TOTAL EVAPORATION ESTIMATION FROM SUGARCANE USING THE SCINTILLATION TECHNIQUE

LW Wiles

Submitted in fulfilment of the
requirements for the degree of MSc in Hydrology

School of Bioresources Engineering and Environmental Hydrology
University of KwaZulu-Natal
Pietermaritzburg
South Africa

December 2006

DECLARATION

The research described in this dissertation was carried out within the School of Bioresources Engineering and Environmental Hydrology at the University of KwaZulu-Natal, Pietermaritzburg under the supervision of Professor GPW Jewitt (School of Bioresources Engineering and Environmental Hydrology at the University of KwaZulu-Natal, Pietermaritzburg)

I hereby certify that the research reported in this dissertation is my own original and unaided work, except where specific acknowledgement is made.

Signed_____
Luke Wilson Wiles

Signed_____
Professor GPW Jewitt

TABLE OF CONTENTS

PART 1: LITERATURE REVIEW AND PLANNING

PART 2: METHODOLOGY

PART 3: RESULTS - TOTAL EVAPORATION ESTIMATION FROM SUGARCANE

ABSTRACT

Ongoing concerns about the efficient and sustainable utilisation of South Africa's water resources have resulted in much interest regarding the water use of different land uses within a catchment. Research has been focussed on water use by different dryland vegetation, in particular commercial forestry which has been declared a Stream Flow Reduction Activity for which a water use license is required for production. Consequently, concerns about the water use of other dryland crops have lead to a need to quantify water use by other land uses, particularly sugarcane.

In this document, previous research focussed on water use by sugarcane is reviewed and summarised, together with an experiment where an energy balance approach has been used to quantify water consumption in the form of total evaporation for an area of sugarcane production in the KwaZulu-Natal Midlands with an assessment of the seasonal variability of this water consumption for a period of 1 year. The study was performed using a Large Aperture Scintillometer to measure sensible heat flux, whilst all other energy balance components, as well as rainfall, soil moisture and other climatic data were obtained using standard methods. Total evaporation was estimated from latent heat flux which was derived as a residual of the energy balance.

Total evaporation varies over the year with substantially higher values occurring in summer in response to high energy and water availability. Over the year, the crop used approximately 630mm of water which equates to 53% of rainfall at the site. The two main factors affecting the seasonal variability of water use by sugarcane are net radiation and soil moisture content. In the wetter months when soil moisture is readily available, net radiation limits total evaporation. In the drier months, soil moisture is not as readily available, and limits total evaporation. Air temperature and relative humidity proved to also be important considerations in their effect on total evaporation.

The total evaporation estimates obtained could be compared to a baseline (grassland) and used in simulations for a better understanding of the stream flow reduction potential of sugarcane and the seasonal variability thereof.

ACKNOWLEDGEMENTS

I wish to express my sincere appreciation for the assistance given by the following persons and organisations:

Professor GPW Jewitt (Associate Professor in the School of Bioresources Engineering and Environmental Hydrology, University of KwaZulu-Natal, Pietermaritzburg) for his supervision, guidance, encouragement and friendship over the project duration.

Ms JJ Blight (Senior Research Fellow in the School of Bioresources Engineering and Environmental Hydrology, University of KwaZulu-Natal, Pietermaritzburg) for her supervision, encouragement and continued support.

Dr CS Everson (Council for Scientific and Industrial Research - Pietermaritzburg) for his guidance.

Mr A Clulow (Council for Scientific and Industrial Research - Pietermaritzburg) for his practical assistance and advice over the field work stage of the project, and for his friendship.

The Water Research Commission (WRC) for funding this project.

Mr DM Knoesen and Mr MJ Bollaert for their assistance, friendship and support over the project duration.

My friends. The many friendships formed over the past few years here in Pietermaritzburg will never be forgotten. Those closest to me (the clique), I thank you for shaping my life the way you have.

My family. The opportunities given to me, consistent support, and love for me I consider to have been a true blessing.

Finally to my Lord, God and heavenly Father for His grace, mercy, and unconditional love shown to me in my life.

LIST OF FIGURES

Appendix A

Appendix B

Appendix C

Appendix D

LIST OF TABLES

LIST OF APPENDICES

PART 1: LITERATURE REVIEW AND PLANNING

1. INTRODUCTION

According to McKenzie and Bhagwan (1999), there has been a growing realisation that increasing water demands are not sustainable and that if this growth in demand is not dealt with, South Africa will face a water crisis in the near future. Since the release of the National Water Act (1998) in South Africa, there has been increased pressure placed on water users to justify their allocations and use. The largest water user from a land use perspective is commercial timber. This has resulted in a large body of research focussed on quantifying water use by timber which includes a large amount of modelling for predictive purposes. Models have been extensively verified and results have been extrapolated from experimental sites to operational areas in South Africa. The most recent research is a set of Stream Flow Reduction Tables used to estimate water use of commercial Afforestation for all the potential timber growing areas in South Africa (Gush *et al.,* 2001). There is however, much concern regarding the accuracy and implementation of these tables as, according to Gush *et al.* (2001), weaknesses in the simulation of low flows were revealed. This research undertaken by Gush *et al.* (2001) has resulted in further research on water use by other potential Stream Flow Reduction Activities (SFRAs). One of these potential SFRAs is sugarcane. According to Schmidt (1997), water use by sugarcane will have to be compared against other land uses in terms of reducing stream flow under rainfed/dryland conditions.

Methods in estimating total evaporation (Et) have advanced considerably in the past decade. Most of the advances are based upon the energy balance where total evaporation is derived from the latent heat of evaporation. Amongst these advances has been the emergence of scintillation as a method to measure average sensible heat flux, a vital component of the energy balance, over an area. The area of measurement may differ in size as well as incorporate different vegetation types. Scintillation has been compared to other techniques commonly used for total evaporation estimates, and the results obtained by scintillation have been found to be accurate relative to measurements by the other instruments (Savage *et al.*, 2004). The mathematical formulae used to derive sensible heat flux using scintillation are rather complex. The scintillometer provides a vital component of the shortened energy balance (sensible heat), with path averaged heat fluxes of up to 10 km being measured. This

sensible heat component is then used in conjunction with corresponding soil heat flux and net radiation data to yield a latent heat flux component of the shortened energy balance and hence, an estimate of total evaporation.

In this dissertation, a study is described in which the evaporative water use of sugarcane was estimated using the scintillation technique and where, in addition to sensible heat flux being measured with a scintillometer, the remaining components of the energy balance as well as soil water content have been measured for one year, from October 2004 to September 2005. The aims and objectives of this study were therefore to:

- become familiar with equipment used in this specific energy balance analysis, especially the scintillometer
- provide estimates of water use by dryland sugarcane for a period of one year
- provide insight into the seasonal variability of this water use by an improved understanding of the limits to total evaporation, with the assistance of Automatic Weather Station (AWS) data
- examine the streamflow reduction potential of dryland sugarcane production

The application of the scintillation technique and the conclusions drawn may aid in decision-making, as knowledge and data obtained improves the support base for decisions related to the declaration, monitoring and management of SFRAs in South Africa.

This document is divided into three parts:

- literature review and planning
- methodology
- results – total evaporation estimation from sugarcane

2. STREAM FLOW REDUCTION ACTIVITIES IN SOUTH AFRICA

Accurate estimation of reference evaporation is necessary for the estimation of actual evaporation for both irrigation design purposes and water resources management (Abezghi, 2003). A recent proposal in South Africa is for there to be a shift towards how land use impacts upon both "blue water" or water flow in a stream and "green water" which focuses on the primary process of evaporation losses from an area of a catchment (Calder *et al*., 2004).

South Africa is a water scarce country and it is for this reason that it is necessary to understand the partitioning of water within the hydrological cycle. A focus of this is to understand how much water certain crops utilize through evaporation and transpiration when growing. The loss of water in this gaseous phase makes up the largest component of the water loss from an area in semi arid regions (Metelerkamp, 1992).

According to the National Water act of 1998, a stream flow reduction activity (SFRA) is defined as any activity "that is likely to reduce the availability of water in a water course to the Reserve; or to meet international obligations; or to other water users significantly." (NWA, 1998) The concept of SFRA has been described as an "innovative concept" and forms the basis for a land and water policy instrument used in addressing issues of equity, economic efficiency and ecology (Calder *et al.,* 2004). In terms of the National Water Act, commercial forestry is the only declared SFRA (DWAF, 2003) where it is listed as such under Section 36 of the Act.

A brief history of SFRA declaration is examined in the next sections followed by a review of the present issues surrounding SFRA declarations.

2.1 History of SFRA Declaration: Afforestation Permit System (APS)

From 1972 until 1995 commercial forestry was regulated through an Afforestation Permit System (APS) (Act No. 72 of 1968) (DWAF, 2003). The reasons for the implementation of this APS were (DWAF, 2003):

- commercial forestry covers only 1 % land area but uses 7% to the country's water use;
- commercial plantation forestry is a permanent change in land use from relatively low water use veld to a higher water use crop;
- afforestation of upper catchments resulted in down-stream rivers drying up, which lead to conflict between foresters and down-stream users, and
- the Department of Forestry deemed that the APS was in the best interests of the country as a whole.

Consequently, in order for a timber grower to plant trees, between 1972 and 1995, a permit had to be obtained before the establishment of commercial plantations on new land or land which after harvesting had not been planted to timber for a period exceeding 5 years (Gush *et al.,* 2001). Quantification of water use by afforestation for the APS was initially based on a model developed by Nanni in 1970 and later improved upon by incorporating additional catchment experimental data by Van der Zel (1995). Some of the major shortcomings of the APS were (DWAF, 2003):

- regulation was based on reductions in Mean Annual Runoff (MAR) at a large catchment scale. Therefore basic needs and ecological requirements at smaller scales downstream were not considered. Other factors such as water demand and supply, impact on available water were also not considered;
- decision-making did not involve local participants, and
- the APS restricted forestry in favour of other uses which may have been far less efficient and used the water less beneficially.

2.2 Introduction of the SFRA Licensing Scheme

Hydrological assessment continued and resulted in a change in the appropriate legislation. In the 1990's streamflow reduction quantification was further improved by the development of two independent estimation techniques. Firstly there was the development of streamflow reduction curves/equations, which were developed by the Council of Scientific and Industrial Research (CSIR). These recognised the significance of low-flows when managing water resources as well as the need to account for climatic differences, management practices and different tree genus (Gush *et al*., 2001). There was also a need to incorporate updated streamflow data from afforested catchments collected from five nation-wide paired catchment studies. Secondly, the ACRU agrohydrological modelling system which had been developed by the then, Department of Agricultural Engineering at the University of Natal was applied to provide estimates of stream flow reduction at sites where experimental data were not available. This model is able to simulate streamflow, total evaporation, and land cover/management and abstraction impacts on water resources at a daily time step (Schulze, 1995). The ACRU model requires input data comprising daily rainfall as well as other climate, soils, and land cover data (Gush *et al*., 2001).

It was proposed that the above two techniques could compliment each other and resulted in a joint research project between the CSIR and members of the ACRU research team between 1999 and 2000. The outcome of this effort was the development of a national set of tables providing estimates of stream flow reduction for each Quaternary Catchment in South Africa, for eucalypt, pine and wattle tree types (Gush *et al*., 2001).

2.3 Stream Flow Reduction Activities Declaration

The Department of Water Affairs and Forestry (DWAF) in South Africa has maintained an interest in the understanding of water use by many different vegetation types. At present (2006), only commercial forestry has been declared a SFRA in terms of the NWA of 1998. There has, however, been increased pressure to consider other crops as SFRAs on the basis of their estimated or perceived water use. According to Anon (2006), the National Water Act proposes licensing of consumptive uses of water that result in streamflow reduction and requires that such uses be estimated with an acceptable degree of accuracy. Various studies that were commissioned to identify other potential SFRAs concluded that these should be

limited to dryland crops (DWAF, 2003). There is thus a need to investigate the water use of these crops. Dryland sugarcane has been at the forefront of investigations and some studies and public perception have suggested that it could be considered an SFRA, and has hence been targeted for declaration by the Department of Water Affairs and Forestry (DWAF, 2003).

There are however many difficulties encountered in declaring a land use to be an SFRA. One of these uncertainties is in the definition of an SFRA as stated in Part Four of Chapter Four of the National Water Act of 1998, in which the Minister must "consider the extent to which the activity significantly reduces the water availability in the watercourse." There is much concern with the meaning of the word "significant" in the Act. At present there is still much debate surrounding SFRAs and how control could be gained over the limited water resources in South Africa, in the best possible way.

Anon (2006) states that evaporation is responsible for the majority of competitive uses of water, yet its exact quantification remains elusive. It is thus important to continue the investigative process using new, more advanced techniques. However, there are many uncertainties in the estimation of evaporation due to a lack of proof brought about by accurate field measurements. In this project, water use by dryland sugarcane was estimated using recently developed technology known as scintillation. It was therefore important to assess any previous research which focussed on the consumptive water use by sugarcane. In the past, there has been a fair contribution in terms of research based upon both understanding and estimating water use by sugarcane using various techniques. These are discussed in the following section.

3. PREVIOUS RESEARCH ON THE WATER USE OF SUGARCANE

In the recent past, there have been a number of attempts undertaken in terms of assessing the water use by sugarcane and the potential impacts of sugarcane on water resources. These range from practical field experimentation to theoretical assumptive work.

Van Antwerpen *et al*. (1996) discussed the complexity in estimating root water use in sugarcane. Van Antwerpen *et al*. (1996) after Philip (1966), described the uptake of water through roots as a dynamic physical continuum which can be divided into a demand and supply component. Philip (1966) also stated that the rate of non-limiting soil water depletion by plants is primarily controlled by the atmospheric demand in combination with characteristic plant and soil properties. However, under limited water conditions, supply to the soil-plant-atmosphere continuum is controlled by the soil-root characteristic (Hillel, 1982). Some of these ideas are discussed further in this dissertation (Section 3.4 of Part 3) with regard to understanding the limits to the total evaporation processes.

Smithers *et al.* (1997) investigated the impacts of grassland, forestry and sugarcane on runoff at the Umzinto research catchments in KwaZulu-Natal using a modelling approach. According to Smithers *et al.* (1997), there is a lack of accurate data and knowledge of the influence of sugarcane production on the water resources of a catchment. Smithers *et al*. (1997) also state that a cost effective and efficient method of assessing the impact of a crop on water resources is to develop credible simulation models. These models should be able to simulate the runoff response from a catchment as well as be sensitive to catchment characteristics such as land cover, management practices and soil characteristics. Smithers *et al*. (1997) stated that an alternative to modelling is long term field monitoring experimentation which is often costly, time consuming and site specific. Notwithstanding, in this dissertation, accurate field data has been collected, analysed and then compared to simulations of total evaporation for different crops, using the ACRU model.

Schmidt (1997) investigated the impacts of sugarcane production on water resources. According to Schmidt (1997), water use by sugarcane will have to be compared to other land uses in terms of the reduction in streamflow under rainfed conditions. Schmidt (1997) also states that the impact of sugarcane on streamflow depends on its location within the river

catchment as well as the soil and slope conditions, stage of crop growth, management practices and the local climate. Approximately 70% of the land under sugarcane production is along the coastal belt of KwaZulu-Natal near the outlet of catchments and within 30 kilometres of the sea. Therefore, most of the runoff entering streams in these areas enter the Indian Ocean (Schmidt, 1997). However, the hydrological impact of different land uses has to be quantified for decisions to be made with regard to land use impacts on water resources, especially in sensitive catchments where there are many competing water users (Schmidt, 1997).

Bezuidenhout *et al*. (2006), estimated the water use of commercial sugarcane in South Africa. According to this study water use of rainfed sugarcane has come under the spotlight in South Africa largely as a result of changes in legislation and a focus on SFRAs as highlighted previously.

The concern raised by Bezuidenhout *et al*. (2006), is that an influential study undertaken by Kruger *et al*. (2000), adopted a methodology whereby candidate SFRAs were determined based upon comparing potential total evaporation rates from the identified crops to corresponding Acocks veld types. Kruger *et al*. (2000) reported that potential total evaporation for sugarcane was approximately 1400 mm per annum and was compared to a country wide average of potential evaporation for Acocks veld types of approximately 1100 mm per annum. This approach could be useful in this research using the data presented in this dissertation.

Bezuidenhout *et al*. (2006) state that the potential total evaporation of a crop assume ideal growing conditions with no soil water limitations. In reality, this rarely occurs. For example, if 700 mm of water was available in the soil profile for a year, both sugarcane and Acocks veld types would consume close to 700 mm as their annual potential total evaporation, are 1400 mm and 1100 mm respectively. Bezuidenhout *et al*. (2006) therefore conclude that actual water use and potential hydrological impacts of different crops is complex and largely dependant on the specific environmental limitations imposed. Thus, to base a crops effect on stream flow reduction on potential total evaporation of a crop and comparing it to the potential total evaporation from the original vegetation, is concluded by Bezuidenhout *et al*. (2006), as not realistic and fundamentally flawed. Rather, the key question should be to find out the actual total evaporation from sugarcane for the regions in which the crop is grown

relative to what it replaces or will be replaced by. In this dissertation, this key question is answered for dryland sugarcane in the KwaZulu-Natal Midlands, albeit for a one year study period.

Bezuidenhout *et al*. (2006) undertook an investigation whereby historical regional sugarcane production records for South Africa were used in conjunction with a robust relationship between sugarcane yield and actual total evaporation, developed by Thompson in 1976. They concluded that the mean water use of sugarcane at an industry scale was 598 mm per annum which amounts to approximately 40 % of the mean annual potential total evaporation for a full vegetative canopy calculated with the Penman-Monteith equation (McGlinchey and Inman-Bamber, 1996) and included irrigated areas. Water use by rainfed sugarcane amounted to approximately 36% of the mean annual potential total evaporation. Clearly, the difference between actual and potential total evaporation for sugarcane is a critical issue in assessing water use of sugarcane.

Burger (1999) compared evaporation measurements above commercial forestry and sugarcane canopies in the KwaZulu-Natal Midlands using the Bowen ratio system. She concluded that during the winter of 1997, mature sugarcane consumed 2.8 $mm.day^{-1}$.Acacia and Eucalyptus canopies over this same period consumed 2.4 $mm.day^{-1}$ and 1.8 $mm.day^{-1}$ respectively. According to Burger (1999), these differences resulted from changes in the leaf area indices and canopy reflection coefficients. The increase in canopy height of the Acacia and Eucalypt tree species over the next year (measured in winter 1998), resulted in increased evaporation rates of 4.9 $mm.day^{-1}$ and 5.4 $mm.day^{-1}$ for Acacia and Eucalyptus respectively.

According to Burger (1999), physiological maturity and high canopy resistance of the sugarcane during the summer of 1997 and winter of 1998 contributed to the lower evaporation rate measured to be 2.1 $mm.day^{-1}$ and 3.7 $mm.day^{-1}$ respectively. Over this same period, no stress conditions were visible for Acacia (3.7 $mm.day^{-1}$ and 4.9 $mm.day^{-1}$ respectively) and Eucalyptus (4.3 $mm.day^{-1}$ and 5.6 $mm.day^{-1}$ respectively) for summer 1997 and winter 1998. This was assumed to be a result of the ability of deep rooted trees to reach water supplies not available to the sugarcane. The research undertaken by Burger (1999) took place at the same site as that undertaken in this project which allow for an increased credibility when comparing results. Total evaporation estimates from dryland sugarcane obtained by Burger (1999), using

the Bowen ratio system compare well to the total evaporation estimates presented in this dissertation as discussed in Section 3.4 of Part 3.

It has thus been seen that in the past, there has been a range of research focussed on understanding and estimating water use by sugarcane and the consequential effects of its production on water resources in South Africa. Much of this undertaken research in terms of both water use and the seasonal variability thereof was confirmed in the study reported in this dissertation. Some of the limits to total evaporation discussed above were evident in this research and are discussed in Section 3.4 of Part 3. In this project, total evaporation has been estimated for dryland sugarcane using an energy balance approach. It is thus important to understand the theory behind estimating total evaporation using an energy balance approach.

4. TOTAL EVAPORATION ESTIMATION USING AN ENERGY BALANCE APPROACH

Water evaporates from soil and plant surfaces and transpires through the plant to satisfy an atmospheric demand (Clark, 1989). The combination of these processes is termed "total evaporation". Evaporation and transpiration occur simultaneously and there is no easy way of distinguishing between the two processes (Allen *et al*., 1998). Evaporation is defined as the physical process whereby a liquid or a solid substance is transformed to the gaseous state (Savage *et al*., 1997), with the evaporation of water occurring everywhere in the hydrological cycle, from rain, land, water surfaces as well as from vegetation in the form of transpiration (Savage *et al*., 2004). There is thus a dynamic state within the soil-plant-atmosphere continuum. The sources of energy in the soil-plant-atmosphere system include (Savage *et al*., 2004):

- solar energy during the day and long wave or terrestrial radiant energy at night;
- heat energy carried into the area by wind (advected energy);
- heat energy stored by vegetation and in land masses;
- heat energy stored in water bodies.

The most important of these energy sources is usually solar energy (Savage *et al*., 2004). The surface energy balance, driven by solar energy, is examined in more detail as follows.

The surface layer is the lowest part of the atmospheric boundary layer (Meijninger, 2003). In this layer turbulent exchange of energy and mass takes place between the earth's surface and the atmosphere. Evaporation of water into the atmosphere is controlled by factors both at the evaporating surface and above it (Metelerkamp, 1992). The amounts of water available as well as the soil characteristics play an important role regarding the supply of water to the soil surface (Metelerkamp, 1992). Furthermore, the vegetation type and its stage of growth will also affect the amount of transpiration occurring. The primary energy input to the system is solar radiation (Clark *et al*., 1989; Savage *et al*., 2004), and it has a significant influence on total evaporation. Some of this solar radiation is reflected while the remaining energy reaching the surface is either absorbed or converted into other energy forms (Clark *et al*., 1989). Therefore the net radiation or radiation balance is defined as the sum of the incoming

short and long wave radiation, less the reflected short wave and emitted long wave radiation (Savage *et al*., 2004). The net radiation provides the driving force behind the energy balance. It is also important to understand that the energy arriving at the surface must equal the energy leaving the surface for the same time period (Allen *et al*., 1998). The simplified version of the energy balance equation for an evaporating surface can be written as (Allen *et al*., 1998; Meijninger, 2003):

$Rn - H - LvE - G = 0$, therefore

$$Rn = H + LvE + G \quad (4.1)$$

where:
Rn = net radiation
H = sensible heat flux density
LvE = latent heat flux density
G = soil heat flux density

According to Allen (1998), all fluxes of energy should be considered when deriving an energy balance equation. It is important to note that in Equation 4.1, only vertical fluxes are considered and the net rate of energy transfer horizontally by advection is ignored. The equation should thus be applied to extensive homogenous vegetative areas (Allen *et al*., 1998).

Sensible heat flux density (H) can be defined as the warming of the air by the underlying surface (Meijninger, 2003). Therefore, the heat transfer is brought about by the temperature difference between two surfaces such as the plant surface and the atmospheric environment (Clark *et al*., 1989). Latent heat flux density (LvE) is the proportion of net radiation that is used to evaporate any water that may be present at the surface (plant or soil). Soil heat flux density (G) refers to the proportion of net radiation which is transferred into the soil (Meijninger, 2003).

The latent heat flux (LvE) component which represents the total evaporation fraction of the energy balance can be derived from the energy balance equation if all other components are known. Net radiation (Rn) and soil heat fluxes (G) can be measured or estimated using measured climatic parameters. Measurements of the sensible heat (H) are more complex and

cannot be easily measured as sensible heat flux estimates require accurate measurements of temperature gradients above the surface (Allen *et al*., 1998).

The energy balance can be linked to the hydrological water balance by the evaporative term. The size of each of the fluxes is determined by the atmospheric and surface properties for the period of interest. For example, in a dry area, soil heat and sensible heat fluxes consume most of the available energy while latent heat flux is dominant in wetter areas (Meijninger, 2003). When there is sufficient water available for a crop, as evaporation proceeds, so the surrounding air becomes increasingly saturated and the evaporation process will slow down if the moist air is not transferred to the atmosphere. The replacement of saturated air with drier air depends greatly on wind speed as this would provide the transport mechanism for the moist air. Solar radiation, air temperature, air humidity and wind speed are thus important climatological parameter considerations, when assessing total evaporation (Allen *et al*., 1998).

In this project, the energy balance approach described above was used to estimate total evaporation by dryland sugarcane. Net radiation was measured using a net radiometer and soil heat flux was measured using a soil thermometer approach. Sensible heat, being more complex in its estimation, can be estimated using various techniques. These include the Bowen ratio, Eddy covariance, and the surface renewal techniques. Savage *et al*. (2004) performed a practical comparative study of the measurement of sensible heat flux from January 2003 until November 2004 above an open and mixed grassland community near Pietermaritzburg using these techniques, as well as a surface layer scintillometer. These techniques were compared by running concurrent field experiments. Savage *et al*. (2004) concluded that the twenty minute measurements of sensible heat flux using the different techniques compared well and were in good agreement for much of the time. A dual beam large aperture scintillometer was used to estimate the sensible heat flux component of the energy balance in this project. This is a relatively new technique used in the estimation of total evaporation from any particular land use or combination of land uses. This technique is discussed in terms of its hydrological applicability in South Africa in Chapter 6 with a detailed review of the scintillation technique in Chapter 5.

5. REVIEW OF THE SCINTILLATION TECHNIQUE

5.1 The Scintillation Phenomenon

Details of sensible heat flux computation are not addressed in this study. This study will just give a brief overview of the scintillation technique as this is sufficient for the purposes of this research. For a more comprehensive overview, Savage *et al*., (1997), Meijninger, (2003) and Savage *et al.* (2004) should be consulted.

Electromagnetic radiation passes through the atmosphere and is distorted by a number of processes such as scattering and absorption by constituent gases and atmospheric particles of the atmosphere, which remove energy from the beam and thus lead to attenuation (Wageningen University and Research Centre, 2003; Meijninger, 2003). The most important mechanism which influences the propagation of electromagnetic radiation, are small changes in the refractive index of air (n). These changes lead to intensity fluctuations in transmitted electromagnetic radiation. These fluctuations are known as scintillations (Meijninger, 2003). An example that clearly shows the distortion of wave propagation by the turbulent atmosphere is the twinkling of stars. This is, the light source is constant but it is distorted to the viewer by atmospheric turbulence described as the existence of three-dimensional air motions or eddies, which have sizes ranging between millimetres to tens of metres (Wageningen University and Research Centre, 2003). Atmospheric turbulence is the most effective transport mechanism for many scalar quantities, including those making up the energy balance such as sensible heat (H) and water vapour (LvE). These eddies transport both heat and water vapour with their refractive indices differing from the surrounding area, hence resulting in refractive index fluctuations or scintillations (Meijninger, 2003; Wageningen University and Research Centre, 2003). Opportunities to utilize the scintillation phenomenon have lead to the development of a range of instruments which attempt to measure these fluctuations.

5.2 Scintillation Measurement Principle

A scintillometer is an instrument consisting of a transmitter and a receiver (Figure 5.1). It functions over a horizontal path by emitting a beam of light (electromagnetic radiation) from the transmitter towards the receiver, which is able to detect scintillations. According to

Savage *et al.* (2004), a scintillometer consists of a light source of known wavelength usually directed over some horizontal distance to a receiver.

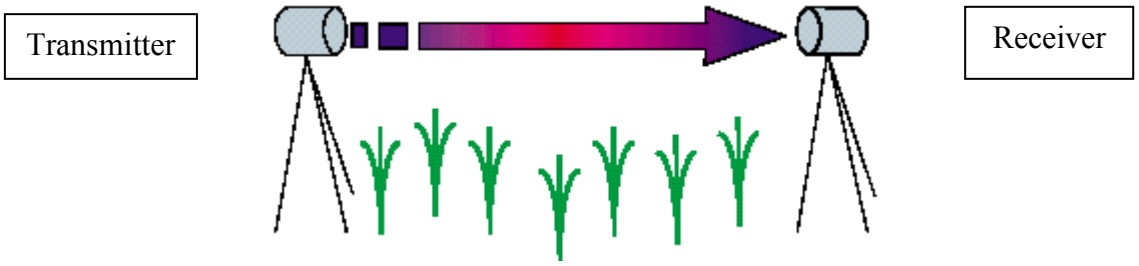

Figure 5.1: Simple illustration of the scintillation technique (Kite and Droogers, 2000b)

The structure parameter of the refractive index of air (C_n^2) provides the expression of the detected scintillations. It therefore describes the atmosphere's ability to transport sensible heat and water vapour. The output from the scintillometer is a path-averaged value of the structure parameter integrated over the optical path. This structure parameter is considered a representation of the "turbulent strength" of the atmosphere (Meijninger, 2003). This is calculated using the following equation (Meijninger, 2003):

$$C_n^2 = 4.48\sigma^2_{\ln A} D^{7/3} L^{-3} \quad (5.1)$$

where:

C_n^2 = structure parameter of the refractive index of air

D = aperture diameter

L = path length

$\sigma^2_{\ln A}$ = variance of the logarithm of amplitude fluctuations

It is also important to note that C_n^2 is path-averaged according to a spatial weighting function. Therefore, scintillations produced by turbulence near the path centre contribute more to the path-averaged C_n^2 (Meijninger, 2003). This is discussed further in Section 3.2.1 of Part 3. It is also important to note that the air passing through the emitted beam of light has often originated from an upwind area. It is thus important that this air passing the emitted beam originated over the vegetative cover which is being researched.

Scintillations are a result of both temperature (C_T^2) and humidity (C_Q^2) fluctuations within the atmosphere. Both C_T^2 and C_Q^2 can be derived from the structure parameter of the refractive index of air (C_n^2) (Meijninger, 2003). According to Hill (1997), structure functions provide the basis for scintillometry. C_T^2 and C_Q^2 are based upon deviations of air temperature and humidity respectively. It can be shown that the relative contribution of these two fluctuations to the fluctuations of the refractive index is dependant on the wavelength of the emitted beam (Meijninger, 2003). Temperature fluctuations dominate at the visible and near-infrared wavelengths. The contribution of humidity increases toward radio wavelengths at the upper end of the scale (Meijninger, 2003). Thus, by selecting a specific wavelength, the scintillations are either produced more by temperature or humidity fluctuations which is an important consideration in the choice of instrument used, to be described in Section 5.4 (Meijninger, 2003).

Using the structure parameters of temperature and humidity, one is able to derive sensible heat and water vapour fluxes, respectively from a scintillometer. This is done using the Monin-Obukhov Similarity Theory (MOST).

5.3 Monin-Obukhov Similarity Theory (MOST)

The lower 10% of the planetary boundary layer is known as the surface layer (Meijninger, 2003). In this zone, vertical fluxes of momentum and conservation scalars (temperature and humidity) are nearly constant with height (Meijninger, 2003). The Monin-Obukhov Similarity Theory (MOST) provides the linkage from the structure parameters of temperature and humidity, to the surface fluxes of H and LvE within the surface layer (Meijninger, 2003). Assuming stationary conditions with a horizontal homogeneous surface, MOST describes the relationship as follows: (Meijninger, 2003).

$$\frac{C_Q^2 (z - l)^{2/3}}{Q_*^2} = \frac{C_T^2 (z - d)^{2/3}}{T_*^2} = f\left(\frac{z - l}{L_{Ob}}\right) \tag{5.2}$$

Where:

C_Q^2 = Structure parameter of humidity

C_T^2 = Structure parameter of temperature

z = Scintillometer height above the surface

d = Displacement

Q_* = Absolute humidity scale

T_* = Temperature scale

L_{Ob} = Obukhov length

L_{Ob} is defined by the following equation (Meijninger, 2003):

$$L_{Ob} = \frac{u_*^2 T}{g k_v T_*} \tag{5.3}$$

Where:

k_v = Von Karman constant

T_* = temperature scale

u_* = friction velocity

g = gravitational acceleration

T = absolute air temperature

The concept of blending height is also an important consideration with regard to MOST. MOST was developed for a stationary atmospheric surface layer over horizontally homogeneous terrain (Green, 2001). As air flows over an area that has a variety of vegetative surfaces, it will be affected in different ways and to different extents. Surface roughness, surface temperature and soil water content could all differ depending on the crop grown (Meijninger, 2003). The question thus arises as to how MOST can be applied to obtain an path-averaged sensible heat flux without violation. As air flows from one vegetation to the next, an internal boundary layer forms. This results in a number of internal boundary layers developing within the surface layer. At a certain level at which the top of the highest internal boundary layer is reached, the signatures of the individual internal boundary layer mix as a result of turbulence (Meijninger, 2003). This level is known as the blending height. The blending height can be defined as the level at which the individual surface element begins to vanish and internal boundary layers merge (Meijninger, 2003). According to Savage *et al*. (2004), the blending height can be defined as the height above which there is horizontal homogeneity by turbulent mixing of fluxes. The blending height will differ depending on the horizontal scale of the inhomogeneities (Mason, 1988; cited by Meijninger, 2003). It has been noted by Meijninger (2003) that the blending height increases with increasing horizontal scale of heterogeneity and instability.

A scintillometer that is placed below this blending height will only detect fluxes from the individual vegetation types (Meijninger, 2003), and thus not satisfy the assumption of homogeneity of cover (Savage *et al*., 2004). Turbulence would thus not be in equilibrium with the local vertical gradients or structure parameters and would result in a violation of MOST. On the other hand, MOST is applicable to a scintillometer placed above the blending height with heterogeneous vegetation (Meijninger, 2003). However, Savage *et al*. (2004) states that "the sensors cannot be too far removed from the surface or else they will be out of the region affected by the surface condition".

5.4 Common/Commercially Available Scintillometers

This scintillation method is used to provide path averaged surface fluxes at spatial scales from 100's of metres to approximately 10 km. There are a number of types of scintillometer available commercially. These scintillometers differ in design according to the type of data which is to be collected. Among commercially available types of scintillometers are:

- radio wave scintillometers;
- surface layer scintillometers;
- large aperture scintillometers.

Radio Wave Scintillometers (RWS) are commercially available but not widely used. With this technique a radio wave is created whenever a charged object accelerates with a frequency that lies in the radio frequency (RF) portion of the electromagnetic spectrum. This type of scintillometer is most sensitive to humidity fluctuations (Meijninger, 2003). It is thus more suited to obtain water vapour fluctuations than temperature fluctuations. However, this is not commonly used due to its expensive components and time-consuming maintenance (Meijninger, 2003). Radio Wave Scintillometers operate at path lengths of approximately 2.2 km (Savage *et al*., 2004).

Surface layer scintillometers (SLS) are instruments targeted for short path lenghs, capable of optically measuring both heat flux and momentum flux in the case of the dual beam version where the laser beam is split into two parallel beams (Scintec, 2003b). Fluctuations in the refractive index caused by thermal changes in the air influence the intensity of the laser light reaching the receiver. These variations are evaluated to yield the turbulent information

(Scintec, 2003c). The SLSs developed by Scintec, Germany, are highly sensitive and allow for even the lowest fluxes and turbulence levels to be measured (Scintec, 2003b). SLSs operate at path lengths between 50 and 250 metres (Scintec, 2003d; Savage *et al.,* 2004). The main advantage of the SLS is its application in the measurement of detailed surface energy budgets (Scintec, 2003d). A major disadvantage however, is that they are affected by strong turbulence which is referred to as saturation (Savage *et al*., 2004), which occurs at path lengths of about 250 metres (Meijninger, 2003).

Large Aperture Scintillometers (LASs) are able to operate at much longer path lengths than SLSs, typically 500 to 5000 m, but with some instruments up to 10000 m. These LASs are also the most common and widely used scintillometer due to the desire for flux measurements at the catchment scale. The ability of the LAS to operate at large scales makes them more applicable to hydrological research and remote sensing than SLSs. They are used when there is a need to estimate atmospheric turbulence or heat flux over an extended area and have also proved to be a practical method in measuring integrated heat fluxes over a mixed canopy (Hemakumara *et al.,* 2003). The large aperture of the instrument allows for the emitter and receiver to be placed far apart but still allow for sufficient signal to be transferred. According to Meijninger (2003), saturation is known to increase with an increase in path length as turbulence is often intense and scattering occurs more than once. Therefore, with the increased path length at which these instruments operate, there is a need to increase the size of the aperture (Meijninger, 2003). According to Meijninger (2003), "when the aperture size of the receiver is larger than the scale of the optically most effective eddies, the receiver will average out fluctuations of the received signal over the aperture area." This process known as aperture averaging thus leads to reduced intensity fluctuations (Meijninger, 2003). Scintec in Germany has provided a large range of both SLSs and LASs which have been widely used in meteorological and hydrological studies. Such an instrument was available for this project and is described below.

5.5 The BLS 900 Scintillometer

The BLS 900 is a LAS made by Scintec (Germany) which has a dual beam (Figure 5.2).

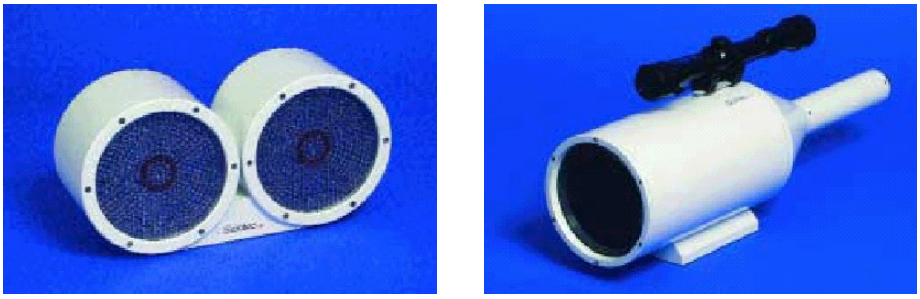

Figure 5.2: Scintec BLS 900 Transmitter (left) and Receiver (right) (Scintec, 2003a)

According to Scintec (Scintec, 2003a), the BLS900 optically measures atmospheric turbulence, heat flux and crosswind over spatial scales of up to 5 kilometres. It contains two disk shaped arrays of 450 light emitting diodes (LEDs). The crosswind speed is determined from the "time lagged cross-covariance between the signals of the two beams". Due to the large transmitting and receiving apertures, saturation and inner scale effects are eliminated. The BLS 900 was used in this project for the measurement of sensible heat flux. Some advantages of the BLS 900 include (Scintec, 2003a):

- minimal transmitter alignment is required;
- accurate and informative data is obtained;
- low noise by using a large number of LED sources;
- insensitive to transmitter vibration;
- relatively low power consumption;
- receiver alignment monitor indicates a need for receiver realignment.

The BLS 900 consists of a dual beam. According to Scintec (2003a), "by evaluating the scintillation from two separate sources, the instrument corrects for transmission changes, increasing the accuracy of the measurement results". The Scintec BLS series scintillometers not only allow for the measurement of turbulence, but also provide the wind speed perpendicular to the optical path.

The BLS 900 scintillometer was used in this project to provide the sensible heat flux component of the energy balance for dryland sugarcane production. The project was undertaken in order to provide a better understanding of water use by sugarcane and the seasonal variability thereof. This better understanding is intended to assist water management authorities in decision making especially with regard to the consideration and possible declaration of SFRAs in South Africa.

6. ISSUES ASSOCIATED WITH THE PRACTICAL APPLICATION OF THE SCINTILLOMETER IN HYDROLOGICAL STUDIES

6.1 Flux Measurements over Heterogeneous Terrain

The natural landscape is heterogeneous with variations of interactions between the soil, plant and atmosphere system and can thus be considered as being in a dynamic state (Allen, 2000; cited by Hemakumara *et al.,* 2003). Surface fluxes of sensible heat and total evaporation are important in many atmospheric processes and can be measured with reasonable accuracy over homogeneous areas (Meijninger *et al.*, 2003). The scintillation technique is one of the few techniques that can provide fluxes at scales of several kilometres (Meijninger *et al.*, 2003). The fact that the scintillometer performs at relatively large spatial scales suggests that the beam can transmit over undulating heterogeneous terrain (Green, 2001).

The scintillation technique could prove to be useful in future hydrological research, and can include flux measurements over heterogeneous vegetation canopies. This could benefit hydrological understanding at a national scale in terms of an integrated water resources management perspective. There is thus a need to use appropriate field techniques, capable of incorporating this landscape heterogeneity. The use of scintillation provides a useful opportunity in this regard. According to Hemakumara *et al*. (2003) "the device is a practical method to measure integrated heat fluxes over a mixed canopy".

6.2 Scintillation as a Tool for Meteorological Research

Meteorology generally deals with processes greater that 1 km on a spatial scale (Green, 2001). This includes weather forecasting and changes to climate. Sensible heat fluxes at spatial scales of greater than 1 km are often important components of meteorological models (Green, 2001). Scintillometers can thus aid meteorological research due to the scales at which they operate.

6.3 Scintillation and Remote Sensing

It has been said (Green, 2001) that the most important feature of scintillometry is that it bridges the gap in spatial scales from point measurement systems to the several kilometre pixel resolution which is demanded by meso-scale atmospheric models, satellite imagery and catchment hydrology. There is a well recognised need to spatially describe total evaporation in hydrological studies (Hemakumara *et al.,* 2003). Satellite imagery and other interpretation tools have allowed for such estimates (Moran *et al*., 1994; cited by Hemakumara *et al.,* 2003). There is, however, a need to obtain independent spatially averaged estimates of both evaporation and transpiration fluxes at the scale of satellite imagery in order to benchmark satellite imagery estimates (Hemakumara *et al.,* 2003).

With the use of a LAS, path averaged surface fluxes at spatial scales up to 10 km may be obtained. This is similar to the pixel size of many remote sensing applications as well as the grid boxes of numerical models (Meijninger *et al.,* 2003; Kongo and Jewitt, 2006). There is thus scope for the two approaches to be linked. Scintillation is able to provide observed data at large scales for heterogeneous vegetation. Remote sensing by satellite provides images at a catchment scale. There is thus potential for practical application of remote sensing to basin scale water balance studies, by incorporating averaged total evaporation estimates over a large area (Hemakumara *et al.,* 2003) and validating such estimates with the use of observed data from a scintillometer. Therefore, calibration of one method against another is possible. This could enhance the management of water in South Africa.

Hemakumara *et al*. (2003) compared total evaporation estimates for a specified area obtained from both a Large Aperture Scintillometer (LAS) and remotely sensed data. Field observations from the scintillometer were compared with SEBAL estimates derived from NOAA satellite images, which were acquired during the same period of time (Hemakumara *et al.,* 2003). The results from this study showed that the satellite images "compared well" with the observed scintillometer data.

It is important to recognise that the net radiation and soil heat flux components of the energy balance used in the estimation of total evaporation described in Chapter 4 are measured at a smaller source area and point source area respectively. This issue of mixing measurements for different spatial scales is one of the shortcomings of this method of estimating total

evaporation. Therefore, it is important to obtain estimates of net radiation and soil heat flux which are representative of the area from which the sensible heat flux component was obtained.

6.4 Scintillation and Water Management

"Increasing competition between industry, agriculture and human consumption for water resources is forcing water resource authorities to improve their management techniques" (Green, 2001). According to Meijninger (2003), "the demand for reliable information of the components of the energy and water balance of land surfaces on a spatial scale of water sheds, river basins, and up to the scale of countries is increasing." It is widely accepted that water resources management strategies should be formulated at river basin scale (Hemakumara *et al.,* 2003). For this to be successful, it is necessary to understand how hydrological processes operate at these scales (Hemakumara *et al.,* 2003). According to Bloschl and Sivapalan (1995), details of the operation of hydrological processes at a catchment scale are important. The processes involved are often complicated as they vary in both space and time. Simulation models are available to help develop and refine our understanding of these processes (Hemakumara *et al.,* 2003). However, most of these models require calibration by the incorporation of sufficient field data. Hydrological models can be run with different levels of data, although the overall data requirements are higher than the other methods (Kite and Droogers, 2000a). These models are often tested using point-source data with high accuracy and then extrapolated to regional scales which then cover a larger area with reduced accuracy (Hemakumara *et al.,* 2003). Mixed vegetation types over an area provide complexities at the basin scale in terms of assessing the validity of total evaporation losses extrapolated from point to basin scale (Hemakumara *et al.,* 2003).

Therefore, scintillation offers an opportunity for total evaporation to be estimated over both homogeneous and heterogeneous vegetation surfaces at river basin scale, at which water management decisions are more sensible. Hydrological research is often focussed upon water use by individual vegetation types produced in the agricultural sector to improve the understanding of potential impacts of certain crops on water resources.

PART 2: METHODOLOGY

1. SITE AND PROCEDURAL DESCRIPTION

1.1 Research Site and Instrumentation Network

The research catchment for this project is located near Greytown in the KwaZulu-Natal Midlands adjacent to the Council for Scientific and Industrial Research (CSIR) Two Streams experimental catchment at which, for a number of years, both water and energy balance research has been undertaken by the CSIR. The research site lies at a latitude and longitude of 29.20 ^{o} S and 30.67 ^{o} E respectively and is considered to be representative of dryland sugarcane production in the KwaZulu-Natal Midlands. The research transect, position of the AWS relative to the transect, and surrounding areas are illustrated in Figure 1.1.

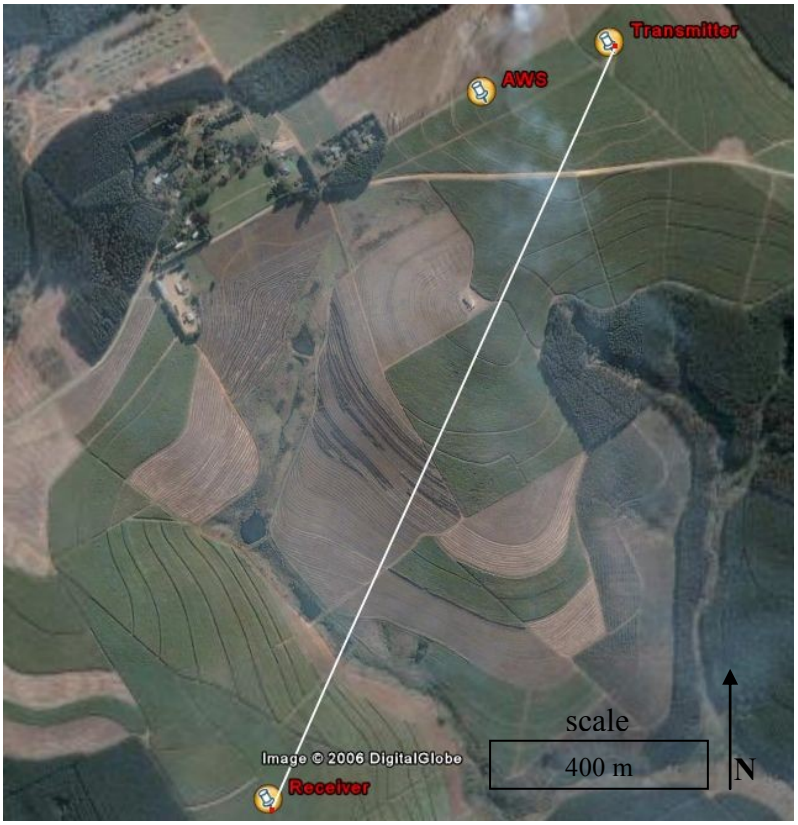

Figure 1.1: Satellite image of the research site illustrating the transect, transmitter, receiver, AWS, and surrounding area (Google Earth, 2006).

At the start of the field work, it was recognised that in order to meet the outcomes of the project, there was a need to measure the following simplified energy balance components accurately:

- Net radiation
- Soil heat flux
- Sensible heat flux

There were numerous issues in terms of temporal spatial scale which needed to be considered as the above listed energy balance components range from instantaneous point measurements to average conditions across the study transect. Therefore data up-scaling in terms of both space and time needed to be done in the most credible method possible.

It was also recognised that additional information which could contribute to the project in terms of interpreting total evaporation results was the change in soil water content over time throughout the transect. Soil water content data that were obtained are not only used in the estimation of soil heat flux, but also assist in the interpretation of when soil water content limits the total evaporation process. Primary data in the form of AWS data were also fundamental to the project, in that solar radiation, air temperature, relative humidity and wind speed all assist in the interpretation of daily total evaporation estimates, as well as in the identification of any anomalies which may exist in the scintillometer estimate of sensible heat and subsequent total evaporation estimate using the shortened form of the energy balance equation.

Consequently, a network of instruments throughout the research site was established as illustrated by Figure 1.2.

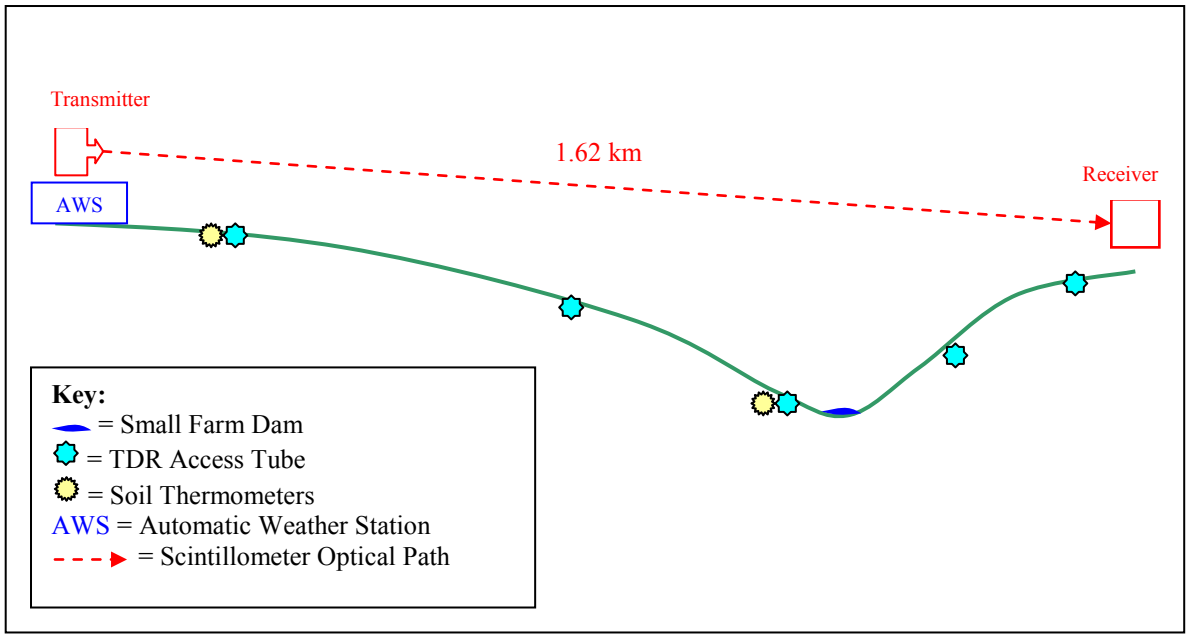

Figure 1.2: Cross section showing network of instrumentation (not to scale).

Figure 1.1 and Figure 1.2 illustrate the 1.62 km transect over which the scintillometer was set up. The cross-section (Figure 1.2) shows the small valley-type transect, over/on which the instrumentation was set up. An AWS - where solar radiation, wind speed, air temperature and relative humidity were measured, is located near to the transmitter of the scintillometer. Five Time Domain Reflectometry (TDR) access tubes were installed at different sites along the transect, and used to estimate soil water content. Soil thermometers were installed at two sites across the transect. The instrumentation and their application and installation are described in greater detail in the appropriate sections below.

The site was visited weekly over the period October 2004 to September 2005 in order to maintain the network of instruments and download data. Solar radiation, air temperature, relative humidity, wind speed and wind direction data are collected at the AWS by the CSIR approximately every two weeks. Net radiation data was collected from a nearby site, by the CSIR. Vegetative changes within the catchment were documented and a photographic record was maintained.

There were a number of issues/problems encountered in the data collection component of the project which resulted in data loss. These were a result of instrument malfunction, depleted batteries, removal of instruments which were occasionally needed elsewhere, as well as late

installation of certain instrumentation. These are best illustrated by Table 1.1 which indicates the duration for which the various instruments successfully logged data.

Table 1.1: Gantt chart illustrating the duration of successful instrument data capture

Date	Oct-04	Nov-04	Dec-04	Jan-05	Feb-05	Mar-05	Apr-05	May-05	Jun-05	Jul-05	Aug-05	Sep-05
Equipment												
Net Radiometer												
Scintillometer												
Hobo Soil Thermocouples												
MCS Soil Thermometers 1												
MCS Soil Thermometers 2												
TDR Moisture Sensor												
Rainfall												
Reliable Total Evaporation												

From Table 1.1, it is evident that the first half of the project was more problematic than the second half in terms of data loss. The major problem over this duration was the lack of soil heat flux data brought about by malfunctioning Hobo soil thermometers. This therefore affected the total evaporation estimation as the soil heat flux provides an important component of the energy balance. Another problem in the first half of the project was the lack of soil water content data as the TDR moisture sensor was only available from late April 2005 following the identification of an instrument malfunction and subsequent repair thereof.

1.2 Crop Management at the Research Site

As highlighted in Part 1, the intention of this project was to investigate water use by sugarcane at a site which is representative of dryland sugarcane production in the KwaZulu-Natal Midlands. It was therefore important to assess the management practices undertaken at the research site to ensure that the management represents the 'norm'. Harvesting of the sugarcane at the research site occurred over the milling season from May until December.

The sugarcane grown at the research site is harvested approximately every 20 months. It is replanted approximately every 5 to 6 cuttings. Therefore, replanting of a field takes place after approximately 8 to 10 years. This is considered to be the 'norm' in the inland high altitude dryland sugarcane production areas.

The sugarcane produced at the research site is burnt rather than greencane harvested. Burning sugarcane is still a common practise within sugar production in South Africa although the drive towards greencane harvesting is being promoted. Conventional tillage is a common

practice on the farm when sugarcane is replanted. Land preparation is performed using conventional rippers, mouldboard ploughs and disc ploughs. Conservation tillage is practised to a lesser extent. At the land preparation phase, a chemical such as Roundup (Glyphosate) is applied at approximately 8 litres per hectare killing both the present sugarcane as well as any weeds. Furrows are then "drawn" a few weeks later and sugarcane is planted with no land preparation taking place, using conventional methods.

Fertilizer at the site is also applied, with the methods and amounts being typical of dryland sugarcane production in the area. To date, granular fertilizer has been used. There may however be a shift to liquid application in the near future. The common granular application method is performed using tractor drawn broadcast application equipment. This method allows for the even spreading of the fertilizer throughout the field. Fertilizer is applied to ratoon cane shortly after harvest (1 - 4 months), depending on the season. Common inorganic fertilizers applied to ratoon sugarcane on the farm are 5:1:5 or 4:1:6 (The ratios indicating Nitrogen, Phosphorus and Potassium). Common application rates for these three elements if 5:1:5 was taken for example, would be approximately 120 kg Nitrogen and Potassium per hectare, and 24 kg Phosphorus per hectare. Micronutrients such as Zinc are also essential in sugarcane production and are included in these mixtures when purchased from fertilizer suppliers.

For plantcane, these ratios differ slightly with a dual application a common practice. Sugarcane is commonly planted with 2:3:4 (N, P, and K) at rates of approximately 44 kg N, 66 kg P, and 88 kg K per hectare, placed in the furrow with the sugarcane. A follow up application when the plantcane has established is common. The follow up application would typically comprise 2:0:3 and rates of approximately 60 kg N and 90 kg K per hectare.

Herbicides are applied to sugarcane shortly after harvest or planting as illustrated in Figure 1.3 and are applied using a tractor and a spray-rig. Four to eight lines (inter-rows) are commonly covered during application (Figure 1.3). A number of chemicals are usually applied including both pre-emergent and post-emergent herbicidal chemicals. These may differ considerably depending on the weeds present, sugarcane variety grown, as well as the farmer's preference. A common combination and rates of chemicals applied at the research site on ratoon sugarcane per hectare are:

- 3 litres Velpar (Hexazinone – pre and post emergent)
- 2 litres Diuron (Diuron – pre and post emergent)
- 0.5 litres Gramoxone (Paraquat – post emergent)

These chemicals have detrimental effects on the growth of the sugarcane for a short period of time. The leaves are often yellow following a large application of for example, Gramoxone. This can affect photosynthesis of the sugarcane for a period of up to 12 weeks.

Figure 1.3: Common application technique of herbicides to sugarcane.

Over the experimental season October 2004 until September 2005, a common management practice adopted on the research farm is the burning of excess 'trash' or vegetative material which remains after harvest has taken place. The amount of vegetation remaining after harvest is determined by the conditions in which the sugarcane was burnt. For example, if there was heavy dew/recent rainfall, the excess vegetation or trash would not have burnt as well as when conditions were drier. If this was the case, the remaining vegetation would often be burnt shortly after harvest. The main reason for this is to 'clean' the field. This is done so as to reduce weed growth by improving the effectiveness of the applied herbicides and fertilizers.

The sugarcane varieties grown at the research site are changing considerably at present and will continue to do so with the release of numerous new varieties by the South African Sugarcane Research Institute (SASRI). New varieties have been developed which may differ in terms of both yield and sucrose, with certain varieties better suited for different areas. The sugarcane variety N12 is the predominantly grown variety on the research farm.

2. THE ENERGY BALANCE

In this project total evaporation was estimated using an energy balance approach as described in detail in Section 4 of Part 1. Each of the instruments used in the energy balance approach, and the calibration thereof, are discussed in more detail below.

2.1 Net Radiation

According to Clark *et al.* (1989), net radiation can be defined as the difference between downward and upward (total) radiation. It is therefore the difference between total incoming and total outgoing radiation (including both short wave and long wave components). Net radiation is typically measured by a net radiometer. A number of radiometers were used in this project to quantify this component.

2.1.1. MCS radiometers

For the estimation of short wave surface reflection, Mike Cotton Systems (MCS) 155 pyranometers were used. The sensor consists of a solar cell fitted in a waterproof housing with a cosine corrected radiation aperture. It is important to note that the spectral response of the MCS 155 radiation sensor does not cover the full range of the solar spectrum. From Figure A1 in Appendix A1, the MCS 155 sensors cover wavelengths ranging from approximately 0.3 to 1.2μm. The error introduced is of the order of 5% under most conditions of natural daylight (Cotton, 2004a). The spectral response curve as well as calibration curves for both incoming and outgoing radiation against a Kipp and Zonen CM3 pyranometer for two MCS radiometers are given in Appendix A. The reflection measurements obtained could however be in error as there is a shift in wavelength (spectral response) when these sensors are inverted. This is due to the calibration of silicon diode sensors taking place under cloudless skies. With regard to the acknowledged error in the MCS 155 readings, it is important to consider that these results were not used in the estimation of total evaporation in this project.

2.1.2 CSIR radiometers

Data from two radiometers (maintained by the CSIR) in the near vicinity of the research site were available for this project. A solarimeter, measuring total incoming solar radiation which is located at the CSIR AWS, was to be used together with site specific reflectivity coefficients to estimate net radiation. The solarimeter data were, however, believed to be erroneous and since the instrument could not be located for re-calibration these data were discarded.

A net radiometer, providing the difference between total incoming and total outgoing radiation is located over a grassed riparian zone at an adjacent site, where a Bowen ratio system has been set up. Although this measurement arrangement was not ideal, the grassed riparian zone was assumed to accurately represent sugarcane in terms of its effects on incoming solar radiation. This aspect is discussed further in Section 1.1 of Part 3.

2.1.3 Reflection coefficient

According to Allen *et al*. (1998), "a considerable amount of solar radiation reaching the earth's surface is reflected. This fraction of the solar radiation reflected by the surface is known as the reflection coefficient." This reflection is highly variable for different incident angles or surface slopes and also varies for different surfaces. For example, freshly fallen snow can have a reflection coefficient of 0.95 (highly reflective) while values of 0.05 for a wet bare soil are typically measured. According to Allen *et al*. (1998), "a green vegetation cover has a reflection coefficient of about 0.20 – 0.25."

The MCS radiometers were used to estimate the reflection coefficient over varying sugarcane canopies. These canopies differed in terms of colour, age, incident angle and density thus producing reflection coefficients ranging from approximately 0.13 to 0.28, depending on the state of vegetation present. The results of this analysis are found in Section 3.2.3 of Part 3.

2.2 Soil Heat Flux

According to Allen *et al*. (1998), soil heat flux is defined as the energy that is utilized in heating the soil. Soil heat flux is positive when the soil is warming and negative when the soil is cooling. Anon (1999) stated that soil heat flux can often consume 5 to 15% of the energy

from net radiation under a vegetative canopy and significantly more where canopy cover is incomplete. According to Burger (1999), in her experiment at a nearby site, soil heat flux comprised up to 40% of net radiation at both Acacia and Eucalypt field experiment sites whilst the sugarcane field experiment site accounted for approximately 10% of net radiation. The difference was due to shade provided by the vegetation canopies (Burger, 1999).

In this project, soil heat flux density (G) was estimated using soil thermometers and estimates of soil heat capacity according to the method described by Blight, (2002).

$$G = z_g(\Delta T)C_G \rho_G \quad (2.1)$$

where:

- z_g = depth of soil heated (m)
- ΔT = the average measured increase in soil temperature over depth z_g (^oC)
- C_G = the specific heat of the soil ($kJ.kg^{-1}.^oC^{-1}$)
- ρ_G = bulk density of the soil ($kg.m^{-3}$)

Savage *et al*., (1997) also used the same technique to estimate the heat energy flux density for soil depths of up to 80 mm, and added this to soil heat flux plate measurements, which were used to estimate soil heat flux below 80 mm. The soil heat flux comprises approximately 10% of the energy balance. Therefore, a small error induced in the calculation of soil heat flux would not have a significant effect on the greater energy balance.

2.2.1 Soil temperature

Soil temperature was measured using a set of two thermometers from October 2004 to September 2005. These data were logged using a Hobo logger in the early stages of the project and were later replaced by new MCS soil thermometers (Appendix B). The thermometers were buried at depths of 50 mm and 250 mm respectively below the surface. According to Blight (2002), the depth to which soil is heated is usually between 200 and 250 mm. It was thus assumed that no heating of the soil took place below a depth of 250 mm.

All soil thermometers were calibrated against mercury measurements. The site within the sugarcane field selected for the installation of the soil thermometers was chosen to represent 'average' vegetative conditions for the area. This represents a vegetative average in terms of both yield and age. The age of the sugarcane in which the thermometers were placed was approximately 12 months and upon harvesting at approximately 20 months, would yield approximately 80 tons per hectare. The thermometers were moved when necessary to maintain these average vegetative conditions.

In this project, one set of Hobo soil thermometers was used initially, with two sets of MCS soil thermometers installed in the latter stages. All of these soil thermometers were calibrated against a mercury thermometer. A linear trend line has been fitted to the data plots for both sets of MCS thermometers. Calibration took place over a range of temperatures from approximately 5 to 45^{o}C. Calibration curves are shown in Appendix B.

2.2.2 Specific soil heat capacity

The specific soil heat capacity (kJ.kg^{-1}.^{o}C^{-1}) is conventionally taken as (Blight, 2002 after Campbell Scientific, 1987):

$$C_G = C_{Gd} + wC_w \qquad (2.2)$$

where

- C_{Gd} = specific heat capacity of the dry soil particles
- C_w = specific heat capacity of water
- w = gravimetric water content of the soil
- C_{Gd} has a value of approximately 0.85 kJ.kg^{-1}.^{o}C^{-1}
- C_w has a value of approximately 4.19 kJ.kg^{-1}.^{o}C^{-1}

C_w is much larger than C_{Gd}. Therefore it is important to have good estimates of soil water content. According to Savage *et al.* (1997), this is a major disadvantage of using this method. In this project, however, reliable soil water content measurements were taken weekly for much of the project period. The analysis of these is found in Section 3.1 of Part 3.

2.2.3 Soil bulk density

Soil bulk density is required in the calculation of soil heat flux as shown by equation 2.1 in Section 2.2. This was estimated at selected representative sites within the catchment. Samples were obtained by using a core sampler which was placed into undisturbed soil within the soil profile and then analysed at the School of Bioresources Engineering and Environmental Hydrology soil laboratory at the University of KwaZulu-Natal. The density was found to be approximately 1390 $kg.m^{-3}$. The procedure undertaken in the estimation of the soil density is explained and illustrated in Appendix B8.

2.2.4 Soil water content

Soil water content is required in the calculation of soil heat flux. This was obtained from gravimetric sampling in the early stages of the research period and Time Domain Reflectometry (TDR) soil water content measurements in the latter stages. Results are presented in Section 3.1 of Part 3. Specific details on the TDR soil water content sensor are found in Appendix D and the monitoring of soil water content is described in the following section.

2.3 Sensible Heat Flux

Surface flux of sensible heat occurs as the air is warmed by the underlying land surface (Meijninger, 2003). In this project, the sensible heat flux component of the energy balance was measured using a BLS 900 Large Aperture Scintillometer (LAS). Specific details on the transmitter, receiver and signal processing unit (SPU), are found in Appendix C.

2.3.1 The scintillometer

The transmitter was located on a fire lookout tower on the Mondi Seven Oaks Estate (Figure C1) with a power supply connected to the national grid. A regulator converts this 220V AC power into 12V DC at which the scintillometer operates. The transmitter has a high power demand and ideally needs to be located near a power source such as this. The receiver uses far less power than the transmitter and can be powered by batteries. Photographic illustrations taken of the instrument at the research site can be found in Appendix C.

2.3.2 Selection of appropriate data resolution

The BLS 900 scintillometer logs minute averages of sensible heat. Figure 2.1 illustrates the '1 minute data' logged at the site using the data viewing software which is provided by the manufacturer. For the purposes of this project, these data were then aggregated up to more meaningful hourly time steps, so that the sensible heat component data corresponded to the remaining energy balance component data collected at the site. The outcome of this was thus a smoother daily trend of sensible heat after hourly averages were determined, rather than highly variable minute measurements, as depicted in Figure 2.1.

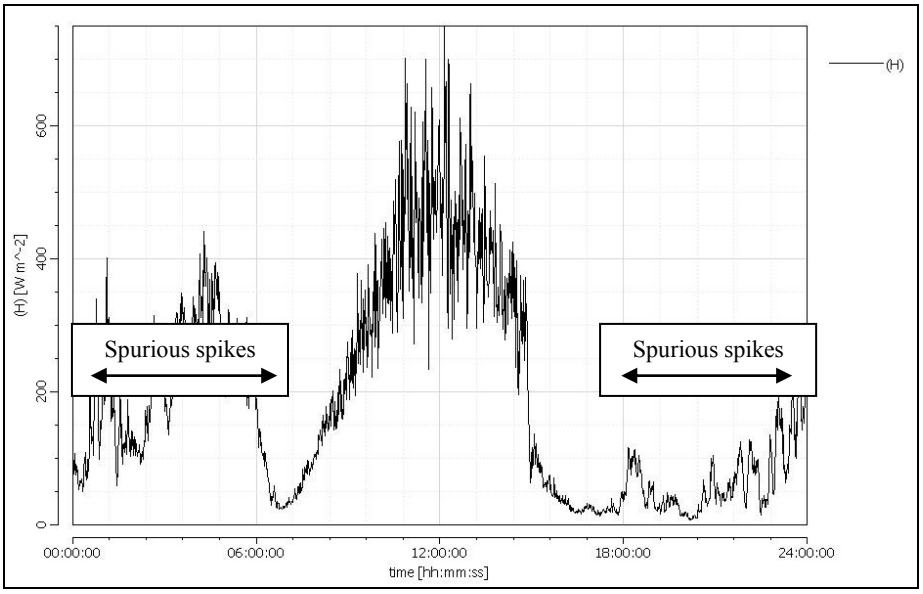

Figure 2.1: 1 minute sensible heat data for 17 November 2004.

A problem encountered with the collection of sensible heat data, were large 'spikes' in the data overnight, especially just before dawn. It was concluded that the cause of these spikes was condensation of water vapour on the scintillometer's receiving lens. This resulted in the refraction of the electromagnetic radiation emitted by the transmitter and thus inaccuracies/anomalies in the sensible heat flux data obtained. Typical recorded data are presented in Figure 2.1 and were useful in identifying this problem. In Figure 2.1, these periods have been labelled as spurious spikes. For these late evening/early morning periods, the sensible heat is expected to be negligible. The daytime period did, however, provide good data with logical trends of sensible heat evident in Figure 2.1, peaking at around midday.

2.4 Latent Heat Flux

Latent heat flux was determined as the residual of the shortened energy balance equation. Latent heat flux can be derived by making it the subject of the energy balance equation. Therefore:

$$LvE = Rn - H - G \quad (2.3)$$

where:
Rn = net radiation ($W.m^{-2}$)
H = sensible heat flux density ($W.m^{-2}$)
LvE = latent heat flux density ($W.m^{-2}$)
G = soil heat flux density ($W.m^{-2}$)

Hourly averages for Rn, H, and G were determined for the duration of the project. For each hour, the evaporative term (LvE) was determined. This was then plotted and the area under the latent heat flux curve was integrated to provide a quantitative estimate of total evaporation in $mm.day^{-1}$. This analysis is expanded upon in Section 2 of Part 3.

3. SOIL WATER CONTENT BALANCE

3.1 Rainfall

The rainfall measured for the duration of the project from October 2004 until September 2005, is represented and discussed in the results Section i.e. Section 3.1 of Part 3. It is however useful to examine historical rainfall records for the area so that the current analysis can be better understood in terms of whether or not the rainfall experienced for a particular year is typical or not. Daily rainfall data have therefore been obtained from the CSIR for the period from November 1999 to August 2005. Figure 3.1 illustrates monthly total rainfall data from 3 separate rain gauges located at the Two streams research catchment.

A general indication of the seasonal rainfall distribution is shown for the period from November 1999 until August 2005. The period over which energy fluxes were recorded was October 2004 until September 2005. From Figure 3.1, it is evident that a similar seasonal rainfall pattern took place over this period, although monthly summer totals were higher than previous years. The maximum monthly total rainfall occurred in December 2004 with approximately 300 mm falling. This rainfall pattern typically results in the recharge of the water table and subsequent runoff resulting in the filling of dams in the early summer. It was observed that a small dam (Figure 1.2) within the catchment was full by the end of November 2004 and was still overflowing in September 2005. This is thought to be a result of the good rains experienced over the summer and early winter months and a relatively high water table level throughout the season. From Figure 3.1, it can be said that the rainfall experienced over the hydrological year of interest is above the long term average rainfall for the research site by approximately 200 mm. A basic water balance calculated for the researched year can be found in Section 3.4.4 of Part 3.

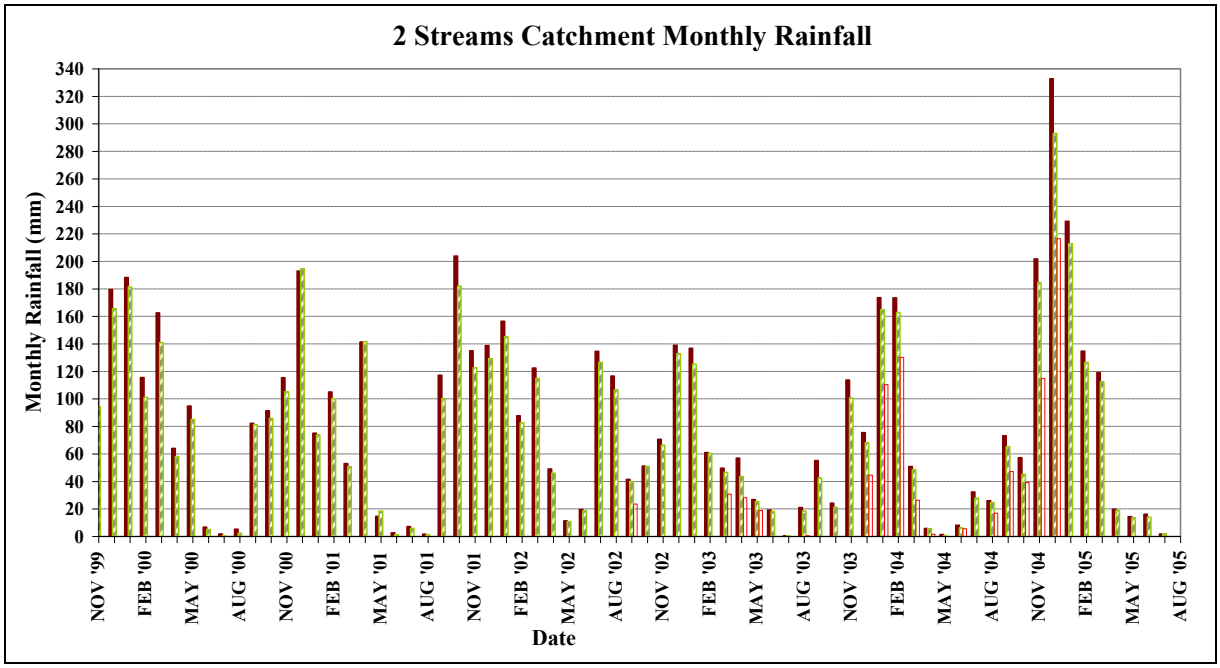

Figure 3.1: Rainfall data from the Two Streams study area at three gauging sites adjacent to the research transect for the period November 1999 to August 2005.

3.2 Soil Water Content Measurement

It is well recognised that available soil water content can limit total evaporation in regions with seasonal rainfall patterns (Calder, 1998). Consequently, the measurement of soil water content was an important part of this project. However, a problem with the TDR instrument in the early stages of the project and difficulties in obtaining regular (i.e. less than weekly) gravimetric samples means that it is necessary to infer soil water content patterns through analysis of the available rainfall records. Notwithstanding, soil water content estimates were obtained both gravimetrically and with the use of a TDR instrument, described in more detail in Appendix D, and these proved to be useful in the analysis of results in terms of understanding water use by sugarcane and the seasonal variability thereof. A number of gravimetric samples were also taken over the season. These were important in the early stages of the project where TDR data were not available, and can be found in Section 3.1 of Part 3.

PART 3: RESULTS - TOTAL EVAPORATION ESTIMATION FROM SUGARCANE

In Part 3, the assumptions made in estimating the energy balance at the site are explained and the data are then presented and analysed. Some conclusions regarding the water use of sugarcane and the representation of this site are then drawn.

1. ASSUMPTIONS MADE IN THE ANALYSIS OF RESULTS

A number of simplifying assumptions were necessary in the process of analysing results. In some cases, these were the results of shortcomings in the equipment used, and in others to simplify the data necessary to resolve the energy balance.

Firstly, condensation observed on the receiving lens of the scintillometer resulted in sensible heat flux estimates being erroneous at times. This occurred some early mornings and evenings and resulted in refraction of the transmitter's emitted electromagnetic radiation. Under these circumstances, sensible heat flux recordings were estimated to be excessively high. Thus, these evening estimates as well as the remaining evening energy balance component estimates were omitted from the analysis. Each day's data were examined manually to identify the condensational effect, with poor data subsequently being deleted. Anomalies were typically found between 6 pm and 6 am. It was thus assumed that:

- The anomalies in the sensible heat flux data are a result of the condensation on the scintillometer's receiving lens
- Such periods were accurately identified
- No evaporation took place over this period

Secondly, all the energy balance components needed to be collected simultaneously for total evaporation estimates to be made. Therefore, if there was a problem with any of the instruments in estimating a component of the energy balance, the remaining data were not useable. It was thus important to ensure that any instrumental problems were solved as soon as possible. A number of instrument problems occurred over the summer period in the estimation of both the sensible heat flux and soil heat flux (Table 1.1 of Part 2). This resulted

in fewer daily evaporation estimates than desired over these months making analysis more difficult. These aspects will be discussed in more detail in the appropriate sections.

Thirdly, it is also necessary that components of the energy balance are measured and analysed at corresponding time steps. For the analyses, data were accumulated and averaged at an hourly time step. It was thus important to ensure that each hour of the energy balance component data were correlated. This was assumed to be the case.

Fourthly, the net radiation data used in this project was obtained from a nearby site in a riparian zone where a Bowen ratio system was operational. Grass and weeds grow in this Riparian Zone, as shown by Figure 1.1. A major assumption of the project is that the short wave reflection as well as long wave radiation from this riparian zone is similar to an average for the sugarcane transect. According to McGlinchey and Inman-Bamber (1996), the reflection coefficient from sugarcane is 0.228. Clark *et al.* (1989), state that a value of 0.23 is often used for green grass/green crops. According to Allen *et al*. (1998) a green vegetation cover has a reflection coefficient of about 0.20 to 0.25 and for the green grass reference crop, is assumed to have a value of 0.23. In Section 3.2.3, the reflection coefficient from the sugarcane site was estimated for varying canopies and found to be approximately 0.23 for a full canopy. Thus, the short wave reflection from the nearby grass site is assumed to be similar to that of the sugarcane.

Fifthly, there is a complication with matching scales of measurement in such research. Some components of the energy balance collected provide a weighted path average (sensible component) while others provide a point estimate (soil component) or over a more localised area (net radiation component). It has therefore been assumed the data obtained at the point estimates are representative of the catchment or transect as a whole, unless specified otherwise.

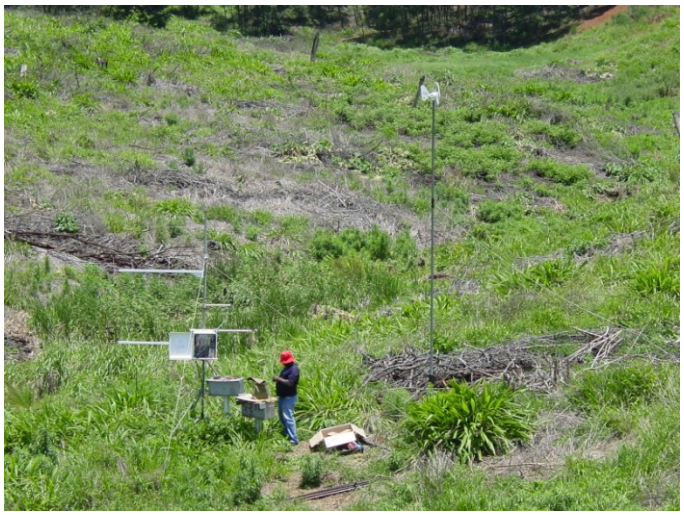

Figure 1.1: Net radiometer on a Bowen ratio system at a nearby site

2. METHOD OF ANALYSIS

In this project, large amounts of data were collected. It was thus important to display these data in an understandable manner and group them appropriately. Ultimately, the goal of this study was to estimate the daily total evaporation of sugarcane. Thus, the output of the data analyses are presented as estimates of daily actual (total) evaporation for representative periods in each month. All components of the energy balance are shown in order to illustrate the methodology used and assumptions made. Actual daily total evaporation estimates have been tabulated in Section 3.3. The total evaporation in $mm.day^{-1}$ was estimated by converting the latent heat of evaporation from $W.m^{-2}$ into a quantitative daily estimate in $mm.day^{-1}$. In this study, as the focus is on studying the water balance in sugarcane growing areas in the context of the possible declaration as an SFRA (Section 3.5), an approach has been taken whereby all energy balance components are expressed as mm of water equivalents. This may be considered unusual in the context of energy balance studies, but given the hydrological focus of this study, it is considered appropriate and was done for comparisons to be drawn between energy balance components data. This is similar to the approach followed by Hemakumara, 2003 as well as Aase and Wright (1972) (Table 2.1).

Table 2.1: Millimetre equivalents for energy balance components in a study undertaken by Aase and Wright in1972 (Aase and Wright., 1972).

TABLE 1. Pan evaporation (E_p), evapotranspiration (ET), net radiation over vegetation (R_{nv}) and over evaporation pan (R_{np}), solar radiation (R_s), and appropriate ratios on native range expressed as mean daily values based on 10-day averages. Energy terms are expressed in equivalent mm of water evaporated (59 cal $cm^{-2} = 1$ mm of evaporation)

	1968			1969									
Period	E_p	ET	$\frac{ET}{E_p}$	E_p	ET	R_{nv}	R_{np}	R_s	$\frac{ET}{E_p}$	$\frac{ET}{R_{nv}}$	$\frac{E_p}{R_{np}}$	$\frac{R_{nv}}{R_s}$	$\frac{R_{np}}{R_s}$
	–mm/day–			– – – – – – –mm/day– – – – – – –									
4/5–4/14	——	——	——	4.78	1.75	2.36	3.36	6.72	.37	0.74	1.42	.35	.50
4/15–4/24	——	——	——	7.01	1.71	3.93	4.21	7.12	.24	0.43	1.66	.55	.59
4/25–5/4	——	——	——	5.84	1.89	4.96	3.24	7.30	.32	0.38	1.80	.68	.44
5/5–5/14	——	——	——	9.14	2.06	5.28	3.68	8.85	.23	0.39	2.48	.60	.42
5/15–5/24	6.2	1.9	.31	5.14	1.68	3.55	4.14	6.98	.33	0.47	1.24	.51	.59
5/25–6/3	6.4	1.0	.16	12.46	2.43	4.15	4.93	7.80	.20	0.58	2.53	.53	.63
6/4–6/13	3.0	2.1	.70	8.73	2.72	4.34	4.30	7.90	.31	0.62	2.03	.55	.54
6/14–6/23	7.2	3.8	.53	6.81	2.58	4.02	4.06	8.67	.38	0.64	1.68	.46	.47
6/24–7/3	5.6	3.1	.55	5.31	3.35	3.12	3.32	7.17	.63	1.08	1.60	.44	.46
7/4–7/13	10.5	3.2	.30	8.89	5.76	3.70	3.92	8.90	.65	1.56	2.27	.42	.44
7/14–7/23	10.0	2.2	.22	6.22	3.26	5.41	5.76	8.06	.52	0.60	1.08	.67	.71
7/24–8/2	8.7	1.3	.15	6.66	3.69	5.99	5.64	8.98	.55	0.58	1.18	.68	.63
8/3–8/12	9.8	0.4	.04	9.35	4.24	5.02	——	8.91	.45	0.84	——	.56	——
8/13–8/22	5.5	1.4	.25	7.29	3.04	——	——	8.37	.42	——	——	——	——
8/23–9/1	7.1	3.4	.48	8.42	2.82	——	——	7.94	.33	——	——	——	——
9/2–9/11	3.8	2.6	.68	6.88	1.83	4.05	4.44	7.32	.27	0.45	1.55	.55	.61
9/12–9/21	——	1.4	——	5.98	1.28	1.56	3.98	5.61	.21	0.82	1.44	.26	.70
9/22–10/1	——	——	——	5.55	0.90	1.23	1.76	4.83	.16	0.73	3.15	.25	.36
10/2–10/11	——	——	——	3.15	0.56	0.60	1.75	3.43	.18	0.93	1.80	.17	.51

Investigations done by Aase and Wright (1972) took place in order to assess total evaporation to net radiation ratios over rangeland vegetation, as well as ratios between evaporation pan and net radiation taking place over the same evaporation pan. Table 2.1 illustrates the expression of these energy balance investigations in millimetre equivalents. Energy balance component data analysis took place at hourly time steps which were then summed to produce daily evaporative estimates. For the purposes of this research, it was necessary to compare the total evaporation estimated to the corresponding net radiation measurement (in mm equivalents) in order to give a broad indication of the proportion of the energy balance met by the latent heat flux component. This was done to assist in the understanding of the seasonal variability of water use by the sugarcane when considered in conjunction with the soil moisture content. According to Aase and Wright (1972), "the upper limit of total evaporation can be predicted from knowledge of the net radiation available to the surface". Aase and Wright (1972) also state that for this upper limit to be reached there needs to be no shortage of water as well as an absence of advective heat transfer which can affect the sensible heat flux estimate, depending on the conditions upwind of the crop. In this project, it has been assumed that the effect of advection is limited due to the surrounding areas consisting largely of the same crop. Hemakumara *et al*. (2003) followed a similar approach in comparing the total evaporation to the net radiation with an evaporative fraction being calculated by dividing the daily total evaporation by the daily total net radiation and assessing this fraction considering the soil moisture content. Rainfall/soil water content was therefore recognised as being an important consideration and likely limitation to total evaporation in the analysis of results. Daily rainfall as well as soil water content estimates taken over the project duration are tabulated in Section 3.1. Air temperature and relative humidity are also tabulated to assist in the understanding of the results presented. These data were obtained from the Two Streams AWS with values from 1pm being used for daily analysis as this was assumed to provide a good representation of daily conditions. Each month's results are discussed separately and then summarised in Section 3.4. All summarised data from each month were tabulated and plotted. Although all daily data are presented, for selected months, a period of 4-5 days has been selected as 'representative' of that month with the energy balance component and primary data being displayed in more detail to aid in understanding the link between primary data and the energy balance. These data were then summarized, plotted and discussed in order to draw conclusions, regarding the consumption of water by sugarcane presented in Section 3.4.

3. PRESENTATION OF RESULTS

In the tables presented in Section 3, the following abbreviations are used:

- DOY = Day of year
- LvE = Latent heat flux component (mm of water equivalents)
- Rn = Net Radiation component (mm of water equivalents)
- H = Sensible heat flux component (mm of water equivalents)
- G = Soil heat flux component (mm of water equivalents)
- Ta = Air temperature at 1pm (^{o}C)
- RH = Relative humidity at 1pm (%)
- Rainfall = Daily rainfall (mm)
- NA = Data not available

3.1 Soil Water Content Balance

The availability of soil water content is vital to processes such as evaporation and transpiration, and thus proved to be a fundamental component of this research. Rainfall for the year will thus be examined and related to soil water content measurements and estimates which took place over the duration of the project.

3.1.1 Rainfall and soil water content samples

Available soil water content is closely related to the rainfall pattern. Figure 3.1 displays daily rainfall for the period October 2004 to September 2005 and provides an important part of the interpretation of results in Section 3. A 5-day moving average has also been plotted to provide a smoother trend of average rainfall. A typical KwaZulu-Natal Midlands rainfall distribution pattern is evident for the study site with significant summer rainfall, peaking in December 2004, followed by a dry winter with very little rain falling between April 2005 and August 2005. Gravimetric soil water content samples were taken over the duration of the project. These have been converted into volumetric soil water content equivalents for comparative purposes with the TDR data discussed in Section 3.1.2. It is unfortunate that only six soil water content samples were taken over the period October 2004 – June 2005, after which a significant amount of soil water content measurements were taken using the TDR soil water

content sensor. The six samples taken do however give a good indication of the seasonal changes in soil water content replicating the rainfall trend in Figure 3.1, peaking in January 2005.

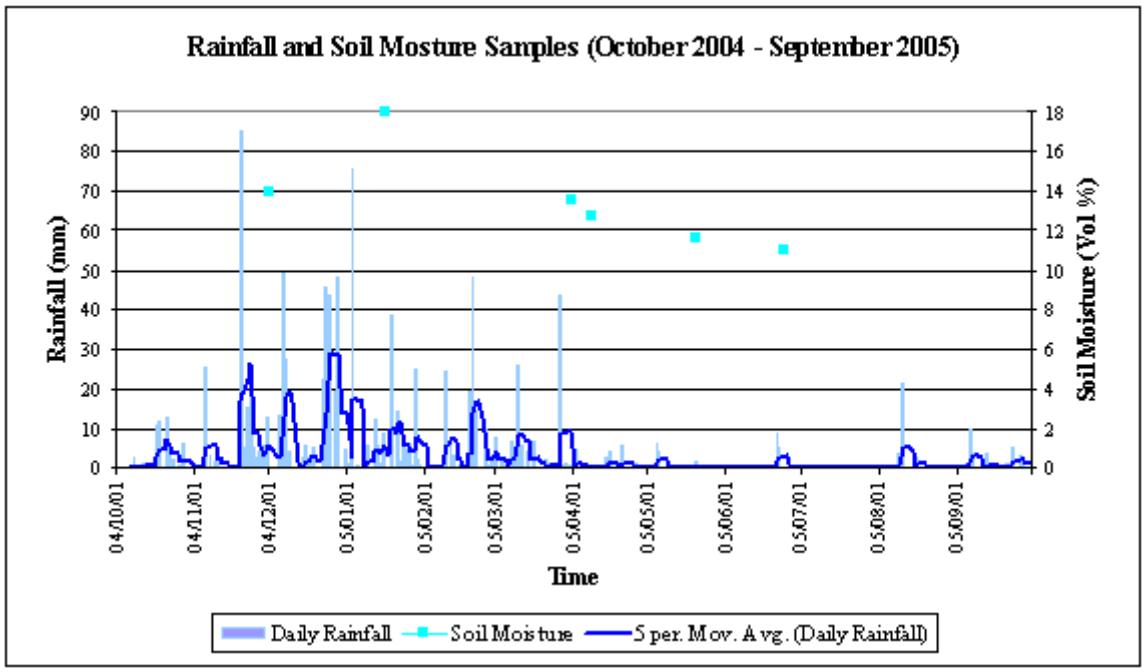

Figure 3.1: Daily rainfall and soil water content samples taken over the period October 2004 to September 2005

3.1.2 TDR soil water content measurements

Measurements were taken at weekly intervals with this instrument (Appendix D) for the period 26 April 2005 until the 19 September 2005, yielding volumetric water content. Five TDR measuring sites/nests were established at different points across the transect. These can be seen in the cross section shown in Figure 1.2 of Part 2. Unfortunately, the first of these nests was not found upon return to the field site due to its position not being clearly identified. Measurements were taken at depths 0.3, 0.6, 0.9 and 1.2 m at the remaining four sites. Figure 3.2 is a summary of the results obtained. For each measured day, soil water content is averaged over the four depths at each nest whilst in Figure 3.3, soil water content for each measured day at a depth of 0.3 m is plotted and provides some differences when compared to the depth-averaged soil water content.

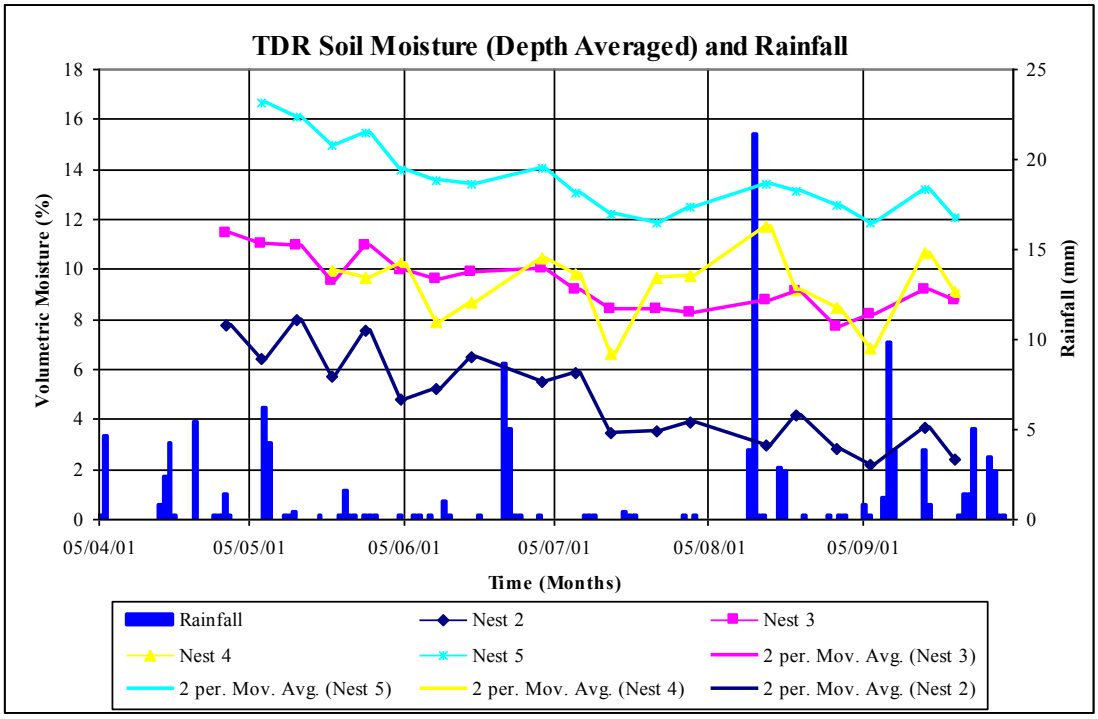

Figure 3.2: Depth-averaged TDR soil water content measurements for nests 2 to 5 for the period April to September 2005

From Figure 3.2, there appears to be clear differences in soil water content between the different nests. Some trends are however evident. The general trend in all nests is a decrease in soil water content over the illustrated period and a clear response to the rainfall events In the analysis of the energy balance, the soil water content estimates obtained at nest 5 were used in the calculation of soil heat flux density as this access tube is located a few metres from the soil thermometers (Figure 1.2 of Part 2). Therefore, soil heat flux density calculations are assumed to be most accurate using soil water content estimates from nest 5.

Nest 2 is located on a relatively steep slope. This may have resulted in an increased surface runoff contribution rather than through flow if compared to nest 5 which is located on relatively flat topography as illustrated by Figure 1.2 of Part 2. This increased slope of nest 2 could result in less infiltration and more water draining away compared to the lesser slopes and correspondingly lower soil water content content. Nests 3 and 4 are located on similar slopes with nest 3 located near the valley bottom and nest 4 located at the mid-slope. Similar soil water content contents were evident at these sites. The access tube at nest 4 was burnt when the sugarcane was harvested in April 2005 but was repaired by mid May.

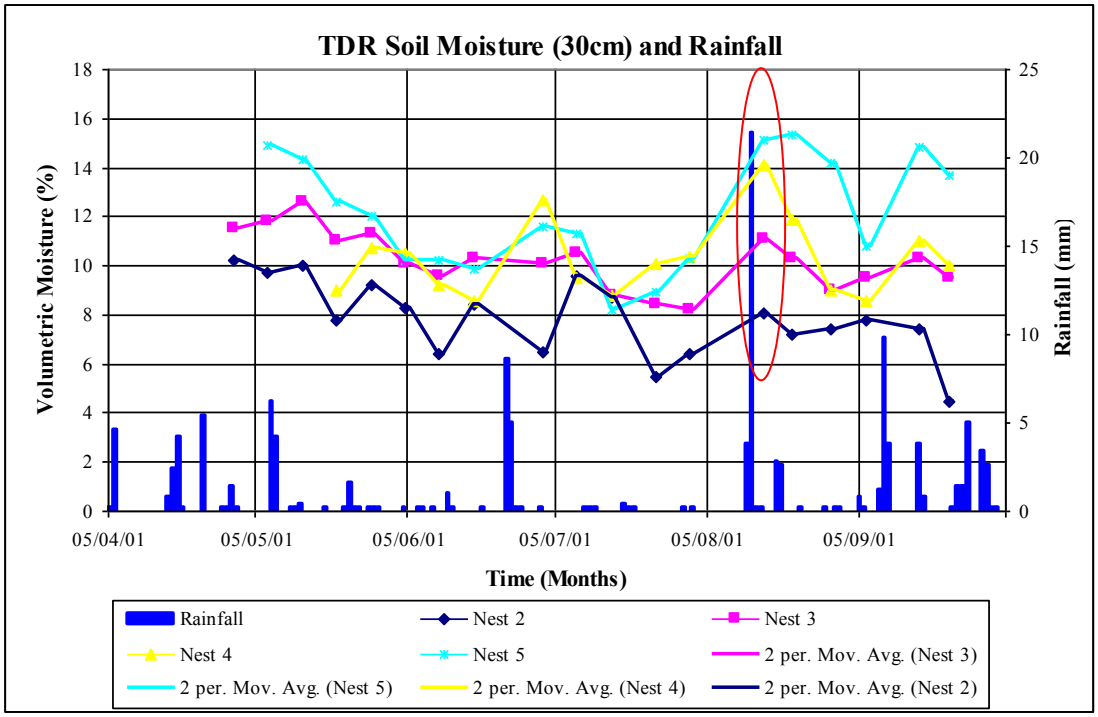

Figure 3.3: TDR soil water content measurements at 0.3 m for nests 2 to 5 for the period April to September 2005

Figure 3.3 provides a more erratic soil water content pattern than Figure 3.2. This reflects the variability of soil water content in the upper soil profile as it undergoes a number of wetting and drying cycles moving through the upper 0.3 m of the soil profile. Relatively small rainfall events result in changes in soil water content at this shallow depth. A seasonal trend is evident from the plots, with the soil water content lowest just after mid winter (July). The effects of individual rainfall events are clearly identified due to the short time taken for the moisture to reach a depth of 0.3 m. For example, on the 12 August 2005 (highlighted in Figure 3.3), soil water content seemed to peak at all nests following a rainfall event. This is confirmed by Table 3.15 (August 2005 monthly analysis) and the rainfall plotted in Figure 3.3 with approximately 25 mm falling over the three days prior to this (9 to 11 August, 2005). The effect of this rainfall on the depth averaged soil water content measurement in Figure 3.2 is more lagged and less pronounced due to the time taken for seepage down the soil profile as well as the distribution of this water though this profile.

3.2 Path Weighting Function for the Energy Balance Components – Incorporation and Significance Testing

In this project, Rn and G have been estimated at a localised source area and point source area respectively whilst H has been estimated using a weighted average across the entire transect. According to Savage *et al*. (2004), the spatial scales of the measurements of the energy balance components differ due to the nature of their measurement. In order test the significance of this weighting function on the other components of the energy balance, A similar weighted distribution across the transect for Rn and G, and thus a weighted estimate for LvE was produced. This was done for selected days when the weighted distribution was thought to have its largest impact on the energy balance components. The estimated weighted LvE values, were then compared to the LvE estimates obtained using the point estimates of Rn and G, in order to test the significance of incorporating the weighted energy balance component distribution.

3.2.1 Sensible heat flux

Estimating the sensible heat flux component of the energy balance (H) is computationally complicated. It is important to understand that sensible heat fluxes measured by the scintillometer are not point estimates, but rather line-averaged values across the transect. Sensible heat flux is thus a spatially weighted function describing the contribution of different regions of the propagation path. Figure 3.4 illustrates the weighted normal distribution of sensible heat flux with an increased contribution near the path centre, and a negligible contribution near the transmitter and receiver of the scintillometer (Scintec, 2004).

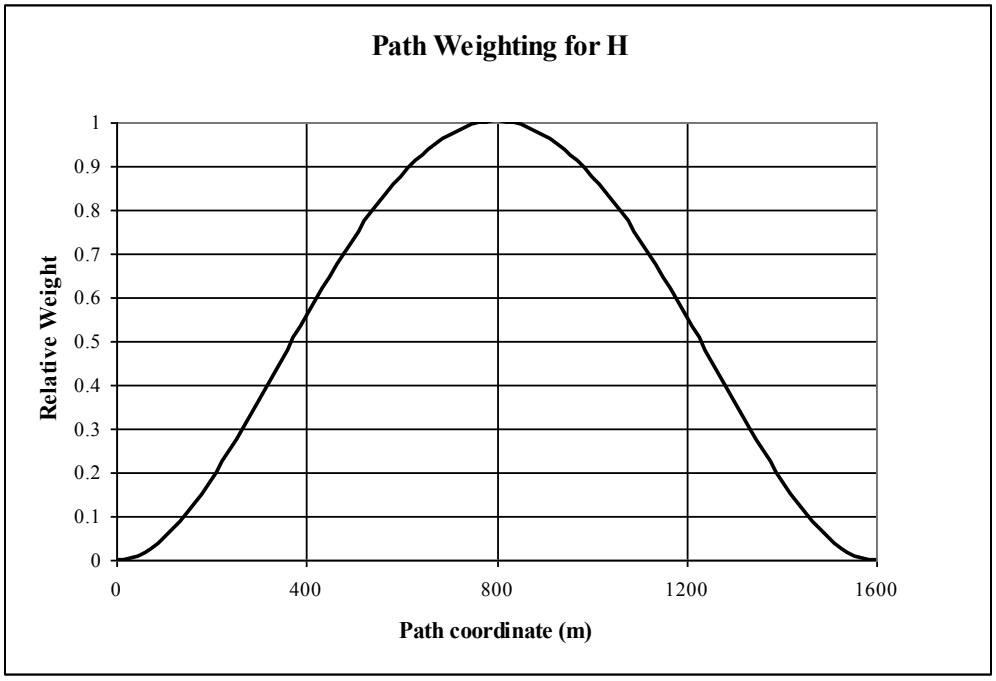

Figure 3.4: Spatial weighting for the sensible heat flux component of the energy balance (Scintec, 2004).

3.2.2 Dynamic vegetation distribution

The research transect has a length of 1.62 km. As the objective of this exercise was to obtain an equal weighting distribution for Rn, G, and H across the transect, Rn and G had to match the distribution of H. Figure 3.4 was thus examined carefully and it was decided to divide the total transect length into four equal quarters, each comprising approximately 400 m. The areas under each quarter of the curve in Figure 3.4 was determined and found to comprise approximately:

- 11%
- 39%
- 39%
- 11%

Rn and G also vary according to the condition of the vegetation at the estimation point. In terms of Rn, both short wave reflection and long wave re-radiation could be affected by the state of vegetation. The change in long wave re-radiation brought about by a change in vegetation has not been considered in section of 3.2 of the project as its contribution is thought to be relatively insignificant. Should this contribution be significant, the path

weighted estimate of Rn could be erroneous. The fraction of solar radiation reflected by the surface, commonly known as the reflection coefficient, could be considerably affected by the vegetative state at the surface. For example, after harvest, a bare soil would be present which, if moist, can have a reflection coefficient of as low as 0.05 or 5% (Allen *et al.,* 1998). The reflection coefficient can also be as high as 0.3 or 30% for a full sugarcane canopy. Trials were set up at the site to determine this variability (Section 3.2.3) and incorporate it into the weighting of Rn over the transect.

The soil heat could also be considerably affected by the state of the vegetation at the point of estimation and although the soil heat flux contribution to the energy balance is small, was also considered as G measured under a dense sugarcane canopy could be considerably less than G measured at a bare surface after harvest has taken place.

In order for the weighting function to be incorporated into calculations of both Rn and G, it was important to consider each of the four equal quadrants as described above. Photographs of the catchment were taken weekly indicating any vegetation changes brought about by crop harvest. This information has been summarized in Table 3.1 with the state of the vegetation across the transect and its variability over time being tabulated. Percentages indicate that the proportion of vegetation remaining i.e. not harvested. From Table 3.1, it is evident that the largest proportion of the sugarcane harvested across the transect, took place near the centre. It can also be seen that for much of the research period, complete vegetation cover is present. This is a result of the 'off season' when sugarcane is not harvested. The off season generally runs from December through until April, depending on the sugar mill to which the sugarcane is sent.

Table 3.1: Vegetation cover across the transect and its variability over time.

Date	0 km-0.4 km	0.4 km-0.8 km	0.8 km-1.2 km	1.2 km-1.6 km
October 2004 - April 2005	100%	100%	100%	95%
May 2005	100%	100%	55%	95%
June 2005	100%	100%	40%	95%
July 2005	90%	50%	5%	96%
August 2005 - September 2005	70%	50%	10%	90%

3.2.3 Net radiation

Two solar radiometers were used to estimate the reflection coefficient of the sugarcane present across the transect. These were calibrated against a pyranometer as described in Appendix A. One of these was faced upwards, to measure the total incoming shortwave radiation, and the other was faced downwards to measure total shortwave radiation reflected at the surface. This was done at four different sites, all with differing vegetative characteristics for a period of 1 to 3 days at each site. One of these was a matter of days after harvest thus providing reflection from a bare soil. Unfortunately, due to instrument failure, measurements from this site were found to be erroneous. At another site, the reflection coefficient was measured a few weeks after the crop was harvested with ratooning commencing. The remaining two of the four, had a full vegetative canopy. The difference between these two was the colour and density of the crop surface. The three sites at which reliable reflection coefficient measurements took place will be discussed.

3.2.3.1 Reflection coefficient: site 1

Figure 3.5 shows the reflection coeffcient being measured over a dense green sugarcane crop. The density of a sugarcane crop is closely related to yield and a dense crop as shown in Figure 3.5 would yield approximately 90 tons per hectare upon harvest. This sugarcane was planted approximately one year prior to the measurements.

Figure 3.5: Reflection coefficient estimation over a dense green sugarcane canopy.

From Figure 3.6, the reflection coefficient measured at this site was high averaging approximately 0.25 (25%) over the three day period of measurements. The effect of the angle of incidence on the reflection coefficient estimates is clearly seen in Figure 3.6 with the least surface reflection occurring at midday when the sun is perpendicular to the land surface.

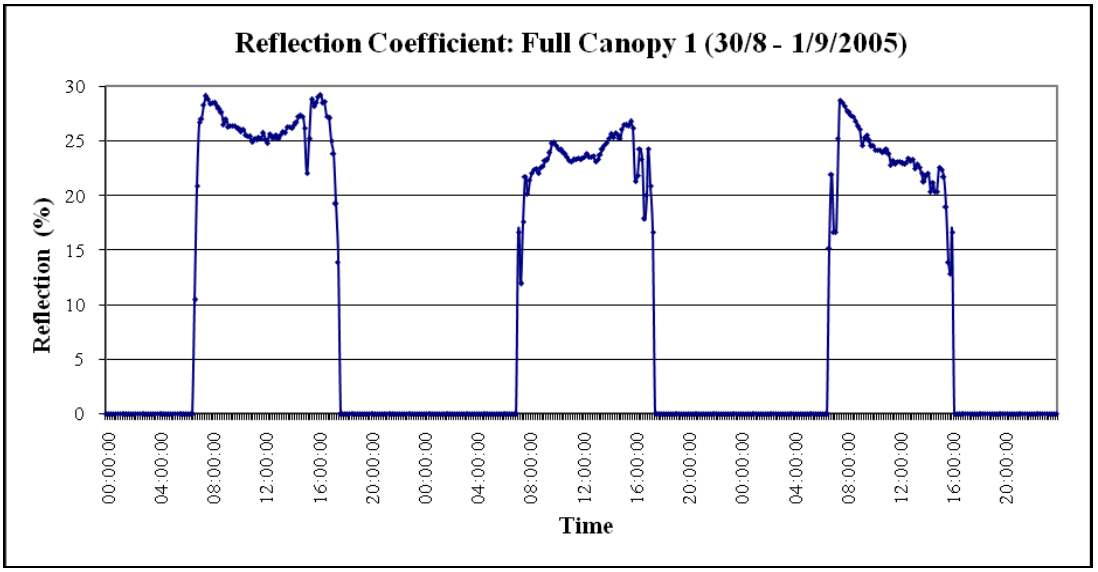

Figure 3.6: Reflection coefficient over a dense green canopy of sugarcane

3.2.3.2 Reflection coefficient: site 2

From Figure 3.7, it is evident that the canopy density for this site is less than that of Figure 3.5. The crop is also drier than that of Figure 3.5 due to the crop being slightly older with evidence of crop senescence. Figure 3.7 thus indicates a lower reflection coefficient measured over a less dense, older crop, which is probably more representative of average sugarcane for the area.

Figure 3.7: Reflection coefficient estimation over a dry sugarcane canopy

One would assume higher reflection from this site when compared to that of Figure 3.5. However, the measured reflection coefficient for this 2 to 3 day period showed a slightly lower reflection coefficient than the sugarcane represented in Figure 3.5. Average reflection coefficient for the measured period was approximately 0.2 (20%) (Figure 3.8). This site would yield approximately 70 tons per hectare upon harvest, which is significantly less than that of Figure 3.5. It can therefore be assumed that reflection coefficient is not only affected by the colour of the crop, but also the density of the crop at the surface.

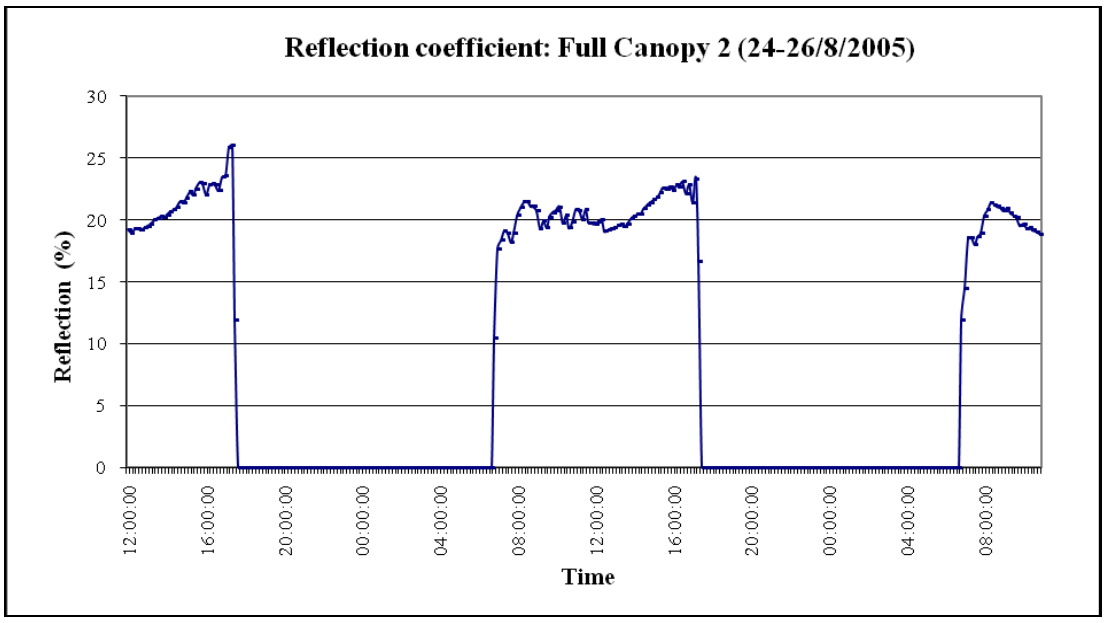

Figure 3.8: Reflection coefficient over a less dense dry sugarcane canopy

3.2.3.3 Reflection coefficient: site 3

A single day's reflection coefficient was measured at a site where harvested sugarcane had been ratooning for approximately 4 to 6 weeks (Figure 3.9).

Figure 3.9: Reflection coefficient estimation over ratooning sugarcane

The result showed an reflection coefficient of approximately 0.13 (13%) as illustrated in Figure 3.10. Thus, for the purposes of the integration of a weighted distribution, a reflection coefficient of 0.1 (10%) will be assumed immediately after harvest. The incident radiation reflection is less evident in Figure 3.10 when compared to that of Figures 3.6 and 3.8 due to there being less surface vegetative cover and an increased proportion of bare soil at the surface.

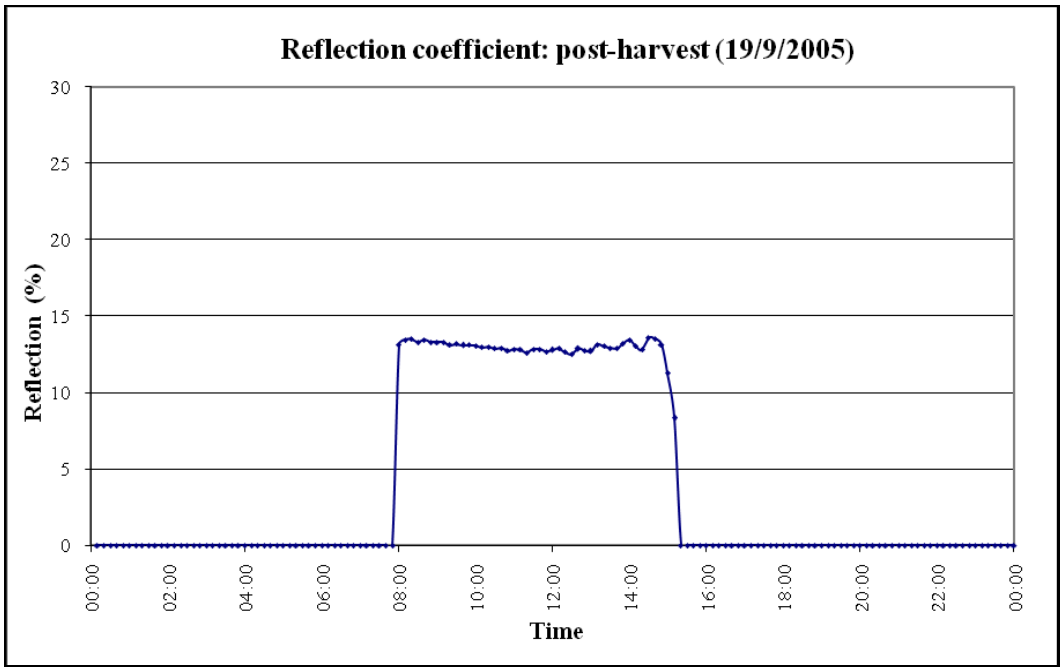

Figure 3.10: Reflection coefficient over harvested sugarcane, after 6 to 8 weeks ratoon growth.

3.2.4 Application of the weighting function

Based on the analysis above it was decided to apply the weighting function to Rn for selected days from July – September 2005 and then compare this weighted Rn distribution to the point source estimate. This was only done from July-September 2005, as this is the period over which significant crop harvesting took place. It is important to note that in this analysis, there were only two vegetative states utilized i.e. full canopy or no canopy. No intermediate stage of growth was selected due to the complexity of incorporating this into the analysis. However, the reflection coefficient immediately after harvest was gradually increased from 0.1 (10%) in July 2005 as ratooning commenced to 0.13 (13%) in September 2005 to incorporate results obtained from Figure 3.10, which had ratooned to a similar vegetative state. It was decided to assign the full canopy with a reflection coefficient of 0.23 (23%) after averaging estimates obtained from Figures 3.6 and 3.8.

Rn for a full canopy was taken from the point source estimate at the CSIR site. With known reflection coefficient estimates for both bare and full canopy conditions, Rn for a bare vegetative condition in this project was estimated using the following equations:

$Rn_{bare} = R_{incoming}$ (1-reflection coefficient $_{bare}$)

$R_{incoming} = Rn_{sugar}$ / (1-reflection coefficient $_{sugar}$)

Therefore: Rn bare = [Rn_{sugar} / (1-reflection coefficient $_{sugar}$)] * (1-reflection coefficient $_{bare}$)

where:

Rn_{bare}= Net radiation for bare vegetative cover

Rn_{sugar} = Net radiation for full canopied vegetative cover

$R_{incoming}$ = Incoming solar radiation at the earth's surface

Reflection coefficient $_{bare}$ = Reflection coefficient for bare vegetative cover

Reflection coefficient $_{sugar}$ = Reflection coefficient for full canopied vegetative cover

These values of Rn_{sugar} and Rn_{bare} were used in calculating the weighted Rn distribution for typical days in July, August and September 2005. For each 400 metre section of the transect, with its attributed weighting function value (0.11 or 11% for section 1, 0.39 or 39% for section 2 etc), the proportion of vegetation present and absent (taken from Table 3.1) was multiplied by the Rn_{sugar} and Rn_{bare} values. This analysis was done quantitatively with Rn represented in $mm.day^{-1}$. The new weighted quantitative estimates for each of the four sections was then summed to provide a weighted daily total for each day analysed as represented in Table 3.2. This method used in the estimation of Rn for both bare and vegetated surfaces could be erroneous due to the incoming and outgoing infrared radiation being neglected, as highlighted in Part 1 Section 2.1.1. Consequently, these results were not used in the estimation of total evaporation, but only to provide a means of comparison between Rn obtained over the riparian area and Rn for the sugarcane crop. As described in more detail in Sections 3.2.5.2 and 3.2.6 all estimates of evaporation reported herein are based on Rn measured using the CSIR net radiometer as described in Part 1 Section 2.1.2.

Table 3.2: Quantitative weighted Rn values ($mm.day^{-1}$) over the transect for one representative day in each month.

Date	0 km-0.4 km	0.4 km-0.8 km	0.8 km-1.2 km	1.2 km-1.6 km	Weighted Total	Point Est.
14/7/2005	0.234	0.884	0.946	0.231	2.295	2.090
6/8/2005	0.402	1.463	1.541	0.391	3.795	3.500
12/9/2005	0.551	2.002	2.100	0.537	5.189	4.820

From Table 3.2, it is evident that the weighted Rn total is slightly higher than the Rn estimated at the point source. This is a result of less reflection of incoming solar radiation

taking place at the surface once the sugarcane had been harvested. The solar radiation available for distribution in the energy balance is thus increased where the reflection coefficient is less. It is important to understand which other energy balance components are affected as a result.

3.2.5 Soil heat flux

Two sets of soil thermometers were installed across the transect. One of these sets was placed under a sugarcane canopy which was assumed to represent average canopy density for the transect. The second set of soil thermometers was placed near the transect centre on 13 July 2005, after the sugarcane had been harvested on 14 June 2005.

3.2.5.1 Comparison of two datasets

Approximately three months of soil heat flux data were obtained from both sites, allowing for a good comparison to be made between heat fluxes under a sugarcane canopy, and the post-harvest site. From Figure 3.11, it is evident that the soil heat fluxes measured at site 2, with no canopy, were significantly higher than those measured at site 1 which had a full canopy. On average, soil heat fluxes were 2.75 times greater where there was no canopy.

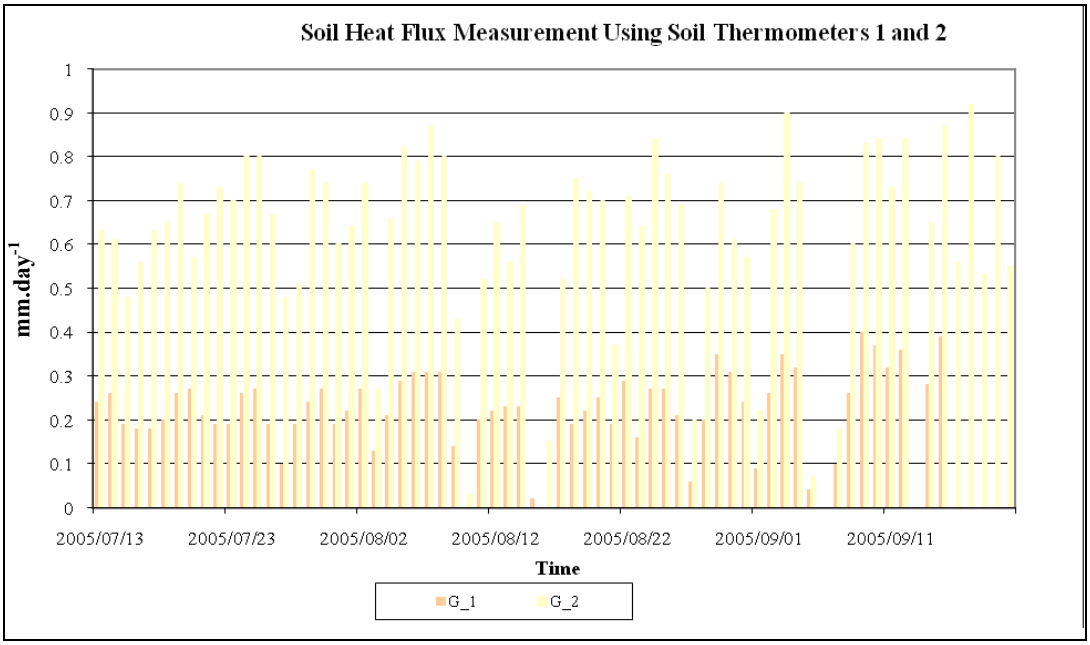

Figure 3.11: Comparison in G using data from soil thermometers from site 1 and 2

3.2.5.2 Weighted distribution

The results presented in Figure 3.11 proved to be useful in adjusting G to incorporate a weighted distribution. This was incorporated in the same manner as Rn. For the same selected days in July, August and September 2005, a quantitative estimate of G, for both full canopy and no canopy was determined. These were then multiplied by the proportion of vegetation present or absent (Table 3.1) for each 400 metre section, and summed together to yield a quantitative weighted distribution for G.

Table 3.3: Quantitative weighted G values ($mm.day^{-1}$) over the transect for one representative day in each month.

Date	0km-0.4km	0.4km-0.8km	0.8km-1.2km	1.2km-1.6km	Total	Point Est.
14/7/2005	0.032	0.170	0.231	0.030	0.463	0.260
6/8/2005	0.054	0.215	0.289	0.039	0.598	0.310
12/9/2005	0.055	0.234	0.309	0.045	0.643	0.360

From Table 3.3, it is evident that the weighted G total are higher than the G estimated at the point source taken from the set of soil thermometers located under the average vegetative canopy. This is a result of less energy reaching the soil surface and thus available to contribution to the energy balance in the form of soil heat flux for the full canopy. Where there is no canopy, more of the incoming solar radiation reaches the soil surface and thus contributes more to the soil heat flux component of the energy balance than under the full canopy.

3.2.6 Summary of the effect of incorporating a weighted distribution

Although only three months (July-September 2005) of soil heat flux estimates were available from both sets of soil thermometers, it must be noted that this was the critical period when sugarcane harvesting took place. Prior to this, localised and a point estimate for both Rn and G respectively is deemed sufficient in the analysis of results, with the whole transect comprising of a full canopy. Table 3.4 provides a summary of the vegetation changes over the transect for one representative day in each month.

Table 3.4: Summary of weighted distribution of energy balance components for the selected days

	Date	0km-0.4km	0.4km-0.8km	0.8km-1.2km	1.2km-1.6km	
Vegetative Cover	Oct 2004 - April 2005	100%	100%	100%	95%	
	May 2005	100%	100%	55%	95%	
	Jun 2005	100%	100%	40%	95%	
	Jul 2005	90%	50%	5%	96%	
	Aug 2005 - Sep 2005	70%	50%	10%	90%	
H weighting Function		11	39	39	11	**Total (mm.day^{-1})**
H Weighted Distribution	14 July 2005	0.122	0.433	0.433	0.122	1.110
G Weighted Distribution	14 July 2005	0.032	0.170	0.231	0.030	0.463
Rn Weighted Distribution	14 July 2005	0.234	0.884	0.946	0.231	2.295
LvE Weighted Distribution	14 July 2005	0.079	0.281	0.282	0.079	0.722
H Weighted Distribution	06 August 2005	0.185	0.655	0.655	0.185	1.680
G Weighted Distribution	06 August 2005	0.054	0.215	0.289	0.039	0.598
Rn Weighted Distribution	06 August 2005	0.402	1.463	1.541	0.391	3.795
LvE Weighted Distribution	06 August 2005	0.162	0.593	0.596	0.166	1.517
H Weighted Distribution	12 September 2005	0.211	0.749	0.749	0.211	1.920
G Weighted Distribution	12 September 2005	0.055	0.234	0.309	0.045	0.643
Rn Weighted Distribution	12 September 2005	0.551	2.002	2.100	0.537	5.189
LvE Weighted Distribution	12 September 2005	0.284	1.019	1.042	0.281	2.626

The incorporation of a weighted distribution of Rn and G results in an increased estimate of these two, relative to the point measurements. The weighted distribution function has also been applied to the estimates of H. These new estimates for the three selected days have thus been used to assess the significance of any changes to LvE. Table 3.5 illustrates the difference in LvE estimates calculated using Rn and G from both point and weighted values. Although Rn and G were both higher for the weighted distribution, their relative increases are similar. It is apparent that the effect which the increases have on LvE is negligible. Table 3.5 indicates that the greatest difference between the two occurred on 12 September 2005, with a difference of 0.076 mm.

Table 3.5: Comparison between LvE from weighted distribution and point source

Date	Total Weighted (mm.day^{-1})	Total Point Est. (mm.day^{-1})
14 July 2005	0.722	0.720
06 August 2005	1.517	1.510
12 September 2005	2.626	2.550

Based on the 3 selected days, it can be concluded that the difference between analysis based on weighted and point source estimates on LvE, are insignificant. Thus, in the further analysis of results, point source estimates of Rn and G have been used.

3.3 Monthly Data Analysis

In this Section, data and results for each of the months analysed are presented.

3.3.1 October 2004

A major problem encountered in October 2004 was a lack of soil heat flux data. However, a number of days with good net radiation and sensible heat data were available. Thus it was decided to average the daily soil heat fluxes totals obtained from November 2004 and September 2005 in the analysis of the data for October 2004. This was done so as to make use of the available net radiation and sensible heat flux data and thereby provide a full year of data from October 2004 through to September 2005. Each day in October 2004 therefore has the same soil heat flux estimate (0.29 $mm.day^{-1}$). This is based on an assumption that the contribution of soil heat to the energy balance is relatively small for this month.

Table 3.6: Summary of analysed data for October 2004

Date	LvE (mm)	Rn (mm)	G (mm)	H (mm)	Rainfall (mm)
2004/10/08	0.41	1.69	0.29	0.99	2.6
2004/10/09	3.01	7.09	0.29	3.78	0.2
2004/10/10	0.21	4.45	0.29	3.96	0.2
2004/10/11	0.12	2.75	0.29	2.34	1.2
2004/10/12	0.70	3.90	0.29	2.91	0.8
2004/10/13	0.71	3.40	0.29	2.40	1.2
2004/10/14	2.70	6.43	0.29	3.44	0.4
2004/10/15	2.66	6.59	0.29	3.64	0.0
2004/10/16	2.17	6.49	0.29	4.03	0.0
2004/10/17	1.73	6.07	0.29	4.04	10.6
Average	**1.442**	**4.886**	**0.29**	**3.153**	**1.72**

Unfortunately, no primary data from the AWS was available for this period to aid in the interpretation of results. It is, however, evident from Table 3.6 as well as Figure 3.12 that the sensible heat component (H) contributes significantly to the energy balance. Over the tabulated duration, averaged sensible heat comprises approximately 65% of averaged net radiation with averaged latent heat comprising a mere 30% of average net radiation. This is assumed to be as a result of a lack in soil water content limiting the latent heat contribution. Unfortunately soil water content measurements are not available to October 2004 to verify

this assumption. From Table 3.6 however, it is evident that minimal rainfall occurred over this period.

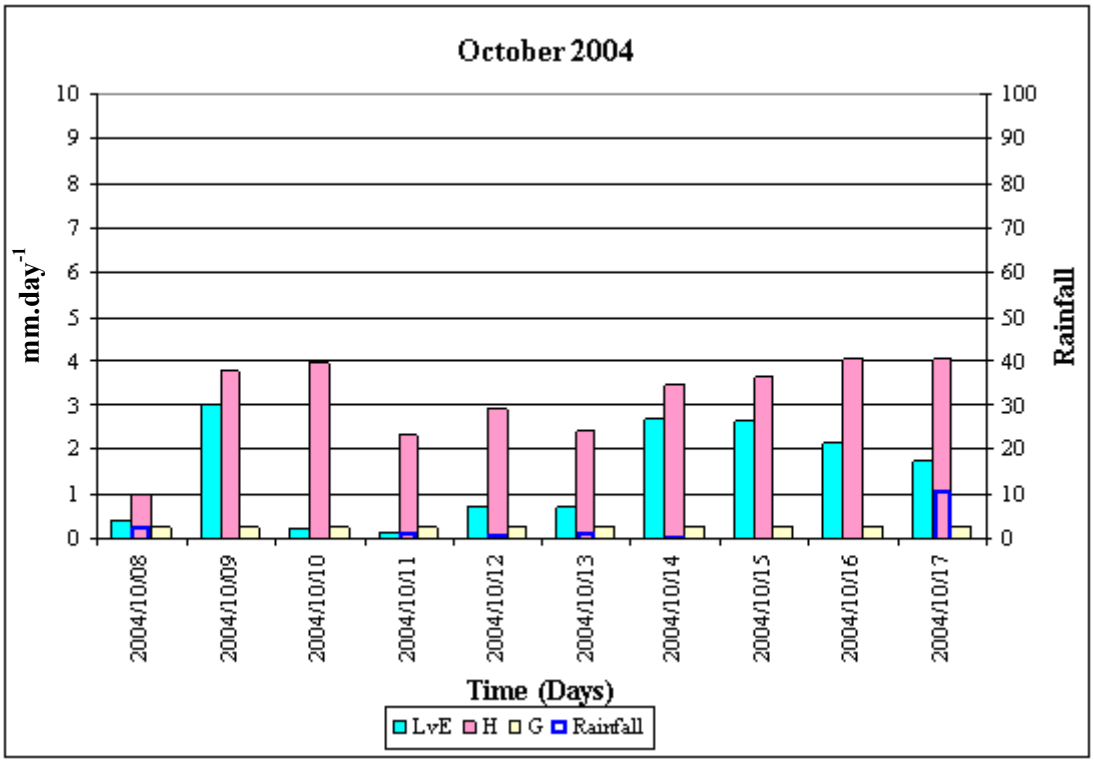

Figure 3.12: Daily summary of energy balance components from 8 to 17 October 2004

Figure 3.12 and Table 3.6 show that there is a significant amount of energy available in the form of net radiation. For the tabulated duration, the quantitative average estimate of net radiation is 4.89 mm.day^{-1}.

3.3.2 November 2004

18 days in November 2004 were analysed and a number of differences were noted when compared to October 2004.

Table 3.7: Summary of analysed data for November 2004

Date	Ta (^{o}C)	RH (%)	LvE (mm)	Rn (mm)	G (mm)	H (mm)	Rainfall (mm)
2004/11/11	16.12	101.30	0.48	1.90	0.16	1.26	0.2
2004/11/12	28.20	45.94	3.34	6.67	0.65	2.67	0.0
2004/11/13	30.88	26.90	3.07	7.24	0.55	3.61	0.0
2004/11/14	21.50	80.20	0.89	2.62	0.03	1.73	0.2
2004/11/15	20.41	83.80	1.52	5.84	0.29	4.03	0.0
2004/11/16	20.35	83.00	1.18	7.47	0.36	5.93	0.2
2004/11/17	31.79	31.13	2.84	7.33	0.68	3.81	0.2
2004/11/18	29.29	49.42	2.01	5.87	0.41	3.44	0.0
2004/11/19	27.80	58.57	1.56	6.62	0.28	4.78	85.2
2004/11/20	28.66	49.43	2.22	7.14	0.52	4.40	8.0
2004/11/21	23.21	64.63	0.38	1.22	0.03	0.81	5.0
2004/11/22	12.60	100.70	0.75	1.36	-0.21	0.81	15.2
2004/11/23	18.95	81.80	NA	NA	NA	NA	18.8
2004/11/24	17.43	83.10	2.18	4.56	0.31	2.07	5.2
2004/11/25	29.90	26.11	4.81	7.77	0.65	2.31	0.2
2004/11/26	22.56	72.70	2.10	5.63	0.34	3.19	2.4
2004/11/27	25.73	67.26	1.67	5.63	0.31	NA	4.2
2004/11/28	27.78	47.28	4.39	6.56	0.55	1.62	6.0
2004/11/29	26.73	46.65	3.68	5.14	0.48	0.98	2.0
Average	**24.20**	**63.15**	**2.17**	**5.37**	**0.36**	**2.79**	**8.05**

Incoming energy in the form of net radiation increased relative to October 2004 reaching a maximum quantitative estimate of 7.77 mm on November 25. Average net radiation average increased from 4.89 mm.day^{-1} in October to 5.37 mm.day^{-1} in November. This is a result of an increased energy as mid summer approaches. A large rainfall event (85.2mm) occurred on the 19 November with a number of smaller events occurring thereafter. This contributed to an increased soil water content (Figure 3.1), and therefore an increased latent heat flux contribution to the energy balance. Quantitative average daily latent heat increased from 1.44 mm.day^{-1} in October to 2.17 mm.day^{-1} in November. The sensible heat flux contribution on the other hand decreased from 3.15 mm.day^{-1} in October to 2.79 mm.day^{-1} in November. It is suggested that this shift from sensible heat to latent heat was brought about by increased soil

water content. This is supported by Figure 3.1 which illustrates the increase in soil water content following rainfall over this period.

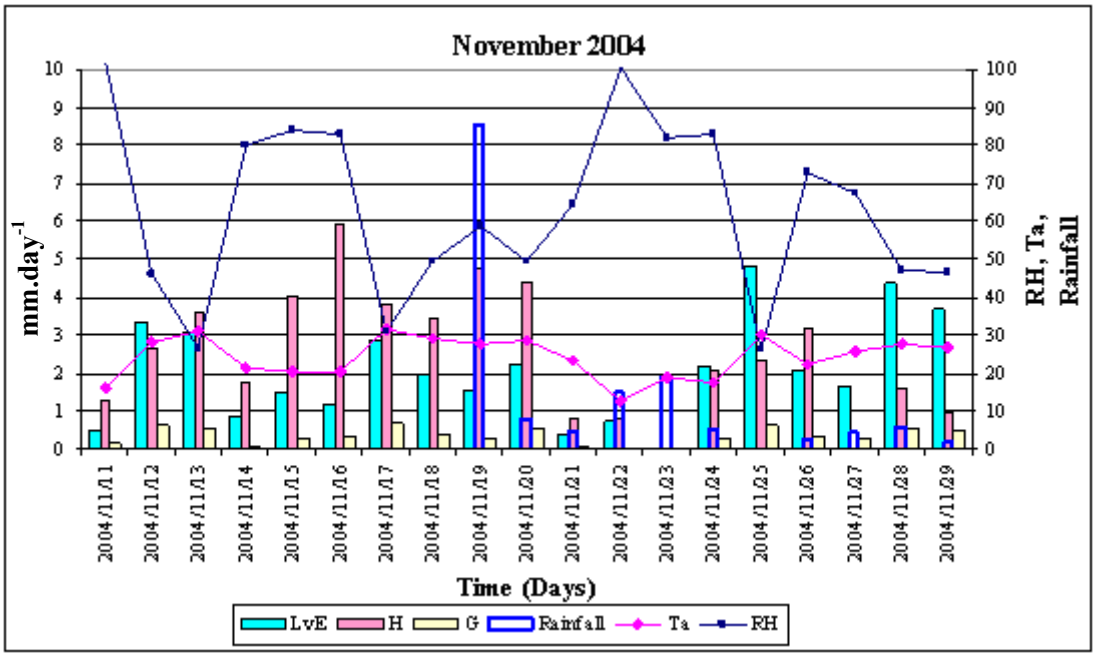

Figure 3.13: Daily summary of energy balance components from 11 to 29 November 2004

From Figure 3.13, the significance of soil water content brought about by rainfall, is evident. There is a definite shift in the contribution of the energy balance components from sensible heat to latent heat following rainfall. Eighty five mm of rain fell on the 19 November which is assumed to have provided a significant amount of moisture to the soil profile illustrated in Figure 3.1. This allowed for increased evaporation from the surface as well as crop transpiration and resulted in large amounts of total evaporation on days such as 25, 28 and 29 November. Relative humidity and air temperature were also conducive to high total evaporative losses on these days. The effect of air temperature and relative humidity on total evaporation should not be overlooked.

Analysis of Figures 3.14 and 3.15 shows that total evaporation, as expected, is closely correlated with net radiation, air temperature and the inverse of relative humidity.

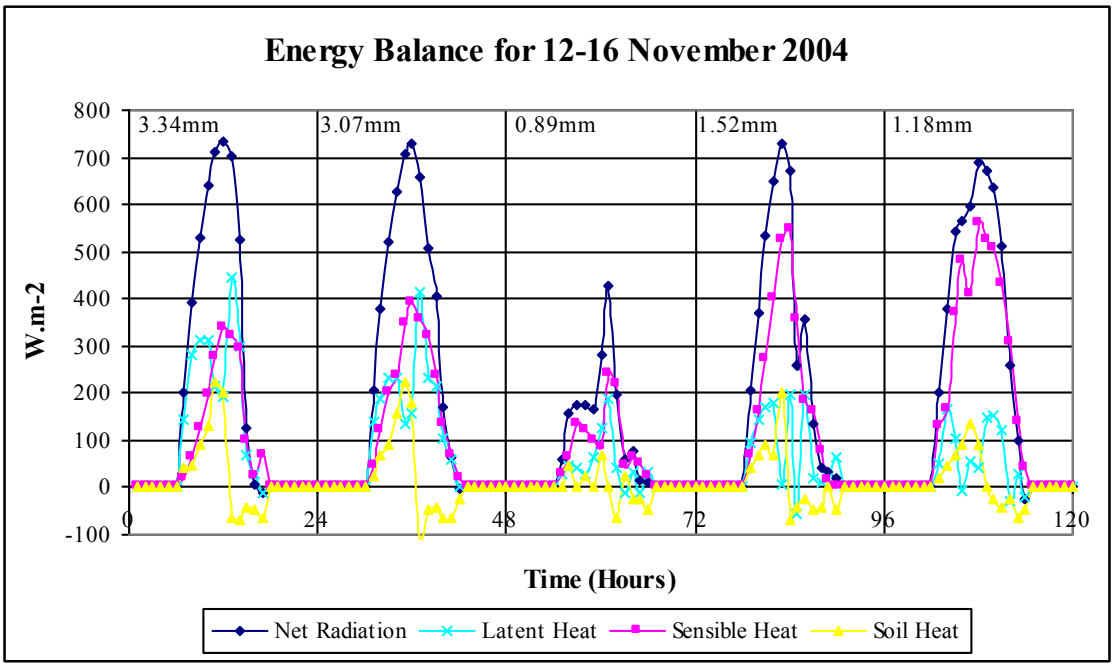

Figure 3.14: Energy balance components for 12 to 16 November 2004. Figures at the top represent daily Et estimates in mm.day^{-1}

The distribution of energy amongst the energy balance components for the period 12 -16 November in energy terms of Watts per square metre (W.m^{-2}) is illustrated in Figure 3.14. The area under the latent heat flux curve was integrated to provide the daily total evaporation indicated on the Figure. For the period 12-16 November the highest total evaporation estimates are 3.34 and 3.07 mm.day^{-1} (12 and 13 November 2004 respectively). These days also record the highest air temperatures (approximately 31^{o}C) and lowest relative humidity (approximately 30%) as illustrated by Figure 3.15.

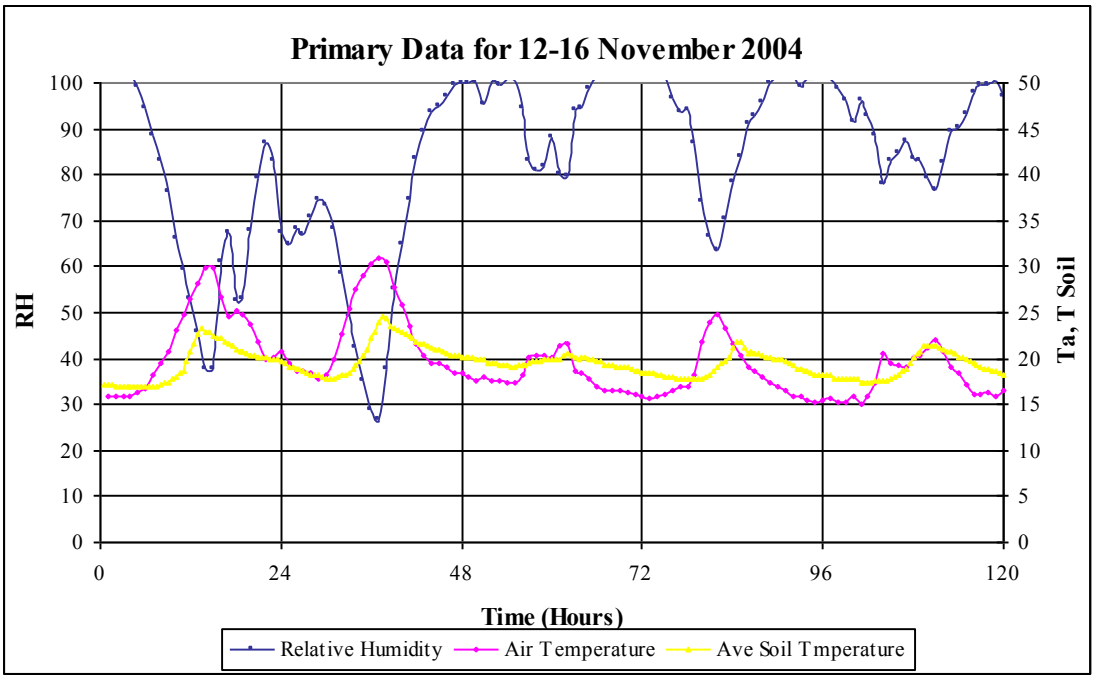

Figure 3.15: Primary data plots for 12 to 16 November 2004

Only 73 mm of rain had fallen by this stage since the start of October 2004 (Figure 3.1). From Figure 3.14 it can be seen that the sensible heat flux component forms a significant portion of net radiation possibly attributed to an assumed lack of soil water content in the profile and hence the inability to meet the atmospheric demand in the form of latent heat. On 12 and 13 November, the latent component is noticeably higher than 14-16 November due to the lack in atmospheric moisture as shown by the low relative humidity values shown in Figure 3.15. Thus it is concluded that the combination of high air temperature and low relative humidity resulted in this higher proportion of latent heat. These trends are evident in Table 3.7. Soil heat flux on these days was significant, reaching values of 200 $W.m^{-2}$. This can be attributed to the lack of soil water content reducing the evaporative cooling effect. The result is a large range of average soil temperature as shown by the change in average soil temperature in Figure 3.15. The rapid decline in soil heat flux after the peak in the afternoon occurs when the soil begins to radiate more heat than it receives from solar radiation and hence a negative flux is recorded.

3.3.3 December 2004

In December 2004, only 7 days were analysed. This was due to a lack in soil heat flux data from 7 December 2004 until 19 January 2005. This lack in data resulted as a consequence of a problem experienced with the Hobo soil thermometer logger. The scintillometer was also removed for security reasons from December 20, 2004 until January 19, 2005. However, sufficient days in December were analysed for trends to be evident.

Table 3.8: Summary of analysed data for December 2004

Date	Ta (^{o}C)	RH (%)	LvE (mm)	Rn (mm)	G (mm)	H (mm)	Rainfall (mm)
2004/12/01	26.95	50.43	3.48	5.54	0.58	1.48	0.2
2004/12/02	22.48	73.70	1.43	4.77	0.35	2.99	0.0
2004/12/03	28.64	45.12	3.09	7.61	0.76	3.76	0.0
2004/12/04	32.06	31.83	4.14	7.24	0.66	2.44	0.0
2004/12/05	32.01	35.06	NA	NA	NA	NA	13.4
2004/12/06	29.47	42.18	2.27	4.92	0.38	2.27	49.6
2004/12/07	22.18	78.40	1.17	1.46	0.07	0.22	27.4
Average	**27.68**	**50.96**	**2.60**	**5.26**	**0.47**	**2.19**	**12.94**

There are noticeable changes from November brought about by the increased air temperature and increased soil water content resulting from increased rainfall. Average air temperature for the analysed period in December was 27.68 degrees which is significantly higher than the average for November which was 24.2 degrees. Quantitative average net radiation for the tabulated duration in December is 5.26 mm.day^{-1} which is similar to that experienced in November (5.37 mm.day^{-1}). The proportion of the energy balance met by the latent heat flux component is however, higher, averaging 2.6 mm.day^{-1} in December as opposed to a 2.17 mm.day^{-1} in November. Sensible heat flux has been reduced from 2.79 mm.day^{-1} in November to 1.88 mm.day^{-1} in December. Soil heat flux has increased slightly from 0.36 mm.day^{-1} in November, to 0.4 mm.day^{-1} in December. Significant rainfall events occurred from the 5-7 December (Figure 3.16). The effect of this rainfall on the energy balance is not evident due to a shortage of energy balance data after this period.

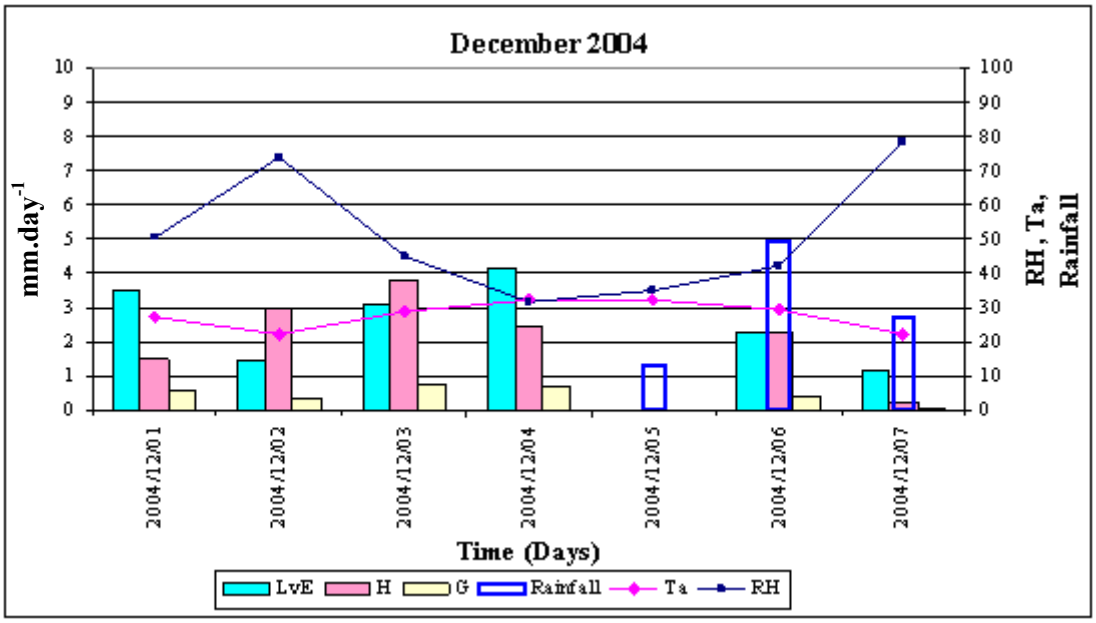

Figure 3.16: Daily summary of energy balance components from 1 to 7 December 2004

Total evaporation reached a maximum on 4 December (4.14mm) for this period. Figure 3.17 shows that the maximum net radiation for 1-4 December 2004 was very similar to that of 12-16 November 2004 (Figure 3.14), with similar relative humidity. The sensible heat flux contributions are lower in December than in November. Latent heat flux on the other hand was higher in December than in November. This increase in total evaporation is a result of increasing soil water content as confirmed by Figure 3.1 with good rain falling in late November resulting in increased soil water content content. Soil heat flux is also very high over this period reaching over 200 $W.m^{-2}$. According to Figure 3.17, the lowest total evaporation occurred on 2 December (1.43mm). On this particular day, relative humidity dropped to approximately 75% at mid day. Air temperatures remained low reaching a maximum of approximately 23^{o}C. This low air temperature resulted in a low average soil temperature and hence a low soil heat flux contribution (0.35mm) i.e. the combination of a high relative humidity and low air temperatures reduces the latent heat flux contribution to the energy balance.

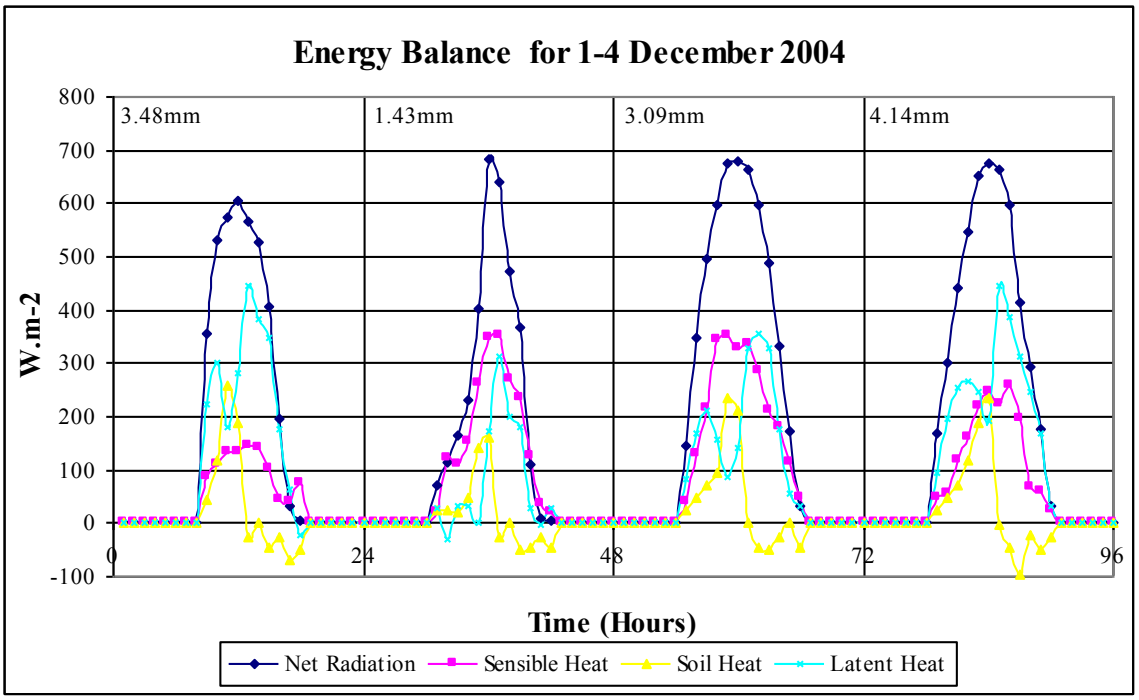

Figure 3.17: Energy balance components for 1 to 4 December 2004. Figures at the top represent daily Et estimates in mm.day^{-1}

According to Table 3.8, the maximum total evaporation over the 7 day period was 4.14mm and occurred on a day when the temperature was 32.06^{o}C day. Examination of data obtained from the AWS showed that there were other days in December which experienced similar maximum air temperatures and relative humidity. It is therefore suggested that this value of 4.14 mm.day^{-1} could have been exceeded in the period when no measurements were available, especially since soil water content is likely to increase after rainfall events during the month, resulting in an increased contribution of latent heat to the energy balance.

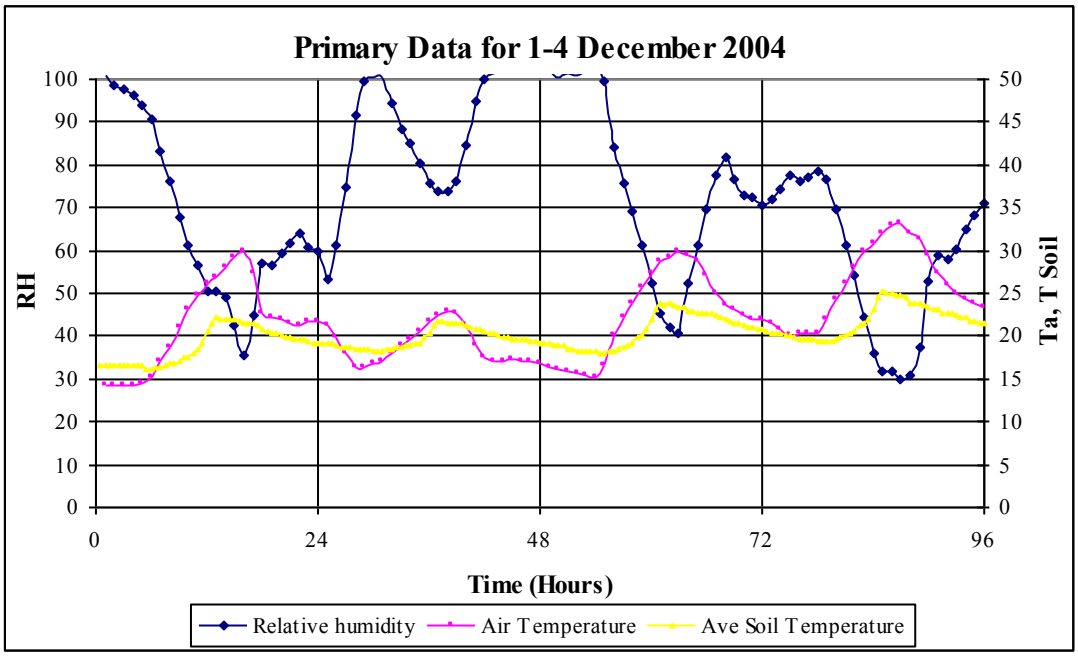

Figure 3.18: Primary data plots for 1 to 4 December 2004

3.3.4 January 2005

Due to security reasons the Scintillometer was removed over the festive season and returned in mid January. This resulted in a shortage of sensible heat flux data for early January. Only 8 days were analysed in January. This is unfortunate, especially since these days are not considered to be very representative of climatic conditions for this time of year. Some interesting results were obtained even though there was a shortage of data for this period. It is unfortunate that limited data are available for this period as this is a key period for this research.

Table 3.9: Summary of analysed data for January 2005

Date	Ta (°C)	RH (%)	LvE (mm)	Rn (mm)	G (mm)	H (mm)	Rainfall (mm)
2005/01/19	24.27	64.09	1.80	2.75	-0.17	1.12	0.2
2005/01/20	26.00	65.46	4.05	6.66	0.39	2.21	3.8
2005/01/21	19.06	88.90	2.64	3.44	0.11	0.69	14.6
2005/01/22	21.92	90.70	2.22	5.20	0.26	2.72	1.8
2005/01/23	17.94	103.30	0.95	1.10	-0.11	0.27	6.6
2005/01/24	21.97	78.90	2.30	5.74	0.37	3.06	2.2
2005/01/25	21.71	92.40	1.65	3.43	0	1.78	4.6
2005/01/26	17.03	99.30	0.60	1.21	-0.07	0.69	6.2
Average	**21.24**	**85.38**	**2.03**	**3.69**	**0.10**	**1.57**	**5.00**

Average air temperatures for January represented in Table 3.9 were lower than expected for this time of year. The analysed days are therefore thought to be cooler than the average in January, reaching a maximum air temperature of only 26°C, at 1pm on 20 January 2005. Using the daily maximum measured air temperature from the site, the analysed days in Table 3.9 from 19-26 January 2005 averaged 23.8 °C. The daily maximum measured air temperature from the site for 1-8 January 2005 for example, was 27 °C. This is a significant difference in air temperature.

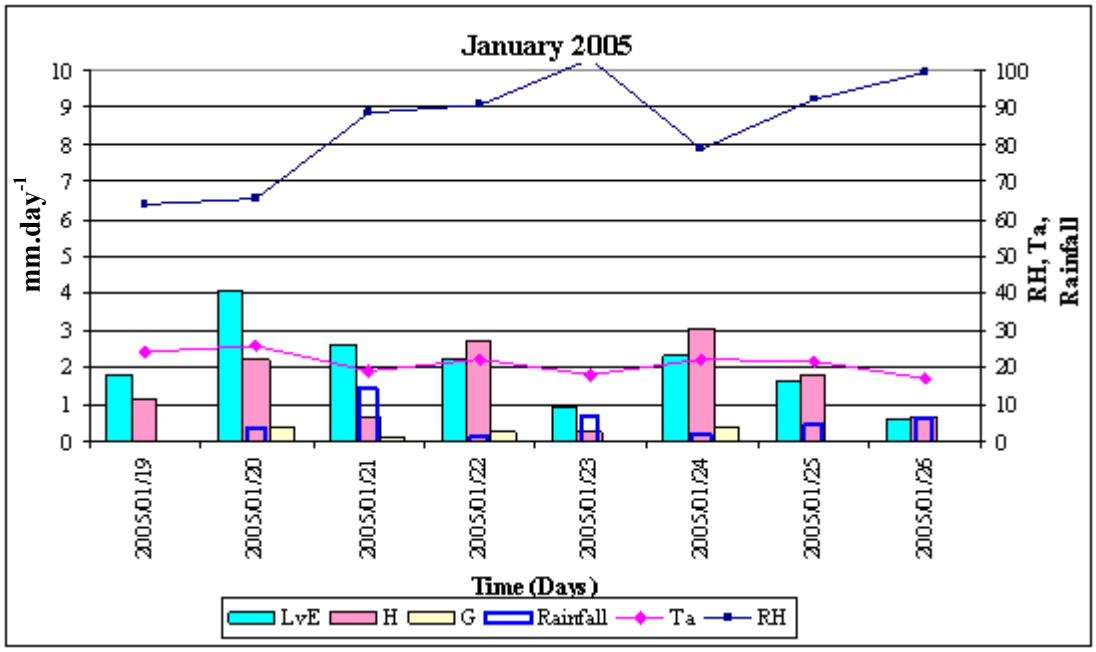

Figure 3.19: Daily summary of energy balance components from 19 to 26 January 2005

Good rains occurred in January and contributed to an increase in soil water content (Figure 3.1) and therefore the major limit to total evaporation for the tabulated period is considered to be incoming radiation. Figure 3.19 indicates the significant proportional contribution the latent component has made to the energy balance. However, there is a reasonable sensible heat contribution showing that radiation is not entirely limiting. Soil heat flux is much lower than it was for November and December indicating that the cooling effect of evaporation from the soil and crop. Soil heat flux reached a maximum of approximately 100 $W.m^{-2}$. The low range in diurnal air temperatures could possibly also contribute to the low range in diurnal average soil temperatures illustrated in Figure 3.21.

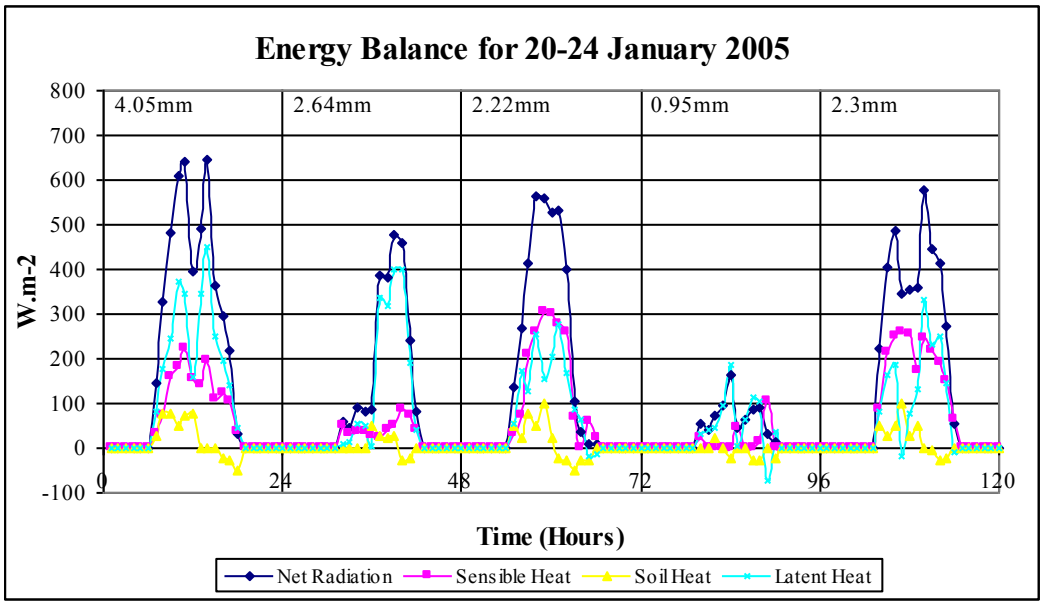

Figure 3.20: Energy balance components for 20 to 24 January 2005. Figures at the top represent daily total evaporation estimates in mm.day^{-1}

These lower temperatures experienced are most likely due to the insulation of clouds with net radiation reaching a maximum of 650 W.m^{-2} on 20 January 2005, and fluctuating throughout the day depending on cloud cover as shown by Figure 3.20. On January 23, the net radiation is well below the daily average for the graphed period, reaching a maximum of only 180 W.m^{-2}.

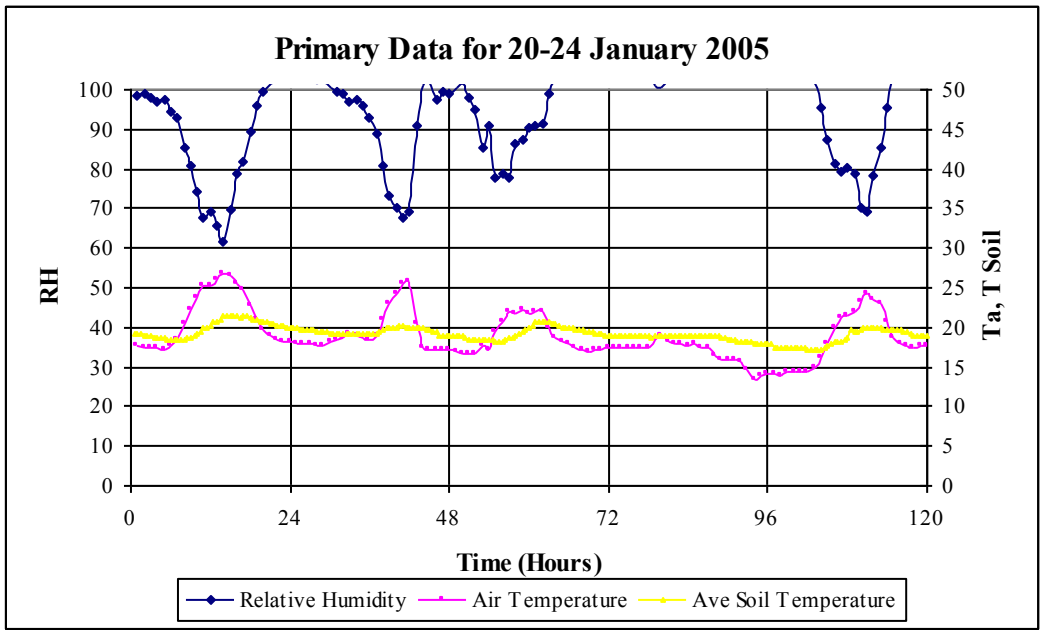

Figure 3.21: Primary data plots for 20 to 24 January 2005.

On 20 January, 4.05 mm evaporated due to the lower relative humidity and higher air temperature, compared to the other days illustrated by Figure 3.21. It is likely that evaporation for a specific day at this time of the year could be significantly higher than this if air temperature was higher and relative humidity was lower. Air temperature reached just over 26 ^{o}C on 20 January whereas air temperatures reached approximately 31 ^{o}C and 33 ^{o}C for days in November and December 2004 respectively. Relative humidity on 20 January dropped to 60% at midday whereas for days in November and December 2004, relative humidity dropped as low as 30%. Thus, if days with air temperature and relative humidity such as this, had been recorded in January 2005, total evaporation would have been significantly higher than 4.05 mm.day^{-1}.

3.3.5 February 2005

Unfortunately, there are no total evaporation estimates for February. A power surge in the power supplied to the transmitter while the scintillometer was being used at another site, resulted in an internal component of the transmitter malfunctioning. Scintec (Germany) were consulted and the new part was delivered and replaced by March 2005. This unfortunate situation is a major downfall of the data collection aspect for project i.e. a lack of total evaporation estimates over the mid summer period.

3.3.6 March 2005

11 days were analysed in March 2005. After 14 March, soil heat flux estimation was found to be erroneous due to faulty soil thermometers. These 11 days did however, prove to be sufficient for typical values to be obtained.

Table 3.10: Summary of analysed data for March 2005

Date	Ta (^{o}C)	RH (%)	LvE (mm)	Rn (mm)	G (mm)	H (mm)	Rainfall (mm)
2005/03/03	18.90	92.20	0.34	2.29	0.04	1.91	2.2
2005/03/04	19.86	75.60	1.41	3.79	0.18	2.20	1.0
2005/03/05	24.82	58.61	2.49	5.49	0.50	2.50	0.0
2005/03/06	28.43	49.64	3.16	5.50	0.53	1.81	0.0
2005/03/07	20.66	79.20	0.43	1.52	0.04	1.27	6.8
2005/03/08	24.66	62.15	2.02	4.47	0.24	2.45	3.4
2005/03/09	22.00	78.30	NA	NA	0.32	3.08	3.4
2005/03/10	27.07	58.81	2.94	4.21	0.10	1.17	26.2
2005/03/11	13.59	88.40	1.55	2.35	-0.04	0.83	5.4
2005/03/12	19.15	64.08	2.89	6.43	0.39	3.16	0.0
2005/03/13	21.07	72.00	2.14	5.65	0.35	3.15	0.0
2005/03/14	15.60	99.10	0.23	1.06	0.03	0.80	4.4
Average	**21.32**	**73.17**	**1.78**	**3.89**	**0.22**	**2.03**	**4.40**

Within these 11 days, there was a high climatic variability. For example, air temperatures at 1pm varied from as low as 13.59 ^{o}C on 11 March to as high as 28.43^{o}C on 6 March. Average daily total evaporation in the form of latent heat for the month was 1.78mm where the sensible heat contributed over the period was 2.03mm. It is assumed that as conditions dry out, the sensible component comprises a correspondingly larger proportion of the energy balance than the latent component.

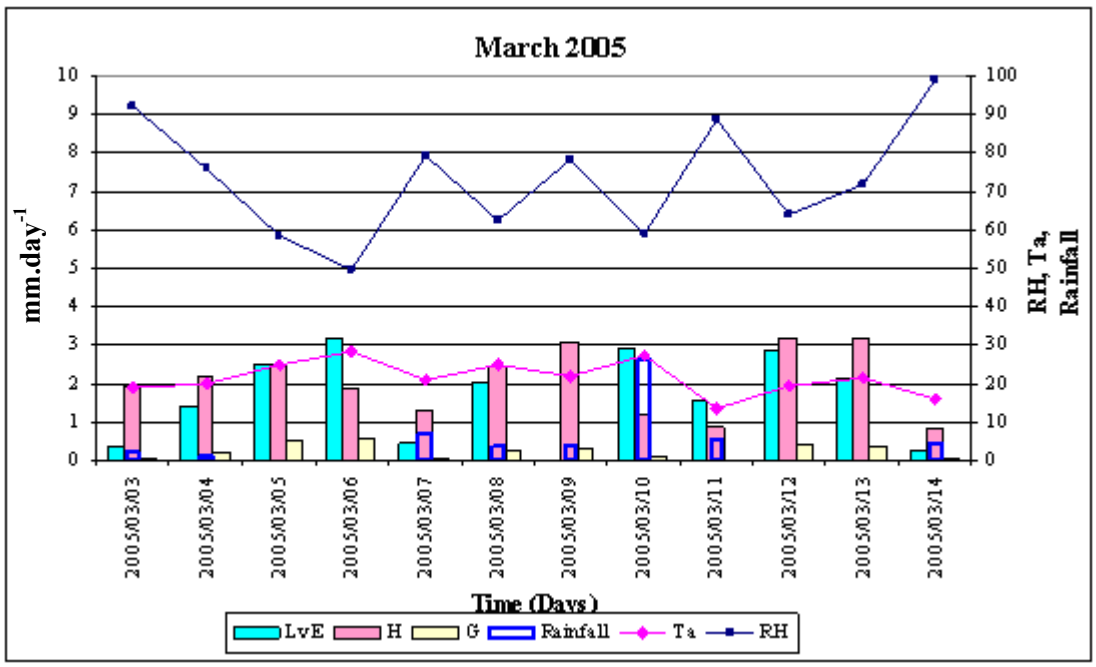

Figure 3.22: Daily summary of energy balance components from 3 to 14 March 2005

A significant amount of rain fell over the analysed period with 26.2mm falling on 10 March (Figure 3.22). This autumn rainfall following good summer rainfall allowed for good crop growth well into the drier winter months and hence resulted in a relatively large proportional contribution of latent heat to the energy balance. Air temperature for this period is substantially lower than that of mid-summer. Average air temperature at 1pm for March 2005 was 21.32 ^{o}C, whereas for December 2004 it was 27.68 ^{o}C. Relative humidity for this period was relatively high averaging at 73.17 % at 1pm, possibly limiting total evaporation.

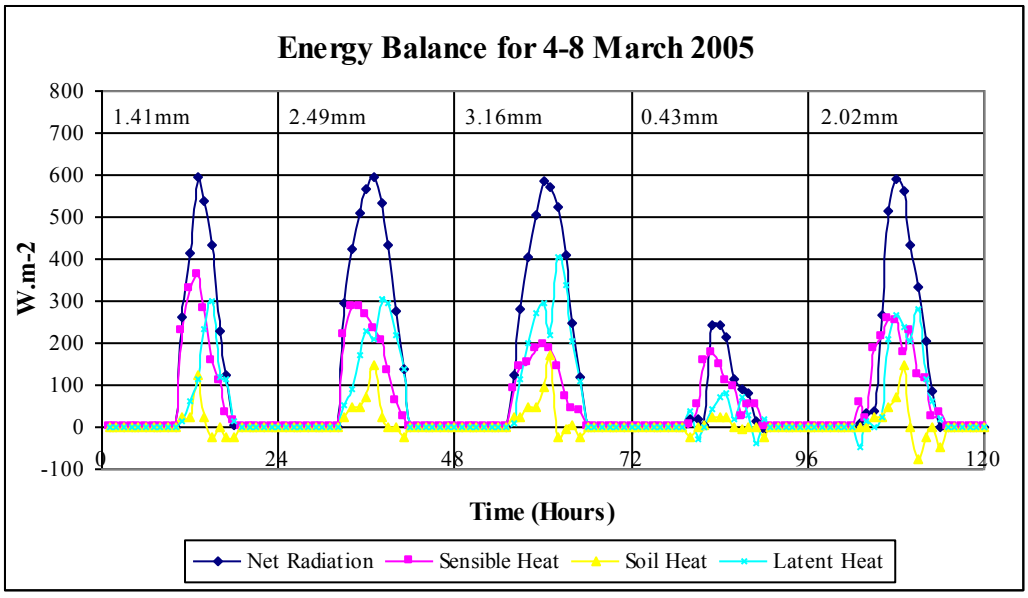

Figure 3.23: Energy balance components for 4 to 8 March 2005. Figures at the top represent daily total evaporation estimates in mm.day^{-1}

The highest total evaporation estimate for March occurred on March 6 with 3.16mm evaporating. This day also experienced the highest air temperature and lowest relative humidity (Table 3.10) thus contributing to this increase total evaporation.

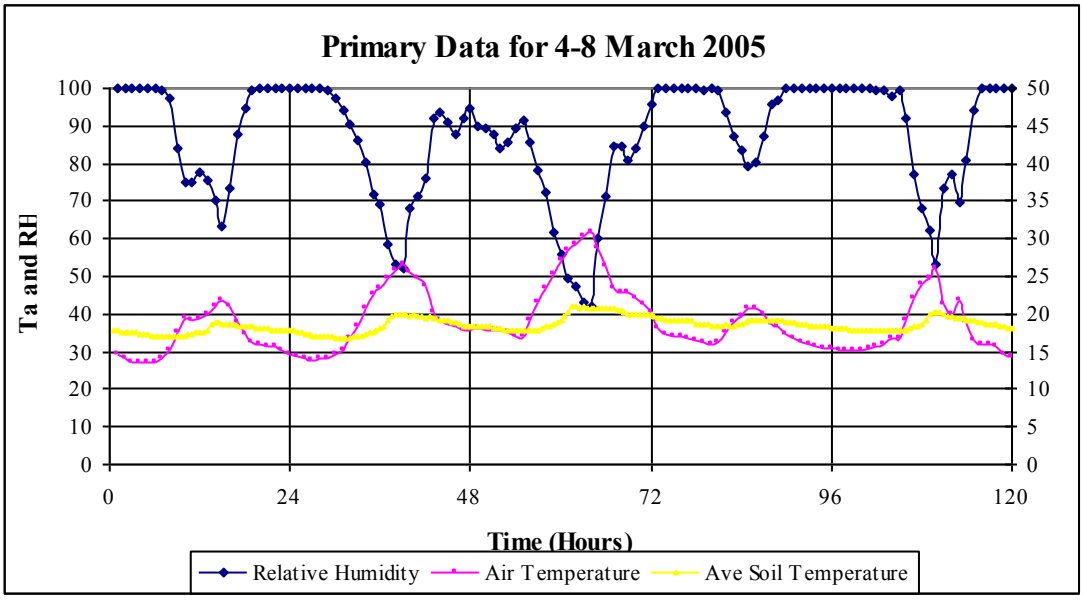

Figure 3.24: Primary data plots for 4 to 8 March 2005.

Total evaporation estimates for March 4-8 (Figure 3.23) are very similar to those obtained for January 20-24 (Figure 3.20). Net radiation reaches a peak of approximately 600 W.m^{-2} as

evident in Figure 3.23. Net radiation was slightly higher for this period in March compared to January due to less cloud cover. This resulted in higher maximum air temperatures than for January and the cooler season resulted in lower minimum air temperatures. This contributed to a higher soil heat flux proportion than experienced in January. The limiting factor to the evaporation process is thus thought to be a combination of both incoming radiation and a drying soil profile for March 2005 as confirmed by soil water content estimates in Figure 3.1.

3.3.7 April 2005

Ten days were analysed in April 2005. Prior to 21 April, soil heat flux data were still erroneous due to faulty soil thermometers. However, from April 2005 until September 2005, the climate variability from day to day is relatively small when compared to the daily variability over the summer period. On April 20, new calibrated soil thermometers were installed as indicated by Table 1.1 of Part 2, and proved to be more reliable than the previous soil thermometers.

Table 3.11: Summary of analysed data for April 2005

Date	Ta (^{o}C)	RH (%)	LvE (mm)	Rn (mm)	G (mm)	H (mm)	Rainfall (mm)
2005/04/21	13.76	88.70	0.18	0.78	0.01	0.58	0.0
2005/04/22	20.90	55.63	2.83	4.30	0.25	1.22	0.0
2005/04/23	21.28	55.95	1.53	2.38	0.18	0.67	0.0
2005/04/24	20.38	64.11	1.76	3.27	0.25	1.26	0.2
2005/04/25	14.83	61.84	1.41	2.82	0.05	1.36	0.2
2005/04/26	11.30	99.30	0.49	1.03	0.03	0.51	1.4
2005/04/27	14.80	75.60	0.65	2.54	0.19	1.70	0.2
2005/04/28	19.41	59.86	1.38	3.85	0.20	2.27	0.0
2005/04/29	17.06	63.58	1.90	3.90	0.20	1.81	0.0
2005/04/30	17.10	68.31	1.40	3.87	0.19	2.28	0.0
Average	**17.08**	**69.29**	**1.35**	**2.87**	**0.16**	**1.37**	**0.20**

Net radiation for this period averaged 2.87 mm per day with a maximum evaporation of 2.83 mm occurring on 22 April. Average daily total evaporation in the form of latent heat for the month was 1.35 mm where the sensible heat contributed over the period was a similar amount (1.37 mm). Soil heat flux contributes an insignificant amount of 0.16 mm on average for the period.

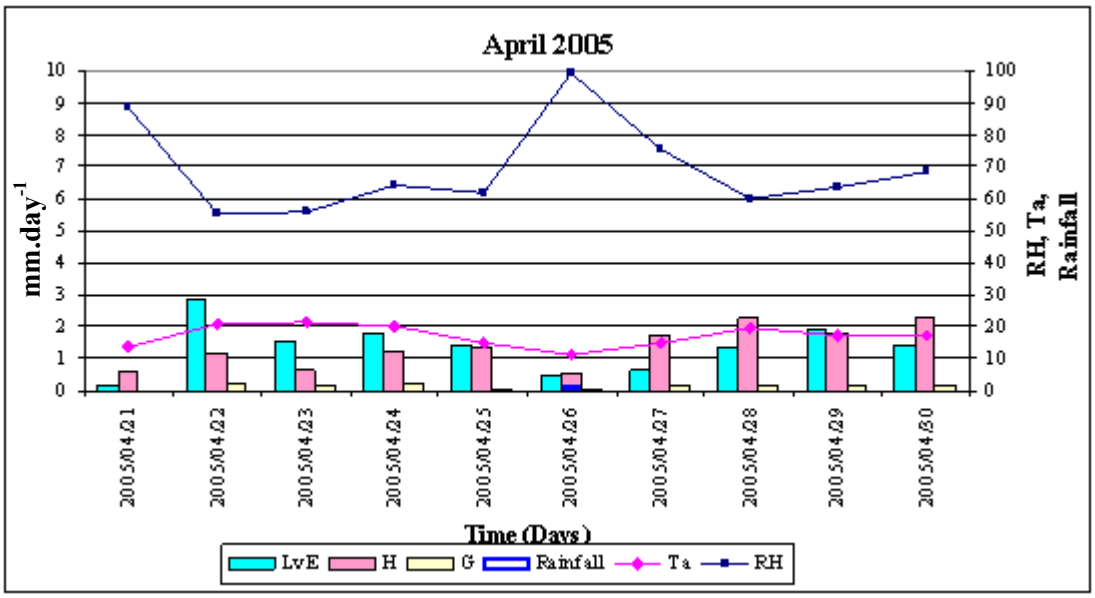

Figure 3.25: Daily summary of energy balance components from 21 to 30 April 2005

As winter approaches, there is a shift to a lower incoming radiation with net radiation reaching a maximum of approximately 500 $W.m^{-2}$ as opposed to over 700 $W.m^{-2}$ in November/December 2004. This has also resulted in lower air temperatures shown in Table 3.11 averaging 17.08°C at 1 pm for the month. The latent component of the energy balance as a proportion of net radiation is still significant indicating that sufficient soil water content is available for the crop to meet much of the atmospheric demand. This is confirmed by the soil water content illustrated in Figure 3.1. This contribution is expected to shift from latent heat to sensible heat as mid winter approaches with a drying out soil profile.

3.3.8 May 2005

From May 2005 until the completion of the fieldwork in September 2005, all equipment functioned well with very few days where data were not available. Where gaps in energy balance data exist, the scintillometer did not produce data due to the atmospheric conditions not being conducive towards measurements. (e.g. 18 to 22 May 2005). This increased data collection allowed for a more representative analysis of data for this period with monthly averages being calculated from significantly more days than the mid-summer months.

Table 3.12: Summary of analysed data for May 2005

Date	Ta (^{o}C)	RH (%)	LvE (mm)	Rn (mm)	G (mm)	H (mm)	Rainfall (mm)
2005/05/01	22.53	36.64	2.50	4.25	0.26	1.49	0.0
2005/05/02	18.80	70.50	0.92	2.88	0.23	1.73	0.0
2005/05/03	20.87	57.89	1.71	3.57	0.22	1.63	0.0
2005/05/04	22.73	45.32	2.18	3.40	0.21	1.01	6.2
2005/05/05	21.06	56.37	3.01	3.85	0.22	0.62	4.2
2005/05/06	23.34	32.70	1.96	3.18	0.21	1.02	0.0
2005/05/07	19.20	51.88	1.98	3.63	0.22	1.42	0.0
2005/05/08	19.90	69.19	1.21	3.52	0.23	2.07	0.2
2005/05/09	22.86	39.41	1.89	3.30	0.21	1.21	0.2
2005/05/10	24.10	39.05	NA	NA	0.11	0.52	0.4
2005/05/11	26.35	27.25	2.10	3.50	0.25	1.15	0.0
2005/05/12	24.74	28.52	2.18	3.52	0.25	1.09	0.0
2005/05/13	24.18	29.94	1.55	3.07	0.23	1.29	0.0
2005/05/14	14.38	92.00	0.22	0.79	0.06	0.52	0.0
2005/05/15	20.52	52.17	2.48	3.42	0.16	0.78	0.2
2005/05/16	19.52	53.78	1.55	3.39	0.18	1.66	0.0
2005/05/17	23.72	26.21	1.70	3.22	NA	NA	0.0
2005/05/18	24.92	20.87	NA	NA	NA	NA	0.0
2005/05/19	16.69	78.90	NA	NA	NA	NA	0.2
2005/05/20	15.48	89.60	NA	NA	NA	NA	1.6
2005/05/21	22.74	50.53	NA	NA	NA	NA	0.2
2005/05/22	22.92	31.30	NA	NA	NA	NA	0.2
2005/05/23	23.75	29.48	1.80	3.14	0.22	1.12	0.0
2005/05/24	8.76	78.10	0.39	0.62	-0.05	0.28	0.2
2005/05/25	15.28	62.84	0.49	2.55	0.21	1.85	0.2
2005/05/26	17.36	51.88	1.74	3.32	0.21	1.37	0.2
2005/05/27	23.05	29.39	1.60	3.11	0.25	1.26	0.0
2005/05/28	17.78	73.40	0.79	2.98	0.21	1.98	0.0
2005/05/29	21.28	47.68	1.65	2.96	0.20	1.10	0.0
2005/05/30	18.32	55.16	1.21	3.08	0.18	1.70	0.0
2005/05/31	18.14	32.33	1.62	3.05	0.16	1.27	0.2
Average	**20.49**	**49.69**	**1.62**	**3.09**	**0.19**	**1.25**	**0.58**

During May 2005, net radiation averaged 3.09mm per day, reaching a peak on 5 May (3.85 mm). The contribution of latent heat to the energy balance proved to be higher than the sensible heat contribution. Average latent heat for the period was 1.62 mm whereas sensible heat was 1.25 mm. Soil heat flux again comprised an insignificant portion of the energy balance. Air temperature is higher than that observed in April 2005, averaging at 20.49 ^{o}C at 1pm.

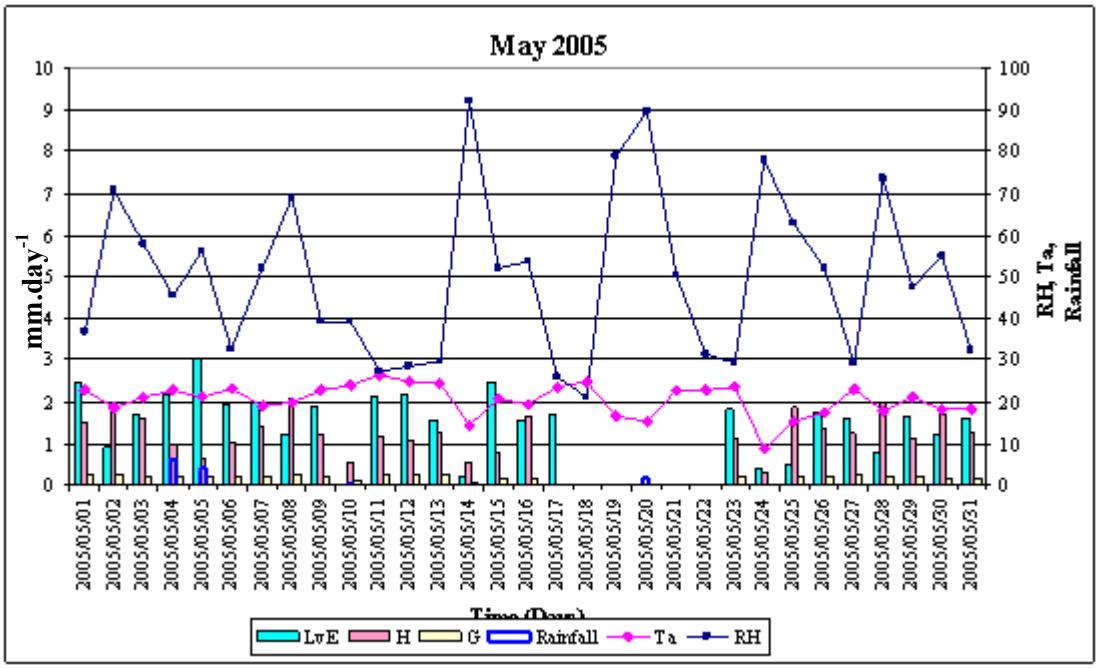

Figure 3.26: Daily summary of energy balance components from 1 to 31 May 2005

Net radiation is low reaching a maximum of approximately 400 $W.m^{-2}$ for the period as the sun is approaching the Southern hemisphere winter solstice. There is thus a lower amount of energy available for distribution amongst the energy balance components. Soil heat flux is low at this stage attributed to lower amounts of energy available to heat the soil compared to the summer months. Moist soils as confirmed by Figure 3.1 which illustrates rainfall and measured soil water content, combined with a lower atmospheric demand in the form of net radiation resulted in the latent flux still comprising a large proportion of the energy balance, even though total evaporation estimates are low. This general trend is once again evident for the plotted period with the highest total evaporation occurring on the days when air temperature is the highest and relative humidity the lowest. Air temperatures are however significantly lower than the summer months with average May temperature around 20.5^{o}C.

3.3.9 June 2005

Data were obtained for June 1 to 30 allowing a more representative analysis of these data.

Table 3.13: Summary of analysed data for June 2005

Date	Ta (^{o}C)	RH (%)	LvE (mm)	Rn (mm)	G (mm)	H (mm)	Rainfall (mm)
2005/06/01	24.61	29.22	1.69	2.84	0.26	0.89	0.0
2005/06/02	23.36	20.82	1.59	2.67	0.22	0.87	0.0
2005/06/03	24.67	20.28	1.19	2.22	0.22	0.82	0.2
2005/06/04	23.81	23.30	1.31	2.66	0.24	1.11	0.2
2005/06/05	14.45	51.52	1.39	2.84	0.11	1.33	0.0
2005/06/06	16.18	51.06	1.33	2.98	0.19	1.47	0.2
2005/06/07	23.58	27.64	1.17	2.39	0.24	0.97	0.0
2005/06/08	25.22	24.21	1.49	2.73	0.23	1.01	0.0
2005/06/09	16.35	72.80	0.71	2.21	0.09	1.41	1.0
2005/06/10	13.48	52.42	0.98	2.56	0.07	1.51	0.2
2005/06/11	19.52	26.71	1.06	2.56	0.19	1.32	0.0
2005/06/12	21.15	35.14	1.61	2.49	0.26	0.63	0.0
2005/06/13	16.09	69.10	1.29	2.51	0.13	1.09	0.0
2005/06/14	18.38	29.45	1.03	2.56	0.16	1.36	0.0
2005/06/15	14.66	46.35	0.95	2.88	0.17	1.76	0.0
2005/06/16	19.94	25.66	1.20	2.71	0.2	1.30	0.2
2005/06/17	19.86	26.63	1.17	2.71	0.23	1.30	0.0
2005/06/18	22.12	20.79	0.99	2.52	0.23	1.30	0.0
2005/06/19	24.74	19.51	1.29	2.30	0.22	0.79	0.0
2005/06/20	15.73	68.39	0.57	2.07	0.15	1.34	0.0
2005/06/21	13.79	87.70	NA	NA	0.11	1.24	8.6
2005/06/22	12.17	99.60	0.33	1.06	0.1	0.64	5.0
2005/06/23	17.08	62.60	2.07	3.01	0.15	0.79	0.2
2005/06/24	18.23	51.54	1.83	2.86	0.18	0.84	0.2
2005/06/25	21.25	33.33	1.48	2.83	0.22	1.13	0.0
2005/06/26	22.07	25.80	1.02	1.98	0.21	0.76	0.0
2005/06/27	20.27	36.41	1.30	2.78	0.19	1.28	0.0
2005/06/28	8.87	77.90	0.21	0.60	0.02	0.37	0.2
2005/06/29	17.11	48.30	1.69	2.98	0.19	1.10	0.0
2005/06/30	22.70	24.14	1.54	2.82	0.22	1.06	0.0
Average	**19.05**	**42.94**	**1.22**	**2.49**	**0.18**	**1.09**	**0.54**

During June 2005, net radiation averaged 2.49mm per day, reaching a peak on 23 June (3.01 mm). The contribution of latent heat to the energy balance once again proved to be higher than the sensible heat contribution. Average latent heat for the period was 1.22 mm whereas average sensible heat was 1.09 mm. Soil heat flux again comprised an insignificant portion of the energy balance averaging 0.18 mm. Air temperature is lower than that observed in May 2005, averaging at 19.05 ^{o}C at 1pm.

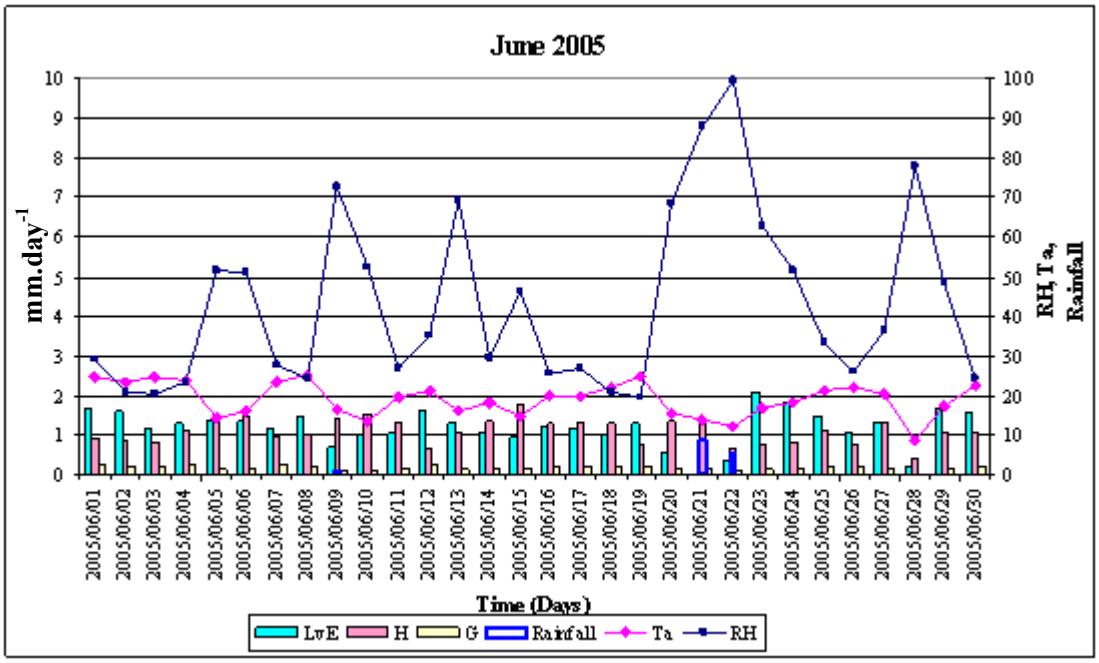

Figure 3.27: Daily summary of energy balance components from 1 to 30 June 2005

Typical net radiation values for June 2005 reached a maximum of approximately 340 $W.m^{-2}$ which is low compared to values of up to 750 $W.m^{-2}$ in November and December 2004.

It is interesting to note that after the rainfall events on 21 and 22 June 2005, there is a definite shift towards an increased proportional contribution of latent heat the energy balance. This is brought about by increased soil water content, clearly evident in the soil water content measurements obtained towards the end of June in Figure 3.2 and 3.3, allowing for a larger portion of the incoming net radiation to be converted into energy of the latent heat form, rather than sensible and soil heat flux forms.

3.3.10 July 2005

A full month's data were obtained in July 2005.

Table 3.14: Summary of analysed data for July 2005

Date	Ta (^{o}C)	RH (%)	LvE (mm)	Rn (mm)	G (mm)	H (mm)	Rainfall (mm)
2005/07/01	14.12	49.30	0.76	2.19	0.10	1.33	0.0
2005/07/02	15.28	46.36	1.23	3.01	0.15	1.63	0.0
2005/07/03	11.14	74.10	0.35	1.38	0.14	0.88	0.0
2005/07/04	13.39	68.39	1.45	2.38	0.15	0.79	0.0
2005/07/05	19.24	41.24	0.95	2.58	0.21	1.42	0.0
2005/07/06	18.04	49.60	0.74	2.42	0.21	1.48	0.0
2005/07/07	16.99	56.06	0.96	2.50	0.19	1.35	0.2
2005/07/08	16.94	47.28	1.20	2.70	0.19	1.32	0.2
2005/07/09	18.75	38.83	1.22	2.78	0.19	1.36	0.2
2005/07/10	22.39	17.86	1.63	3.07	0.24	1.19	0.0
2005/07/11	20.96	20.06	1.00	2.31	0.20	1.11	0.0
2005/07/12	22.74	17.03	1.42	2.95	0.25	1.28	0.0
2005/07/13	22.66	20.29	0.98	2.49	0.24	1.28	0.0
2005/07/14	21.96	20.81	0.72	2.09	0.26	1.11	0.0
2005/07/15	18.62	36.85	0.97	2.46	0.19	1.31	0.4
2005/07/16	15.23	55.60	1.11	2.92	0.18	1.64	0.2
2005/07/17	17.40	50.40	NA	NA	0.18	NA	0.2
2005/07/18	21.15	19.68	1.34	2.89	0.20	1.35	0.0
2005/07/19	23.87	19.03	1.12	2.76	0.26	1.38	0.0
2005/07/20	19.69	26.56	0.80	1.76	0.27	0.69	0.0
2005/07/21	17.65	44.57	0.87	3.17	0.21	2.09	0.0
2005/07/22	17.65	53.56	0.82	3.29	0.19	2.29	0.0
2005/07/23	23.47	27.78	1.34	3.19	0.19	1.66	0.0
2005/07/24	25.47	17.37	1.52	3.26	0.26	1.48	0.0
2005/07/25	28.84	9.18	1.34	3.21	0.27	1.60	0.0
2005/07/26	16.87	61.89	0.54	2.88	0.19	2.15	0.0
2005/07/27	16.88	42.19	1.02	3.32	0.10	2.19	0.2
2005/07/28	15.70	55.97	0.35	2.53	0.19	1.99	0.0
2005/07/29	23.08	22.37	1.48	3.34	0.24	1.62	0.2
2005/07/30	24.34	20.17	1.07	3.24	0.27	1.90	0.0
2005/07/31	17.58	55.44	0.68	3.19	0.19	2.32	0.0
Average	**19.29**	**38.25**	**1.03**	**2.74**	**0.20**	**1.51**	**0.06**

During July 2005, net radiation averaged 2.74 mm per day, reaching a peak on 29 July (3.34 mm). There is a definite shift as the month progresses, towards an increase in energy available in the form of net radiation. This is understandable with the mid-winter solstice having past a month prior to this. The contribution of latent heat to the energy balance is lower than the sensible heat contribution. Average latent heat for the month was 1.03 mm whereas sensible heat was 1.51 mm, which is a significant difference. Soil heat flux again comprised an

insignificant portion of the energy balance, averaging at 0.2 mm. Average air temperature is slightly higher than that observed in June 2005 (19.29^{o}C at 1pm)

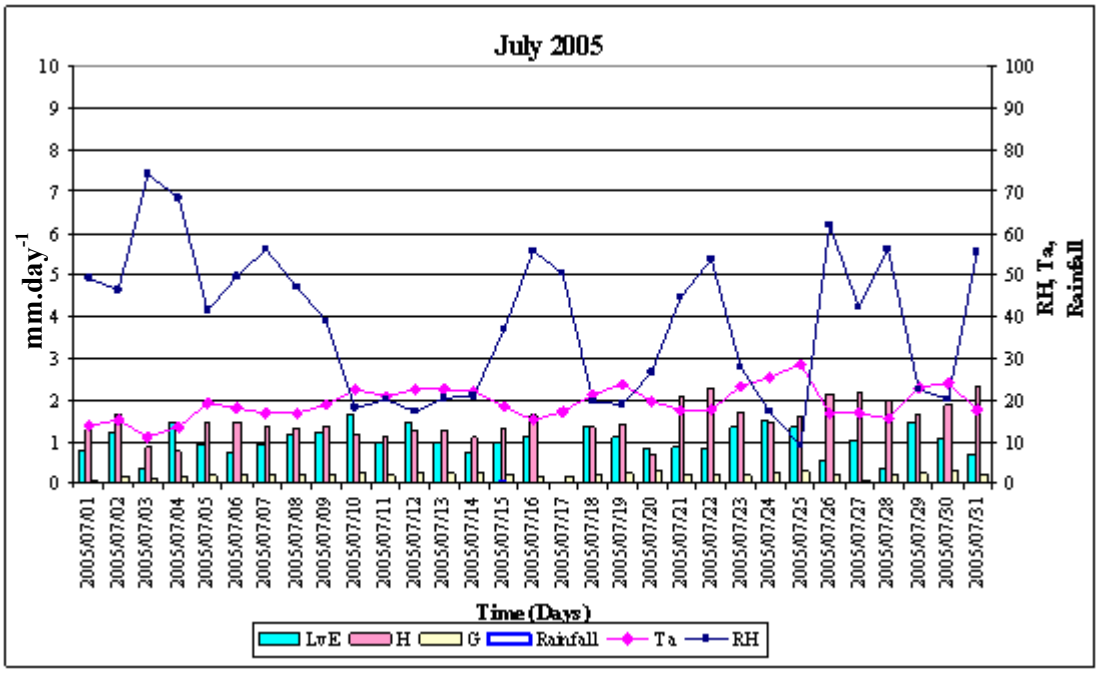

Figure 3.28: Daily summary of energy balance components from 1 to 31 July 2005

From Figure 1.29, it is evident that with the progression of the month, there is a shift towards an increased proportional contribution of sensible heat to the energy balance, relative to the remaining energy balance components. This is closely related to the increased energy available in the form of net radiation as time progressed, as well as the moisture availability within the soil profile. From Figure 1.29 it can be seen that no rain fell during the month of July resulting in a drying soil profile. This is once again confirmed by the decreasing soil water content measured over July in Figure 3.2 and 3.3. Therefore, the increase in net radiation was unable to be met by energy in the latent form and was thus met by energy in the form of sensible heat.

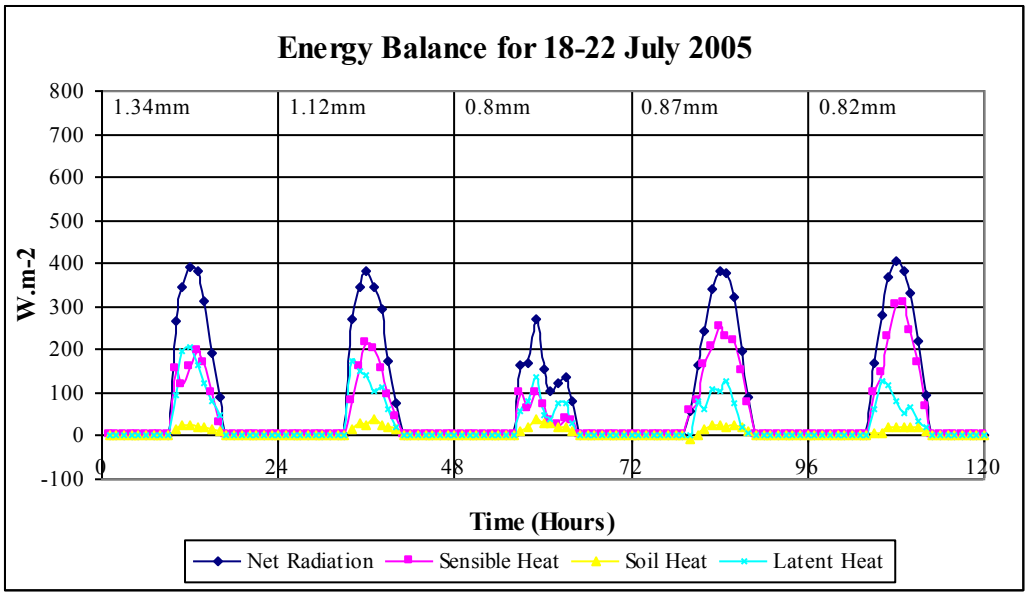

Figure 3.29: Energy balance components for 18 to 22 July 2005. Figures at the top represent daily total evaporation estimates in mm.day^{-1}

Figure 3.29 illustrates the decrease in net radiation when compared to the summer months, reaching a maximum of approximately 400 W.m^{-2} for the plotted period. This is however higher than that of June 2005, indicating the passing of mid-winter, and the approach of summer. On 21 and 22 July, the sensible heat component comprises the majority of net radiation, whilst on 18 and 19 July, latent heat and sensible heat contribute approximately equal proportions to a similar net radiation to that of 20 and 21 July. The difference between these varying contributions is best explained by examining the primary data in Figure 1.31.

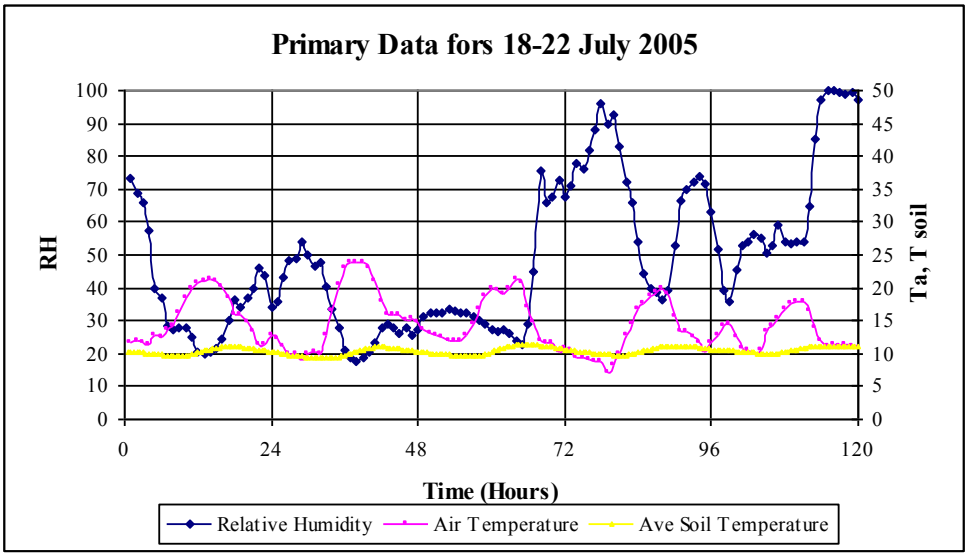

Figure 3.30: Primary data plots for 18 to 22 July 2005.

For 18 and 19 July, air temperature was relatively high compared to the remaining days reaching a maximum of approximately 25^{o}C which is possibly associated with Berg wind conditions. These same days also experience the lowest relative humidity dropping as low as 20%. On the other hand, day 21 and 22 July experienced colder temperatures reaching a maximum of approximately 20 ^{o}C. Relative humidity for these same days also only dropped to as low as approximately 40%. The combination of this lower air temperature and high relative humidity thus limited the amount of energy converted to the latent heat form, and resulted in an increased sensible heat contribution to the energy balance, as depicted by Figure 3.30.

3.3.11 August 2005

For August 2005, a full month of energy balance component data were obtained. The primary data obtained from the AWS on the other hand provided data until 18 August after which no data is available due to it being deleted.

Table 3.15: Summary of analysed data for August 2005

Date	Ta (^{o}C)	RH (%)	LvE (mm)	Rn (mm)	G (mm)	H (mm)	Rainfall (mm)
2005/08/01	19.38	46.12	1.71	3.39	0.22	1.46	0.0
2005/08/02	22.98	19.96	1.51	3.37	0.27	1.60	0.0
2005/08/03	12.73	89.70	0.36	1.72	0.13	1.23	0.0
2005/08/04	18.72	46.58	1.74	3.58	0.21	1.63	0.0
2005/08/05	26.60	16.53	1.45	3.34	0.29	1.60	0.0
2005/08/06	24.76	20.64	1.51	3.50	0.31	1.68	0.0
2005/08/07	28.49	13.48	1.29	3.48	0.31	1.88	0.0
2005/08/08	27.21	12.72	1.30	3.54	0.31	1.93	0.0
2005/08/09	15.56	67.96	0.20	1.99	0.14	1.66	3.8
2005/08/10	10.17	100.00	0.10	0.34	-0.03	0.27	21.4
2005/08/11	18.36	58.01	2.30	3.97	0.20	1.48	0.2
2005/08/12	19.04	47.24	1.55	3.72	0.22	1.95	0.2
2005/08/13	24.99	22.59	2.27	3.94	0.23	1.44	0.0
2005/08/14	22.48	37.13	2.97	4.08	0.23	0.88	0.0
2005/08/15	13.43	95.80	NA	NA	0.02	0.63	2.8
2005/08/16	8.12	99.80	0.28	0.73	0	0.45	2.6
2005/08/17	20.22	55.10	2.98	3.89	0.25	0.65	0.0
2005/08/18	18.26	28.29	1.45	4.11	0.19	2.47	0.0
2005/08/19	NA	NA	3.20	4.58	0.22	1.17	0.0
2005/08/20	NA	NA	1.94	4.02	0.25	1.83	0.2
2005/08/21	NA	NA	NA	NA	0.19	1.96	0.0
2005/08/22	NA	NA	2.39	3.94	0.29	1.26	0.0
2005/08/23	NA	NA	1.55	4.38	0.16	2.67	0.0
2005/08/24	NA	NA	1.41	4.40	0.27	2.73	0.0
2005/08/25	NA	NA	0.93	4.48	0.27	3.27	0.2
2005/08/26	NA	NA	3.41	4.69	0.21	1.07	0.0
2005/08/27	NA	NA	NA	NA	0.06	1.98	0.2
2005/08/28	NA	NA	0.77	2.72	0.20	1.76	0.2
2005/08/29	NA	NA	1.94	3.92	0.35	1.63	0.0
2005/08/30	NA	NA	2.17	3.47	0.31	0.98	0.0
2005/08/31	NA	NA	0.74	3.45	0.24	2.47	0.0
Average	**19.53**	**48.76**	**1.62**	**3.46**	**0.21**	**1.60**	**1.03**

During August 2005, net radiation averaged at 3.46 mm, reaching a peak on 26 August (4.69 mm). Once again, there is a definite shift as the month progresses, towards an increase in energy available in the form of net radiation attributed to the approach of summer. The contribution of latent heat to the energy balance is virtually equal to the sensible heat contribution. Average latent heat for the month was 1.62 mm with sensible heat contributing 1.60 mm. Soil heat flux again comprised an insignificant portion of the energy balance, averaging at 0.21 mm. Average air temperature is slightly higher than that observed in July 2005 (19.53^{o}C at 1pm).

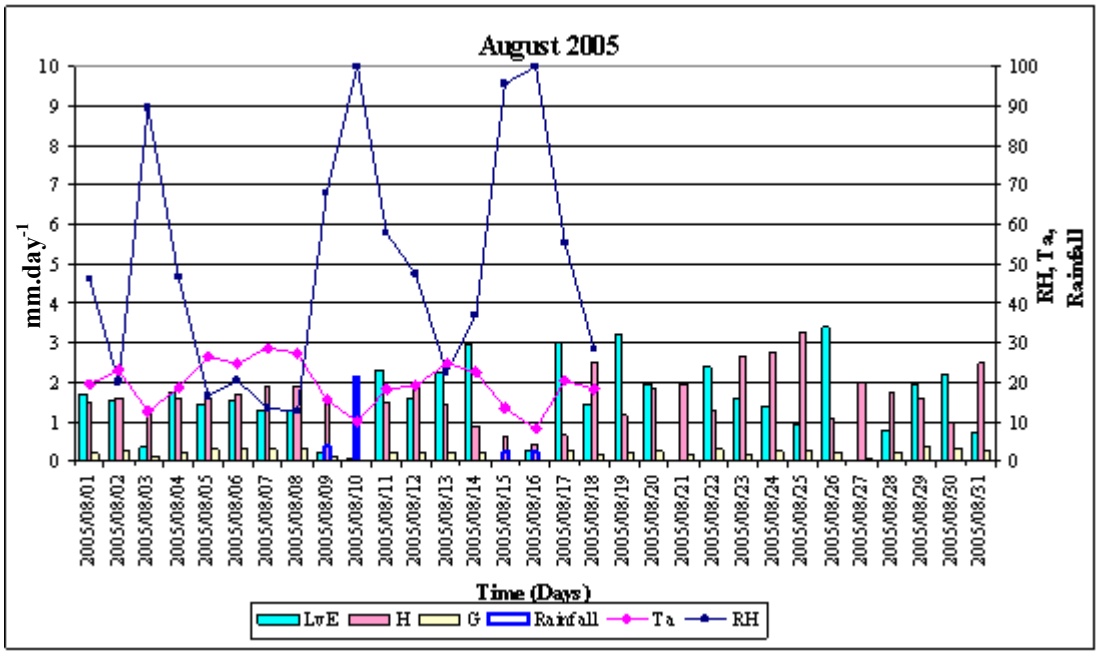

Figure 3.31: Daily summary of energy balance components from 1 to 31 August 2005

Berg wind conditions occurred over the period 7-10 August. Air temperatures dropped rapidly from extremely warm to cold and relative humidity increased to 100%, followed by approximately 25 mm of rainfall. These occurrences are typical for this area at this time of the year. The effect of increased soil water content brought about by rainfall is once again evident by observing Figure 3.31. Prior to the rainfall event (21.4mm) on 10 August, the sensible and latent heat contributions are approximately equal. However, immediately after the rainfall event, the latent heat contribution appears to be significantly higher than the sensible heat contribution. This continued until approximately 22 August after which this reverses to a higher sensible heat contribution than latent heat contribution. This is a result of a drying out soil profile after the rainfall on 10 August.

3.3.12 September 2005

The field work component was completed in September 2005 with energy balance data being obtained until 20 September.

Table 3.16: Summary of analysed data for September 2005

Date	LvE (mm)	Rn (mm)	G (mm)	H (mm)	Rainfall (mm)
2005/09/01	1.03	2.18	0.09	1.07	0.8
2005/09/02	2.19	4.93	0.26	2.48	0.2
2005/09/03	2.02	4.83	0.35	2.45	0.0
2005/09/04	2.64	4.66	0.32	1.70	0.0
2005/09/05	NA	NA	0.04	0.70	1.2
2005/09/06	NA	NA	-0.05	0	9.8
2005/09/07	0.18	0.76	0.10	0.47	3.8
2005/09/08	1.95	5.48	0.26	3.27	0.0
2005/09/09	2.67	5.22	0.40	2.15	0.0
2005/09/10	1.91	4.74	0.37	2.46	0.0
2005/09/11	1.08	4.87	0.32	3.48	0.0
2005/09/12	2.55	4.82	0.36	1.92	0.0
2005/09/13	0.68	1.08	0	0.41	3.8
2005/09/14	2.02	5.13	0.28	2.84	0.8
2005/09/15	2.51	4.97	0.39	2.07	0.0
2005/09/16	NA	NA	NA	NA	0.0
2005/09/17	2.51	5.32	0.43	2.38	0.0
2005/09/18	NA	NA	NA	NA	0.0
2005/09/19	2.36	5.16	0.39	2.41	0.0
2005/09/20	1.01	4.78	0.26	3.51	0.2
Average	**1.83**	**4.31**	**0.25**	**1.99**	**1.03**

During September 2005, net radiation averaged 4.31 mm per day, reaching a peak on 8 September (5.48 mm). The contribution of latent heat to the energy balance is slightly less than the sensible heat contribution. Average latent heat for the month was 1.83 mm with sensible heat contributing 1.99 mm. Soil heat flux again comprised an insignificant portion of the energy balance, although it increased slightly when compared to that obtained in the winter months, averaging 0.25 mm.

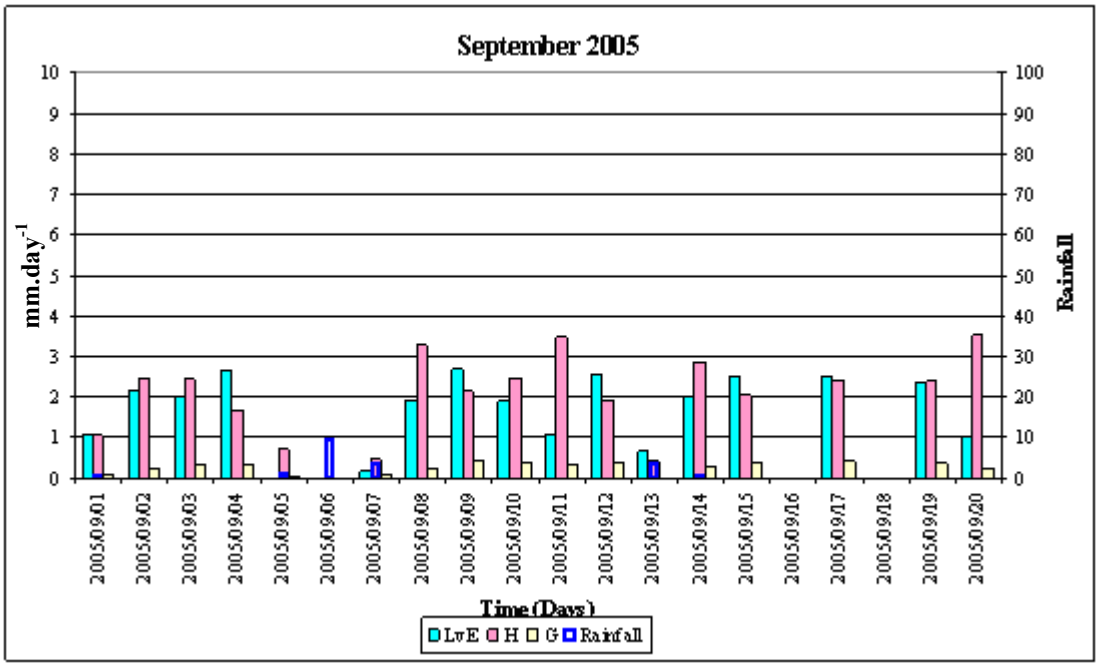

Figure 3.32: Daily summary of energy balance components from 1 to 31 July 2005

Air temperatures are thought to have increased considerably since mid winter brought about by an increased net radiation. The sensible component of this is still high due to the increasing atmospheric demand not being able to be met by the soil water content and hence latent heat component. The increase in soil heat flux is thought to be primarily a result of increased air temperatures.

3.4 Summary/Discussion of Results

Each month has been examined by looking at a detailed energy balance and primary data and noting changes at a daily/monthly time step. The effects of the change in net radiation as well as the change in soil water content on total evaporation have been noted to be significant in Section 3.3. In the context of the stated aims in Section 1 of Part 1, it is important that these smaller temporal effects (daily/monthly) are summarised to produce a longer record and a broader (seasonal/annual) understanding of the changes in both primary data and energy balance component data.

3.4.1 Average daily total evaporation and net radiation estimates

Each month analysed in this project consisted of a number of daily estimates of total evaporation. This differed from month to month depending on the availability of the required energy balance data. This meant that for certain months (December 2004 and January 2005), only a few daily total evaporation estimates were possible. However, the majority of months have a large number of daily total evaporation estimates. Figure 3.33 shows a simple average of each month's daily quantitative estimates of net radiation and latent heat based on the number of days analysed in that month. The months with few analysed days, hold more uncertainty than months with more analysed days. For example, in January 2005, only 8 of the possible 31 days were analysed due to a lack of energy balance data. Had more days been analysed, a more representative total evaporation and net radiation estimate would have been possible. Air temperatures of these 8 days are very low and may not give a good representation of average conditions in January. This needs to be taken into account in interpreting the results presented in this section. The summarised data has been expressed in mm equivalents.

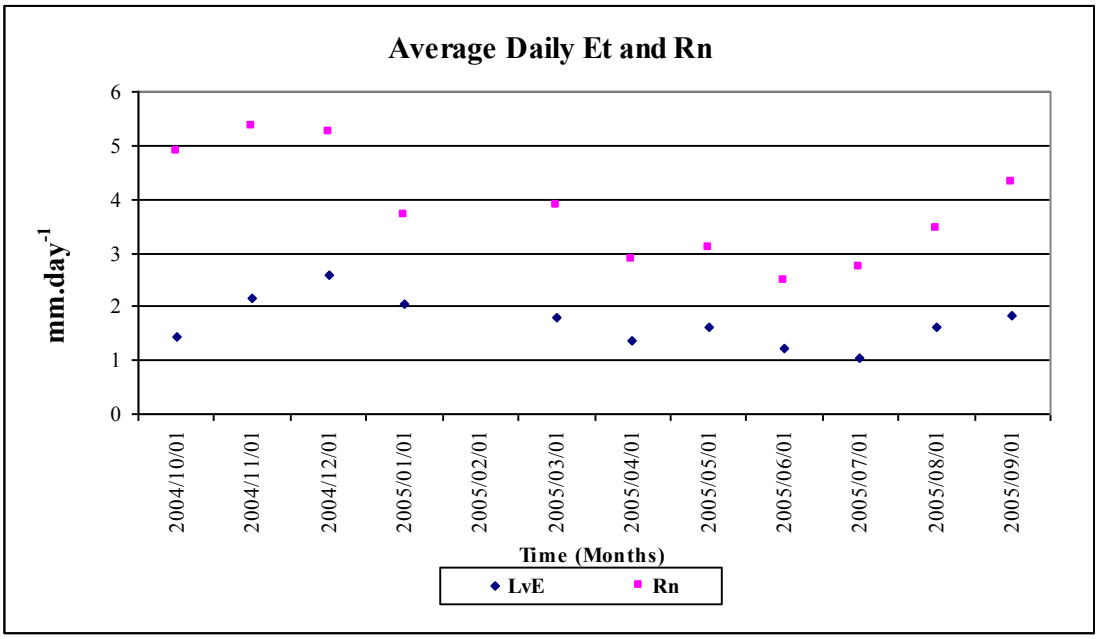

Figure 3.33: Average daily total evaporation and net radiation data in mm equivalents.

The pattern is typical of southern hemisphere summer rainfall area with substantially more evaporation occurring in the summer where soil water content limits the evaporation process less than in the winter months. Net radiation is also at a peak for these months. Thus, the combination of both the increased atmospheric demand in the form of Net radiation and the presence of water in the soil profile during summer, lead to higher total evaporation losses. It can be said that Net radiation and available soil water content provide the basis for total evaporation and that in line with the concepts of Calder (1999), soil water content provides the primary limit to evaporation. According to Muchow *et al*. (1994), the three main climatic elements which affect crop growth are net radiation, temperature and rainfall. Seasonal variability of these components will thus affect the seasonal variability of total evaporation. Total evaporation, as expected, was lowest in mid winter over the June/July months. Considering Figure 3.33 in three different sections aids the consideration of net radiation and soil water content and their impact on total evaporation.

1) In November 2004, the atmospheric demand in terms of net radiation is high, averaging 5.37mm/day. At this stage of the season, the soil profile is relatively dry following winter. The crop and soil are thus not able to meet this demand and hence the average actual total evaporation for this period is only approximately 2.17 mm/day. In December 2004, good rains had fallen resulting in a increased soil water content in the soil profile. This resulted in more of the atmospheric demand being met. The average demand for the days analysed in

December is virtually the same as that for November 2004 averaging at 5.26 mm/day. A large difference is however, noticed in the actual total evaporation which occurred, averaging 2.6 mm/day. The increased actual total evaporation is brought about by an increase in available moisture in the soil. A similar trend is evident for January 2005 as available soil water content was still high as a result of rainfall over that period (Figure 3.1). The atmospheric demand was slightly lower than for November/December. However, it must be noted that the days analysed may not be a good representation of climatic conditions in January. None the less, much of this 3.69 mm/day demanded was met by values of 2.03 mm/day in actual total evaporation as described in Section 3.3.4.

2) From March 2005 until June 2005, the atmospheric demand decreased slightly with actual total evaporation decreasing by the same proportion. This is expected with the winter solstice occurring on June 21. Over this duration, total evaporation comprised approximately 50 % of net radiation. Soil water content got progressively drier over this period (Figure 3.1) with net radiation also decreasing (Figure 3.33). The combination of this decreasing demand and the drying soil profile resulted in the same proportion of net radiation being met by total evaporation. This shows that the availability of moisture cannot merely be compared from one month to the next but needs to be considered in conjunction with the net radiation demand.

3) From July 2005 until September 2005, there is a definite shift towards increased net radiation. This is seen by the rapid climb in the net radiation presented in Figure 3.33. Total evaporation on the other hand did not show a corresponding increase for this period. This is due to a lack in soil water content (Figure 3.1). In September 2005, only 42 % of net radiation was met by total evaporation. Soil water content is believed to be a major determining factor in the amount of total evaporation occurring at this time, a conclusion supported by Figure 3.1 in conjunction with Figure 3.33.

It is concluded that the availability of soil water content is the major factor limiting evaporation in the late winter/early summer months whilst it is not the major limit during the mid/late summer and early winter months. The reason for this is the accumulation of water in the soil profile over the rainy season. As winter approaches, this supply is gradually depleted resulting in a soil profile which is unable to meet the atmospheric demand in the early summer where net radiation is substantially higher than in the winter months. Once

spring/summer rainfall begins to raise the water table and increase the soil water content, so to, the proportion of net radiation which is met by total evaporation, increases.

3.4.2 Maximum daily total evaporation and net radiation estimates

Figure 3.34 indicates days on which maximum total evaporation and net radiation, rather than averages, were selected from within each month.

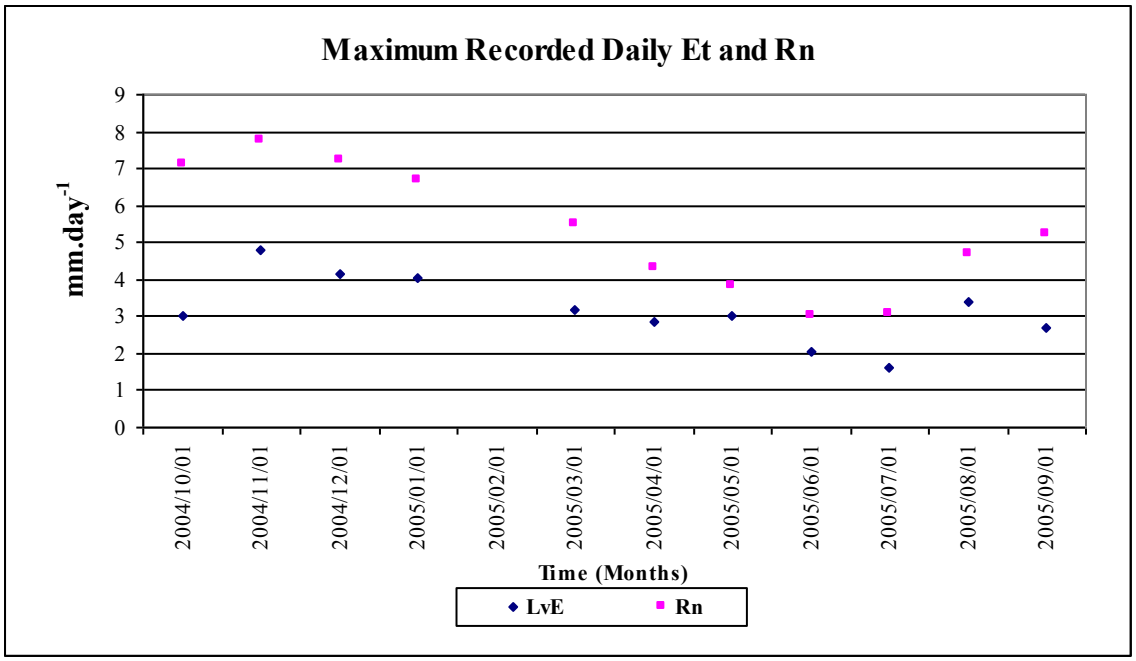

Figure 3.34: Maximum daily total evaporation losses and Net Radiation in mm equivalents.

A similar pattern was found when compared to that in Figure 3.33. The difference between Figure 3.34 and Figure 3.33 is that total evaporation and net radiation are substantially higher in Figure 3.34. Another major difference is that the proportion of net radiation being met by total evaporation is substantially higher when using these maximums. The reason for this is that on these days selected, air temperature was high and relative humidity low allowing for the latent heat component to comprise a large proportion of the net radiation. These maximums are significant in that they provide insight into the potential total evaporation rates of sugarcane. It also becomes useful to understand how much water sugarcane consumes under for example, irrigated conditions where soil water content is not a limiting factor to total evaporation.

3.4.3 Annual summary of energy balance and primary data

In Figure 3.35, energy balance component data is plotted for each day on which data were obtained for the period October 2004 until September 2005. Figure 3.35 therefore gives an indication of the periods when there was a problem in terms of data capture. All available data are plotted, including times when a complete energy balance data set was not available. It is also important to consider that all energy balance data analysis took place using data obtained over the period of daytime hours. This was done as it was recognised that an energy balance approach is driven by energy from the sun and hence sunshine hours. The evening data obtained for the energy balance components was thus ignored especially since the sensible heat flux component was erroneous as explained in Section 2.3.2 of Part 2.

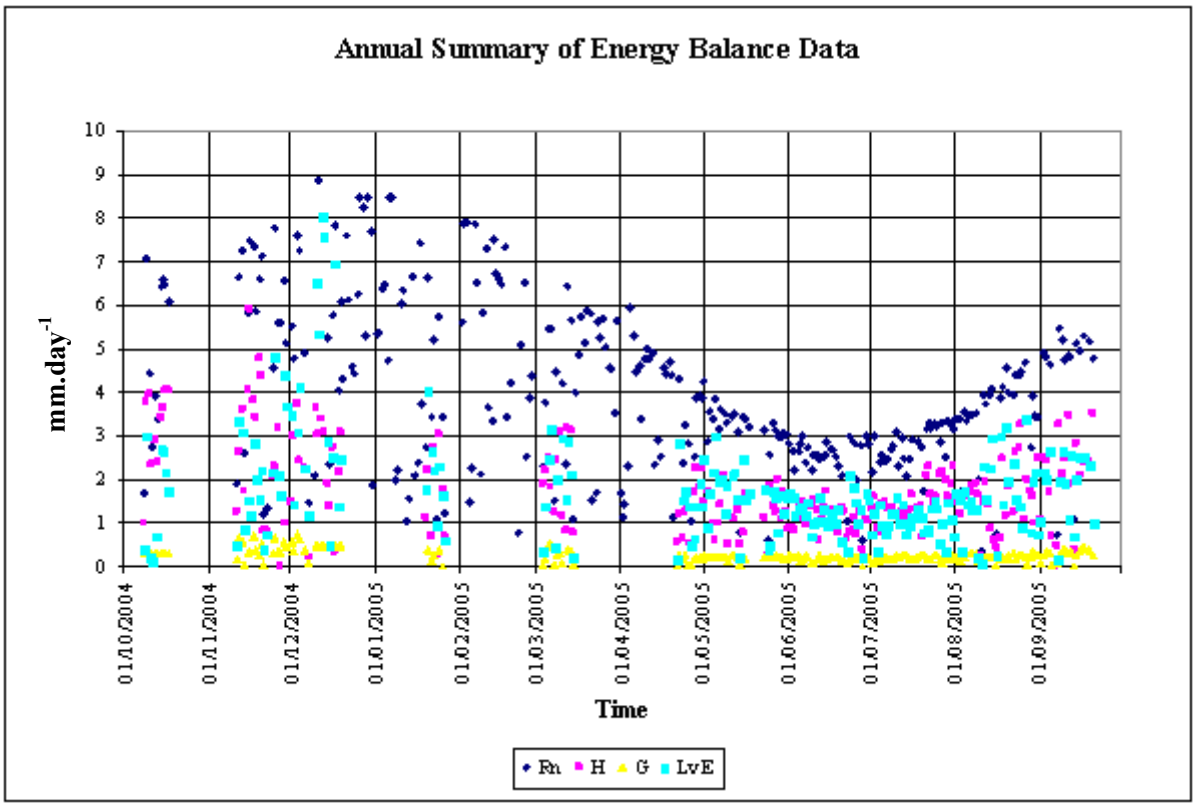

Figure 3.35: Annual summary of energy balance data

Net radiation was the most consistently available data. Soil heat flux and sensible heat flux data are not as consistently available due to equipment malfunction over certain periods. Consequently, the energy balance could not be completed and thus latent heat flux data are missing for certain periods. The problem periods occurred over the summer from December 2004 until April 2005, after which there were very few gaps in the data as depicted by the

density of data points from May 2005 onwards. It is important to note that for the period December 8 until December 19, soil heat flux was assumed by taking an average from December 1 until December 7. This was done as sensible heat flux data were available and proved to be useful as this period was thought to be vital one due to the lack of data over the summer period. In the following section, these data will be discussed in the light of the energy balance component seasonal variability and how this relates to water used by sugarcane. For clarity, primary data in the form of average air temperature, average relative humidity and rainfall are plotted in Figure 3.36. Good seasonal variability/trends are evident.

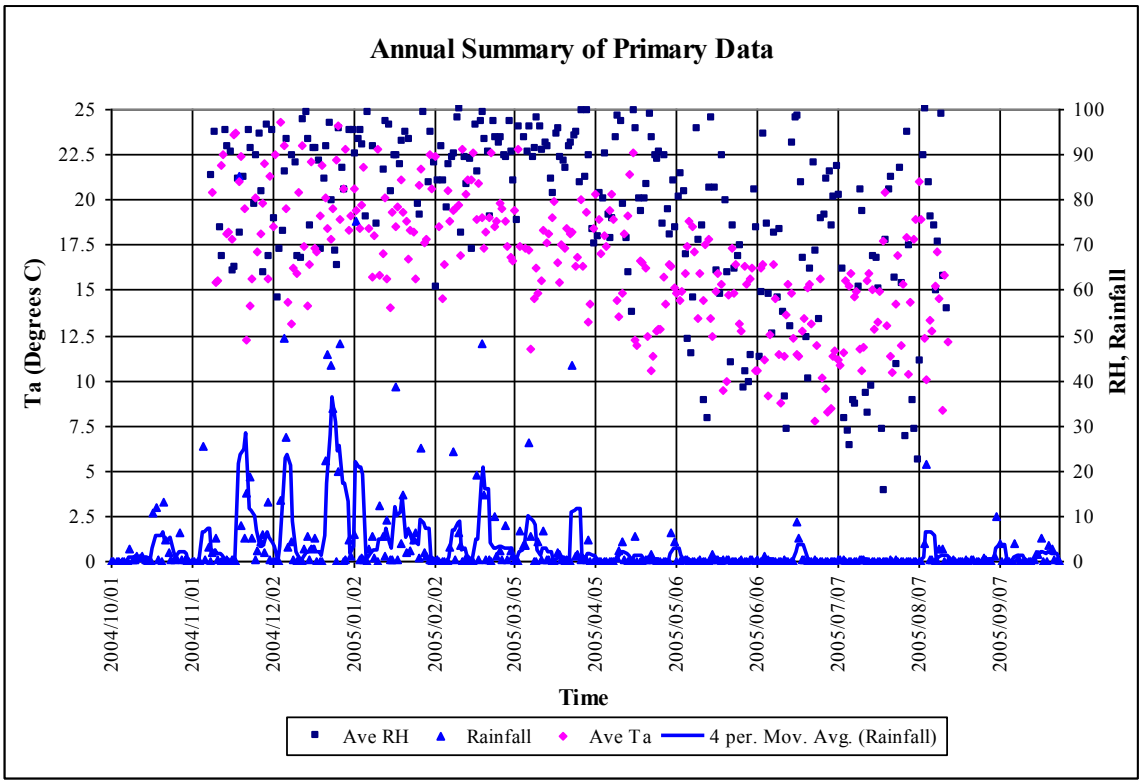

Figure 3.36: Annual summary of primary data (RH, Ta, and rainfall)

Both average relative humidity and average air temperature follow the same trend, peaking around January 2005, which is also when the majority of rainfall fell. These two variables then dropped steadily until about July 2005, when rainfall was also at a minimum. Average air temperature dropped from approximately 20^{o}C in mid-summer to approximately 13.5 ^{o}C in mid-winter. Relative humidity dropped from approximately 92% in mid-summer to approximately 60% in mid-winter. These two variables, when combined with the availability of soil water content, affect the distribution of the energy balance components considerably. In theory, for increased total evaporation to occur, there needs to be sufficient soil water

content available, high air temperature, and low relative humidity. This would allow the latent heat flux component to meet much of the atmospheric demand which is in the form of net radiation. The seasonal variability of energy balance components in Figure 3.35 reflect limits imposed by these parameters.

Figure 3.35 shows that net radiation follows a typical seasonal incoming radiation trend, peaking in mid-summer and dropping steadily until mid-winter, thereafter climbing once again as summer approaches. It is interesting to note the variability of net radiation within the seasons in terms of its range. From Figure 3.35 it is evident that there is a great range over the summer period as seen by the scattered data points. Over the winter period this range is significantly less, as seen by the density of data points. This indicates the variability of atmospheric conditions over summer and their relative consistency over winter.

From Figure 3.35 it seems that soil heat flux contributes a relatively minor component to the energy balance. It does however, follow a seasonal trend, peaking in early November 2004, and dropping as winter approaches. After having considered the component which drives the energy balance (net radiation), and the insignificance of the soil heat flux contribution, the seasonal variability of the remaining sensible and latent flux contributions are vital to this research in terms of understanding seasonal variability of water use by sugarcane.

Figure 3.35 shows that sensible heat flux peaks in the late winter and early summer months, with the maximum contribution occurring around September through to November. Over this period, a significant amount of energy (net radiation) is available for distribution amongst the energy balance components. Soil water content is often limited over this period for this type of climate, as is the case in this scenario with minimal rain falling over this period. This meant that the available energy could not be significantly consumed by processes such as evaporation and transpiration, hence resulting in an increased sensible heat flux contribution. From Figure 3.35, sensible heat flux then decreases steadily through the summer, into the winter. From Figure 3.35, it can be seen that the sensible heat flux contributes more to the energy balance than the latent heat flux from approximately June until mid November.

From Figure 3.35 it can also be seen that the latent heat flux contributes more to the energy balance than the sensible heat flux from approximately mid November until the end of May. It is evident that the latent heat flux seasonal trend follows that of net radiation, peaking in mid-

summer with an average of approximately 3 mm.day^{-1} dropping steadily until July with an average of approximately 1.2 mm.day^{-1}. It is therefore somewhat dependant upon the energy available in the form of net radiation. However, the latent heat flux seasonal trend also follows a similar pattern to that of rainfall shown in Figure 3.36. Soil water content is dependant upon rainfall, and is the source of water used in the evaporation of surface moisture (soil and crop surface) as well as transpiration from the sugarcane. It can thus be said that the contribution of latent heat flux to the energy balance is also dependant upon the availability of soil water content. Therefore, where adequate soil water content is available, the latent heat flux will contribute significantly to the energy balance. From Figure 3.36, average air temperature and average relative humidity should also be considered in the light of their effect and possible seasonal contribution to total evaporation. High air temperature and low relative humidity result in increased total evaporation. On days when this occurs and adequate soil water content exists, total evaporation, or the contribution of latent heat flux to the energy balance, is high. Average air temperature is affected by the amount of incoming solar radiation. Relative humidity, however, has proved to limit the amount of total evaporation. From Figure 3.36 it is evident that relative humidity is higher in summer than in winter. In the summer period, energy in the form of net radiation and soil water content are not limited. Therefore, if relative humidity was low for this period, the latent heat flux contribution to the energy balance would contribute a vast majority. Therefore, relative humidity can often limit the amount of total evaporation over this period.

3.4.4 Accumulated rainfall and energy balance component data plots

In Figure 3.37, the energy balance components as well as rainfall have been represented in the form of accumulated plots from October 2004 until September 2005. This was done to give an indication of the annual proportional contributions of the energy balance components.

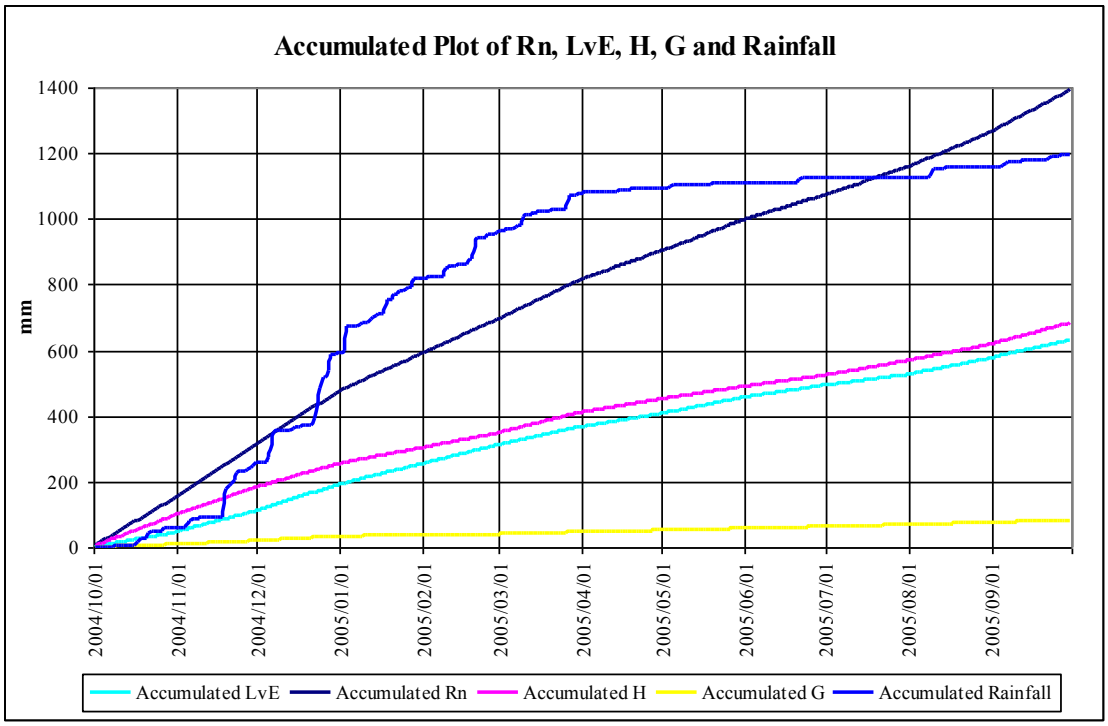

Figure 3.37: Accumulated plot of net radiation, latent heat flux, sensible heat flux, soil heat flux and rainfall.

It is important to note that for these accumulated plots in Figure 3.37, due to there not being a complete daily data set for the period, daily means were calculated for each month, using the available data to produce the accumulated plots. The accumulated rainfall plot is also useful in that it gives an indication of total rain which fell, and when it fell, for this period. From Figure 3.37 it is evident that approximately 1200 mm fell over the period suggesting that a significant amount of moisture was added to the soil profile. Although this was totalled over a hydrological year, when compared to previous Mean Annual Precipitation (MAP), it was on average, 200 mm higher as discussed in Section 3.1 of Part 2. For the same period, net radiation totalled approximately 1400 mm. Latent heat flux totalled approximately 630 mm and proved to be similar to the sensible heat flux total of approximately 680 mm. Soil heat flux, however, was significantly less, totalling approximately 80 mm over the season.

With the energy balance approach undertaken in this project, it was important to accurately estimate net radiation, sensible heat flux and soil heat flux so that estimates of total evaporation from sugarcane in the form of latent heat flux could also be accurate. If this is so, it is evident from Figure 3.37 that the contributions of sensible heat and latent heat are very similar, contributing approximately 49% and 45% of net radiation respectively. Therefore 45% of the energy which was available in the form of net radiation was converted into latent heat, and thus used to evaporate moisture at the surface (crop/soil) or crop transpiration.

Water use by sugarcane therefore varied seasonally due to limits to the evaporative process in the form of both radiation and moisture limitations. These seasonal changes in total evaporation have been discussed. They are however, depicted by the slopes of the lines representing the energy balance components in Figure 3.37. Four distinct slopes are evident over time:

1. October 2004 – December 2004
2. January 2005 – March 2005
3. April 2005 – July 2005
4. August 2005 – September 2005

In general, the changes in slope occur for all the energy balance components. The steepest of these are for periods 1 and 4, indicating substantial daily additions to the energy balance components when compared to the lesser slopes for periods 2 and 3. From Figure 3.37, period 3 shows the gentlest gradient, indicating significantly less daily additions to the energy balance components when compared to periods 1 and 4. The slope gradients are a direct result of the combination of moisture availability and solar energy. Therefore, in spring and summer, when significant amounts of moisture and solar energy are available, there are significant daily additions to the energy balance components, resulting in the steeper slopes. In autumn and winter, when moisture availability and solar radiation are limited, daily contributions are less, resulting in more gentle slopes.

From Figure 3.35 it has been seen that water use by sugarcane varies seasonally depending upon the amount of energy supplied in the form of net radiation, the availability of soil water content, as well as the average relative humidity. From the accumulated plots of the energy balance components in Figure 3.37, the latent component contributed approximately 630 mm

to the energy balance. Therefore, the water consumption by the sugarcane present at the research catchment was approximately 630 mm for the period from October 2004 until the end of September 2005. The majority of this was consumed over the summer months. When this amount consumed by the sugarcane is compared to the amount of rain which fell over the same period, amounting to approximately 1194 mm, it is evident that the crop did not use a significant amount. Approximately 564 mm was not consumed by the sugarcane, which suggests that a large amount of water contributed either to groundwater through seepage, or stream flow through surface runoff. It must be considered however, that much of this rainfall was event based and hence fell over a very short time period. For example, 85.2 mm falling on 19 November 2004. This would have resulted in a large amount of surface runoff, and hence immediate stream flow contribution, and would thus not have been available for crop growth. A large proportion of the rain fell over the summer and contributed to increased soil water content. Soils would thus often be near saturation, in terms of water content, which results in surface runoff if a significant amount of rain fell. Therefore, a large proportion of the 564 mm which was not consumed by the sugarcane could have runoff the surface as a result of a few large rainfall events over the summer period, especially if the events were in quick succession. It can be postulated that had this rain fallen more evenly, more of this 1194 mm would have been consumed by sugarcane growth.

In this dissertation, water use by sugarcane has been quantified with the seasonal variability thereof, better understood. The question still remains however, as to the stream flow reduction potential of dryland sugarcane production. In order for this to be answered, a comparison between water use by sugarcane and a baseline is required.

3.5 Stream Flow Reduction Potential of Sugarcane

Energy balance data from one year (October 2004 to September 2005) has been obtained and could prove to be useful in assessing the stream flow potential of sugarcane. This would require comparison with a baseline (grassland) and then used in a modelling approach. Although this is beyond the scope of this project, the following times of the year (season) should be considered important with regard to understanding the stream flow potential of sugarcane.

From the data presented in this dissertation, the response of the crop following rainfall has been rapid and has been highlighted on numerous occasions. Therefore, the response of the crop with the onset of spring rains and the effect on total evaporation will need to be compared closely to the baseline and used in the verification/validation of the model.

The maximum total evaporation from the crop over the summer is also important as this indicates the maximum potential evaporation from the crop due to non-limiting soil moisture and maximum demand in terms of solar radiation. One of the major weaknesses in this project was the lack of critical data over the December/January period due to unforeseen circumstances.

The data presented in this research is detailed enough for this to be undertaken. It should however be noted that there will be uncertainties as the data obtained is for a single year and the representativeness of this data for this area has not been confirmed due to the scope of this research. Further research of this nature should be undertaken or a number of years in the future for stronger conclusions to be drawn in this regard.

4. DISCUSSION, CONCLUSIONS AND RECOMMENDATIONS

The aims and objectives highlighted in the introduction have been met in this study. In this dissertation, comprehensive results have been presented based upon an energy balance approach using a scintillometer, in the estimation of water use by dryland sugarcane for one year resulting in an improved understanding of the water use by dryland sugarcane and the seasonal variability thereof. Streamflow reduction potential of sugarcane has also been discussed.

Total evaporation varies significantly over the year with substantially more evaporating over summer than winter. Consequently, the maximum total evaporation estimates are significantly higher in summer than winter. This is brought about by the major limits to total evaporation varying seasonally. The two main limits identified in this research are net radiation and soil water content. As expected, net radiation provides the driving force to total evaporation and fluctuates depending on the time of year. The availability of soil water content also varies seasonally and has proved to be a limiting factor to total evaporation for some of the year. In the wetter (late) summer months and early winter months however, when soil water content is readily available, soil water content limits total evaporation less than in the late winter and early summer. In these months with a wetter soil profile (late summer/early winter), net radiation is more of a limiting factor to total evaporation than soil water content. In the late winter and especially the early summer, net radiation increases significantly. Soil water content on the other hand is at its lowest at this time following the dry season, and is thus a major limit to total evaporation. The effect of relative humidity should not be overlooked and can also limit total evaporation.

In this project, the sugarcane grown in the area studied was estimated to have utilized 630 mm of the 1194 mm which fell as rainfall, proving to be approximately 53% of the available moisture. Thus, a significant amount of rainfall was not consumed by sugarcane. This is possibly due to the nature of the rainfall being strongly event based over the study period, therefore resulting in increased surface runoff.

The atmospheric demand assessed in the form of net radiation for the year was 1392 mm equivalents. Therefore, approximately 45% of the energy which was available in the form of

net radiation was converted into latent heat, and thus used to evaporate moisture at the surface (crop/soil) or crop transpiration.

A number of problems were encountered in terms of instrumentation in this project. The results presented in this dissertation could have been improved upon by the use of a net radiometer at the sugarcane site instead of using data from a nearby site over riparian vegetation. The TDR soil moisture sensor was problematic in the early stages of the project and resulted in the inferring of soil moisture from rainfall data instead. Soil moisture was also only measured weekly and it would have been beneficial if this was measured at a daily time step. Consistency of instruments used for the duration of the project would have resulted in more credible results, especially if these operated without malfunctioned and thus result in a complete data set.

In terms of future recommendations, this research could be improved upon in various ways in the near future. According to Savage *et al*. (2004), the energy balance components of net radiation and soil heat flux density in estimating latent energy flux density from measured sensible heat flux density, is important and will need to be considered in more detail in future energy balance based research. The scintillometer is a relatively new technique used in the estimation of sensible heat flux and will require further refining and testing in the near future in order to improve the credibility of this technique in energy balance research. In order to provide further insight into the water use by sugarcane and the seasonal variability thereof, as well as to verify the results presented in this dissertation, it would be beneficial to establish a similar study to the one discussed in this dissertation over both drier and irrigated sugarcane crops. Comparisons made would assist in further understanding the limits to total evaporation under these extreme cases, and provide insight into transpiration limitations brought about by vegetative characteristics under non-limited soil water content conditions. The actual measured total evaporation estimates presented in this dissertation could be used for modelling purposes. The total evaporation estimates obtained could be compared to a baseline (grassland) and used in simulations for a better understanding of the stream flow reduction potential of sugarcane and the seasonal variability thereof.

5. REFERENCES

Aase, JK and Wright, JR. 1972. Energy balance investigations on native range vegetation in the northern great plains. *Ecology*. 53: 1200-1203.

Abezghi, TW. 2003. Estimation of Reference Evaporation and Comparison with ET-Gage Evaporimeter. Unpublished MSc. Agric. Dissertation, School of Applied Environmental Sciences, University of Natal, Pietermaritzburg, South Africa.

Allen, RG. 2000. Using the FAO-56 duel crop coefficient method over an irrigated region as part of an evapotranspiration intercomparison study. *Journal of Hydrology*. 229: 27-41.

Allen, RG, Pereira, LS, Raes, D and Smith, M. 1998. Crop Evapotranspiration – *Guidelines for computing crop water requirements* – FAO Irrigation and drainage paper 56 FAO – Food and Agriculture Organization of the United Nations. Rome, Italy.

Anon. 1999. Micromet Systems. Soil Heat Flux Instrumentation. [Internet]. http://snrs.unl.edu/agmet/408/instruments/soilheat.html Accessed [2 March 2005].

Anon. 2006. Building an Evaporation Monitoring Toolkit. In: *The Water Wheel*- Evaporation in the Spotlight. 5 (4):12-15. ISSN 0258-2244 South Africa.

Beven, K. 1989. Changing Ideas in Hydrology – The case of physically based models. *Journal of Hydrology* 105: 157-172.

Bezuidenhout, CN, Lecler, NL, Gers, C and Lyne, PWL. 2006. Regional based estimates of water use for commercial sugarcane in South Africa. *Water SA*. 32: 219-222

Blight, GE. 2002. Measuring Evaporation from Soil Surfaces for Environmental and Geotechnical Purposes. *Water SA* 28: 381-394.

Bloschl, G and Sivapalan, M. 1995. Scale issues in hydrological modelling: A review. In: Kalma, JD and Sivapalan, M. (Eds). Scale Issues in Hydrological Modelling. John Wiley and Sons, Chichester, United Kingdom pp. 9-48.

Burger, C. 1999. Comparitive Evaporation Measurements Above Commercial Forest and Sugarcane Canopies in the KwaZulu-Natal Midlands. Unpublished MSc. Dissertation. School of Applied Environmental Sciences, University of Natal, Pietermaritzburg, South Africa.

Calder, IR. 1998. Review outline of Water Resources and Land Use Issues. SWIM paper 3. Colombo, Sri Lanka: *International Irrigation Management Institute (IIMI).* ISBN: 92 9090 361 9.

Calder, IR Bosch, J and Jewitt, GPW. 2004. Recommendations for Improving the SFRA Policy Instrument Through Focussing on Green Water Impacts. [Internet]. A Briefing Paper for the Department of Water affairs and forestry. Available from: www.cluwrr.ncl.ac.uk/projects/camp/CAMP-RSA-SFRA.pdf Accessed [26 July 2004].

Campbell Scientific Ltd. 1987. Bowen Ratio System User Guide.

Campbell Scientific Ltd. 2005. Solar Radiation Sensor. Model CM3. South Africa [Internet]: http://www.campbellsci.com/documents/lit/b_cm3.pdf Accessed [2 Oct 2005]

Clark, GA, Smajstrla, AG, and Zazueta, FS. 1989. Atmospheric Parameters Which Affect Evapotranspiration. Circular 822, Florida Cooperative Extension Service, University of Florida. USA.

Cotton, M. 2004a. MCS 155 Pyranometer. South Africa. [Internet]: Available from: http://www.mcsystems.co.za/html/mcs_155.html Accessed [2 Oct 2005]

Cotton, M. 2004b MCS 486TLW - 2 Channel Soil Temperature and Moisture Data Logger. South Africa. [Internet]: Available from: http://www.mcsystems.co.za/html/mcs_486tsm_.html Accessed [2 Oct 2005]

De Bruin, H and Moene, AF. 2003. Sri Lanka Experiment, A Meteorology and Air Quality Group (METAIR). [Internet]: Research projects and experiments, Wageningen University and Research Centre. Available from:http://www.met.wau.nl/index.html Accessed [19 Jan 2004].

DWAF, 2003. The Identification and Declaration of Stream Flow Reduction Activities in Terms of the National Water Act. A Discussion Paper Drafted by the Subdirectorate: Stream Flow Reduction, Unpublished Draft copy, Department of Water Affairs and Forestry, Pretoria, South Africa.

Green, AE. 2001. *The Practical application of Scintillometers in Determining the Surface fluxes of Heat, Moisture and Momentum*. Wageningen University, The Netherlands.

Gush, MB, Scott, DF, Jewitt, GPW, Schulze, RE, Lumsden, TG, Hallowes, LA and Görgens, AHM. 2001. *Estimation of Streamflow Reductions Resulting from Commercial Afforestation in South Africa.* Report No. TT 173/02, Water Research Commission, Pretoria, South Africa.

Hemakumara, HM, Chandrapala, L and Moene, AF. 2003. Evapotranspiration fluxes over mixed vegetation areas measured from large aperture scintillometer. *Agricultural Water Management* 58: 109 – 122

Hill, RJ. 1997. Algorithms for obtaining atmospheric surface-layer fluxes from scintillation measurements. *Journal of Atmospheric and Oceanic Technology*. 14: 456-467

Hillel, D. 1982. *Introduction to Soil Physics*. Academic Press, New York

Kite, G and Droogers, P. 2000a. Comparing estimates of actual evapotranspiration from satellites, hydrological models, and field data. *Journal of Hydrology* 229: 3–18

Kite, G and Droogers, P. 2000b. *Comparing estimates of actual evapotranspiration from*

satellites, hydrological models, and field data: A Case Study From Western Turkey. International Water Management Institute, Colombo, Sri Lanka.

Kongo, VN and Jewitt, GPW. 2006. Preliminary investigation of catchment hydrology in response to agricultural water use innovations: a case study of the Potshini catchment – S. Africa. *Physics and Chemistry of the Earth* 31 (15–16): 976–987.

Mason, PJ. 1988. The formation of areally-averaged roughness lengths. *Meteorological Society* 114: 399-420

McGlinchey, MG and Inman-Bamber, NG. 1996. Predicting Sugarcane water use with the Penman-Monteith equation. *Proceedings of Evapotranspiration and Irrigation Scheduling Am. Soc. Agric. Eng*. San Antonio, USA. 592-597

McKenzie, RS and Bhagwan, JN. 1999. Some Recent Developments in Water Demand Management In South Africa. In: *Proceedings of the Ninth South African Hydrology Symposium,* Nov 1999, Western Cape, South Africa.

Meijninger, WML. 2003. *Surface Fluxes Over Natural Landscapes Using Scintillometry*. Grafisch Service Centrum Van Gils BV, Wageningen, The Netherlands.

Meijninger, WML, Beyrich, F, Luedi, A Kohsiek, W and De Bruin, HAR. 2003. Scintillometer fluxes of sensible and latent heat over a heterogenous area—a contribution to LITFASS-2003 [Internet] Wageningen University, Wageningen, Netherlands.Availablefrom:http://ams.confex.com/ams/BLTAIRSE/techprogram/paper_77904.htm Accessed: [9 Aug 2004].

Metelerkamp, BR. 1992. The use of the Bowen Ratio Energy Balance Method for the Determination of Total Evaporation over a Grassed Surface. Unpublished MSc. Agric. Dissertation, University of Natal, Agrometeorology, Pietermaritzburg, South Africa.

Micromet Systems. 1999. Soil Heat Flux Instrumentation, Seattle, USA. [Internet]: available from: http://www.snrs.unl.edu/agmet/408/instruments/soilheat.html Accessed [15 Oct 2005]

Muchow, RC, Spillman, MF, Wood, AW and Thomas, MR. 1994. Radiation interception and biomass accumulation in a sugarcane crop grown under irrigated tropical conditions. *Australian Journal of Agricultural Res*earch. 45: 37-49

NWA. 1998. National Water Act, RSA Government Gazette No. 36 of 1998: 26 August 1998, No. 19182. Cape Town, South Africa.

Savage, MJ. 2005. Personal Communication. Agrometeorology, University of KwaZulu-Natal, Pietermaritzburg, South Africa.

Savage, MJ, Everson, CS, and Metelerkamp, BR. 1997. *Evaporation measurement above vegetated surfaces using micrometeorological techniques.* Water Research Commission Report No. 349/1/97. Pretoria, South Africa.

Savage, MJ, Everson, CS, Odhiambo, GO, Mengistu, MG and Jarmain, C. 2004. *Theory and Practice of Evaporation Measurement, with Special Focus on SLS as an Operational Tool for the Estimation of Spatially-Averaged Evaporation.* Water Research Commission Report No. 1335/1/04. Pretoria, South Africa.

Schmidt, EJ 1997. Impacts of sugarcane production on water resources. *Proceedings of the South African Sugar Technologists Association* 71: 73-75

Schmidt, EJ, Smithers, JC, Schulze, RE and Mathews, P. 1998. *Impacts of Sugarcane Production and Changing Land Use on Catchment Hydrology.* Report Number 419/1/98. Water Research Commission, Pretoria, South Africa.

Schulze, RE . 1995. *Hydrology and Agrohydrology: A Text to Accompany the ACRU Agrohydrological Modelling System.* Report Number TT69/95. Water Research Commission, Pretoria, South Africa.

Scintec. 2003a. Boundary Layer Scintillometer, Turbulence, Heat Flux, Crosswind Over Large Spatial Scales. Germany. [Internet]: Available From: http://www.scintec.com/Site.1/PDFs/01_LayBLS.pdf Accessed: [19 Jan 2004].

Scintec. 2003b. BLS Series Scintillometers. Germany. [Internet]: Available From: http://www.scintec.com/Site.1/scintisls.htm Accessed: [21 Sep 2004].

Scintec. 2003c. Surface Layer Scintillometers, The Ultimate Sensors for Turbulence, Heat Flux, Momentum Flux, Crosswind. Product Summary. Germany. [Internet]: Available From: http://www.scintec.com/Site.1/PDFs/SLSsummary.pdf Accessed: [21 Sep 2004].

Scintec. 2003d. Surface Layer Scintillometers, The Ultimate Sensors for Turbulence, Heat Flux, Momentum Flux, Crosswind. Germany. [Internet]: Available From: http://www.scintec.com/Site.1/PDFs/01_LaySLS.pdf Accessed: [21 Sep 2004].

Scintec. 2003e. Boundary Layer Scintillometer, Turbulence, Heat Flux, Crosswind Over Large Spatial Scales. Product Summary. Germany. [Internet]: Available From: http://www.scintec.com/Site.1/PDFs/BLSsummary.pdf Accessed: [21 Sep 2004].

Scintec. 2004. Scintec Boundary Layer Scintillometer, User Manual BLS 900/BLS 2000. Scintec Tubingen, Germany.

Smithers, JC, Schulze, RE and Schmidt, EJ. 1997. Modelling the impacts of grassland, forestry and sugarcane run-off at the Umzinto research catchments. *Proceedings of the South African Sugar Technologists Association* 71: 15-17

Van Antwerpen, R, McGlinchey, M, Inman-Bamber, NG, and Bennie, ATP. 1996. Estimating root water use in sugarcane. *Proceedings of the South African Sugar Technologists Association* 70: 57-58

Van der Zel, DW. 1995. Accomplishments and dynamics of the South African Afforestation Permit System. *South African Forestry Journal* 172: 49-58.

Wageningen University and Research Centre. 2003. The Scintillation Method- a First Introduction, Meteorology and Air Quality Group (METAIR) [Internet], Research projects and experiments, Available from: http://www.met.wau.nl/index.html Accessed: [19 Jan 2004].

APPENDICES

Appendix A: MCS Radiometer Calibrations

Two MCS radiometers were used in this study. Both of these were calibrated against a Kipp and Zonen CM3 pyranometer where calibration took place both with the pyranometer orientated upward (Figure A4) and downward (Figure A7) in order to obtain a calibration equation for both incoming and outgoing radiation. The spectral response curve for the MCS radiometers is illustrated below in Figure A1. The CM3 has a flat spectral sensitivity from 0.305 to 2.8µm. This instrument therefore detects a wider spectral range than the MCS radiometers. Long wave radiation range is usually considered to extend up to 50µm. Unfortunately there is no spectral response curve available for the CM3.

A1: Spectral Response for the MCS Radiometers

The spectral response for the MCS radiometers is illustrated by Figure A1.

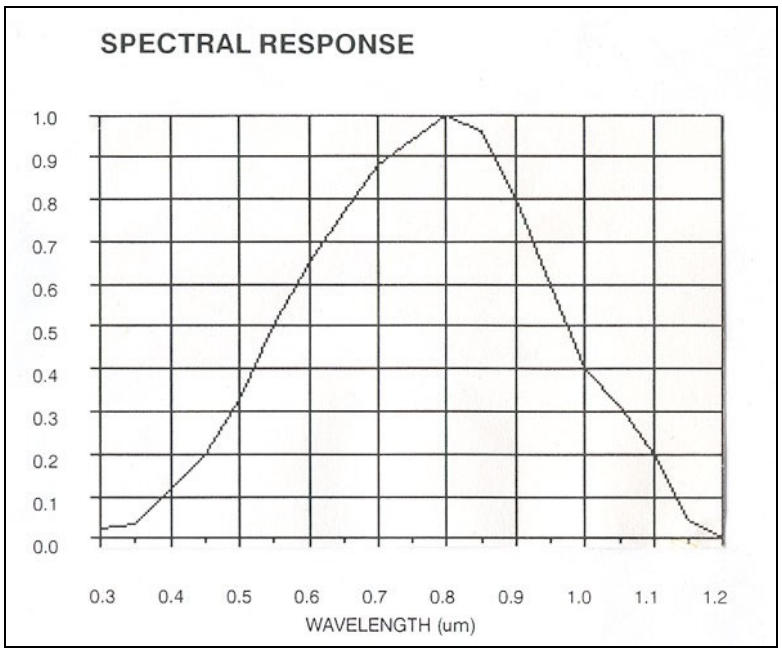

Figure A1: Spectral response of the MCS 155 radiation sensor (Cotton, 2004a)

A2: Calibration of Mike Cotton Systems (MCS) Radiometers for Incoming Radiation

A linear trend line has been fitted to the upward calibration of both radiometers illustrated in Figure A2. The linear fit accurately represents the data points as indicated by R^2 values of 0.9984 and 0.9991 for each of the radiometers. The calibrations indicate that a single unit logged on the MC system (y axis) represents approximately 20 $W.m^{-2}$.

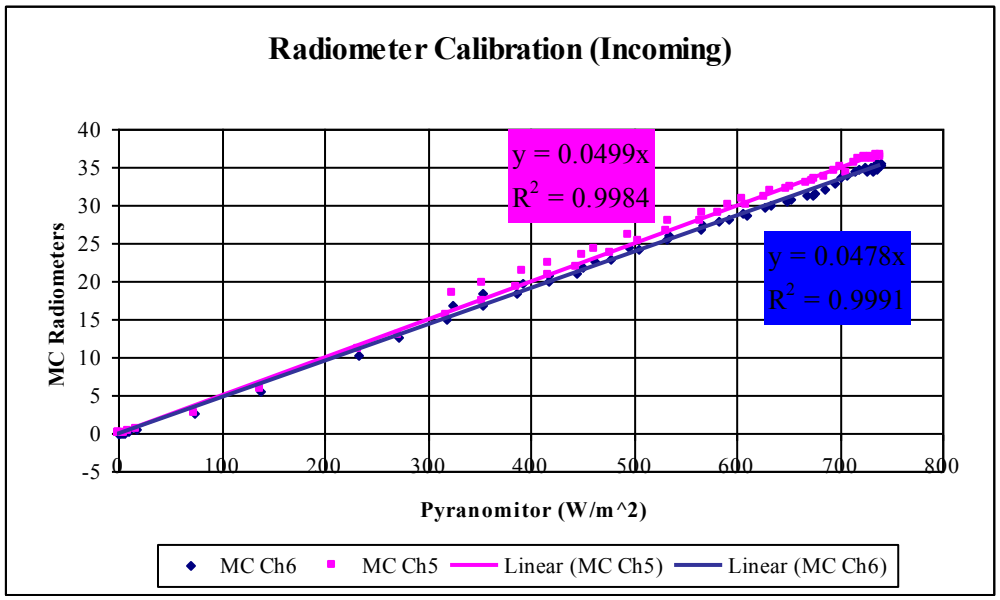

Figure A2: Incoming calibration of MC radiometers against a Kipp and Zonen CM 3 pyranometer.

In Figure A2, MC represents Mike Cotton, the manufacturer of the radiometers. Ch5 and Ch6 represent the channel of the Mike Cotton Systems logger.

An assumption in the calibration of these instruments is that the Kipp and Zonen pyranometer accurately records incident solar radiation for the given spectral range. For the calibrated time period, with the application of the correction factor derived from the gradient of the linear trend lines, the day-time trend/pattern is satisfactory as illustrated by Figure A3. A sunny day was selected in April 2005, which was thought to represent average conditions for this time of the year, in this compaison. This resulted in a good range and distribution of radiation for that day. Incoming solar radiation for the specified spectral distribution was estimated at 10 minute averages.

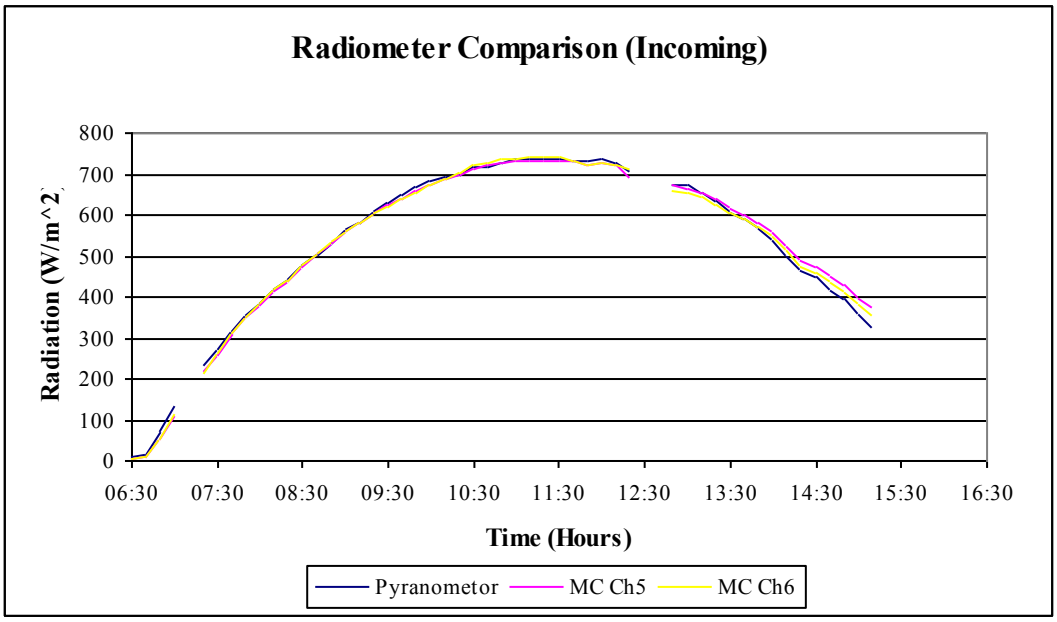

Figure A3: Incoming radiation comparison between MCS radiometers (MC Ch5 and MC Ch6) and a Kipp and Zonen pyranometer.

From Figure A3 it is evident that there are two periods in which no data were logged. These appear at 7:10am as well as 12:30-12:40pm. The reason for this is that data over these periods was erroneous due to a shadow being cast over the radiometers, hence affecting the radiation recorded. In this project, due to limitation of available finances, it was decided to use cheaper instruments as the primary data source (Mike Cotton Systems) and to calibrate these against more expensive ones (Kipp and Zonen). Reliable calibration coefficients were then fitted to estimates of radiation, measured in the field by cheaper instruments.

Figure A4: Calibration of the MCS radiometers (middle and right) with a Kipp and Zonen CM3 pyranometer (left) for incoming radiation.

A3: Calibration of Mike Cotton Systems (MCS) Radiometers for Outgoing Radiation

Calibration of the MCS radiometers for outgoing radiation (downward facing) took place in the same way. The only difference is that the radiometers were inverted in order to detect radiation reflected from the surface (Figure A7). It is important to note that the radiometers were only able to detect the spectral distribution in the ranges described previously and illustrated by Figure A1. As this does not include the long wave component, it is important to note that these radiometers were only used in the estimation of the reflection coefficient which, according to Allen *et al*. (1998), is the fraction of solar radiation reflected by the surface. The wavelengths which are commonly reflected at the surface, fall within the range of spectral response wavelengths illustrated in Figure A1.

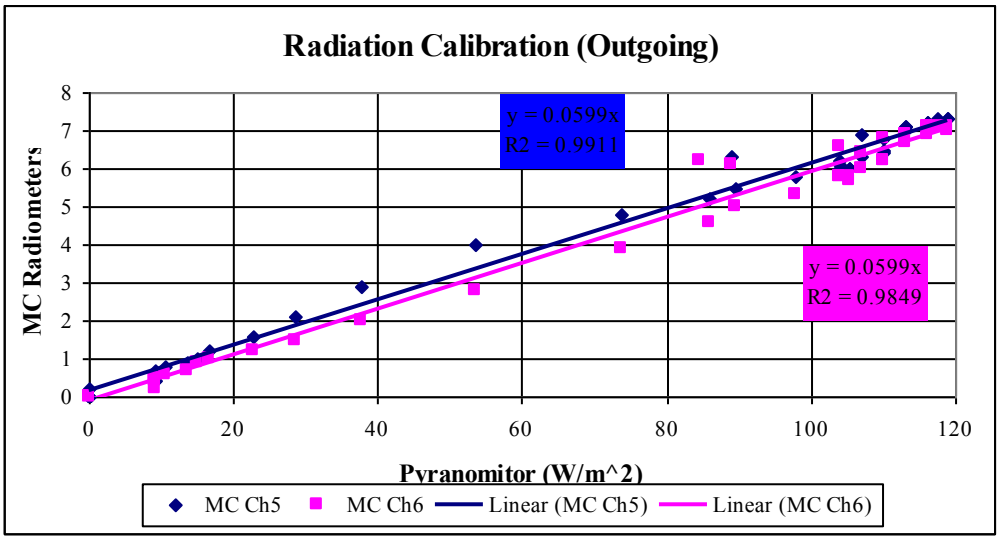

Figure A5: Calibration of MC radiometers against a Kipp and Zonen CM 3 pyranometer.

It was again assumed that the Kipp and Zonen pyranometer records accurate solar radiation for the given spectral range. For the calibrated time period, with the application of the correction factor, the day-time trend/pattern is satisfactory as illustrated by Figure A5. Incoming solar radiation for the specified spectral distribution was again averaged over a 10 minute period.

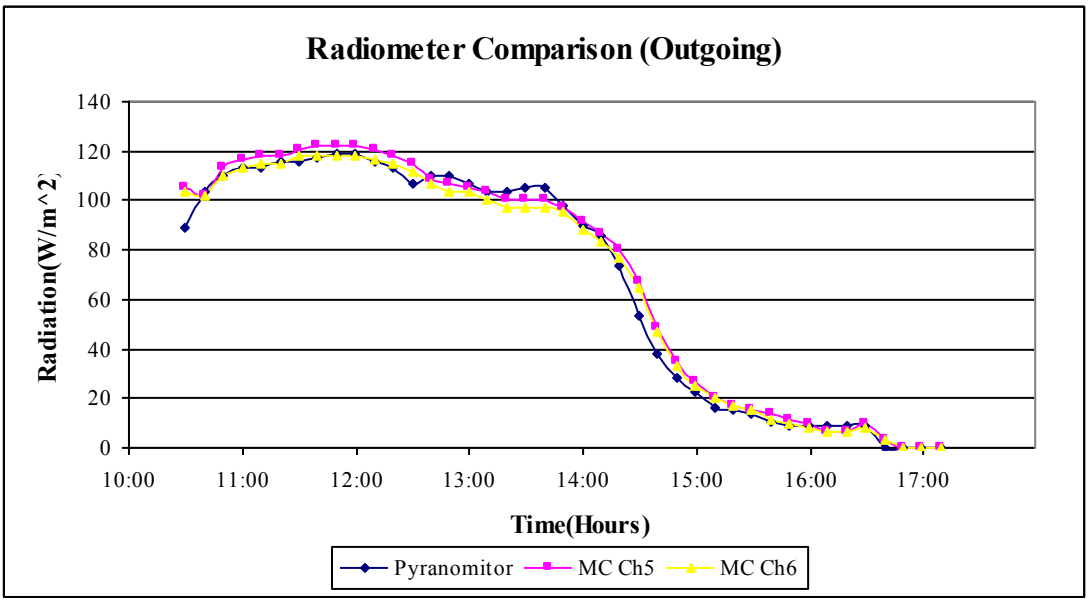

Figure A6: Radiation comparison between MCS radiometers and a Kipp and Zonen pyranometer.

Data plots of the outgoing calibration in Figure A5 are more scattered than those from the incoming calibration in Figure A2 with lower R^2 values of 0.9911 and 0.9841 for channel 5 and 6 respectively. This is however to be expected given fewer data points and the difference is thus thought to not be practically significant. From Figure A7, it is evident that the vegetation, over which the radiometers were placed, was grass. Although numerous obstacles and trees/shrubs are noted in Figure A7, the area in the local vicinity beneath the instruments was grass. Thus the reflection coefficient estimates obtained at this calibration site are not important, but the calibration correction factors are vital. These were assumed to be as measured.

Figure A7: Outgoing calibration of the MCS radiometers (left and right) with a Kipp and Zonen pyranometer (middle)

A4: Comments

The MCS logger used in this project houses 10 channels, where channels 5 and 6 host the radiometers. The above calibrations were applied in the determination of the reflection coefficient or reflected solar radiation. For this, the incoming calibration of the MCS channel 5 was used and the outgoing MCS channel 6 calibration. The MCS channel 5 was thus positioned facing upward and with the MCS channel 6 positioned facing downward. The reflection coefficient or short wave reflection was then determined by calculating the proportion of outgoing radiation, relative to the amount of incoming radiation at a corresponding wavelength.

However, there are some uncertainties in the determination of the far infrared wavelengths within the project. As stated above, the wavelengths measured by the Kipp and Zonen pyranometer, against which the MCS radiometers were calibrated, range between 305 to 2800 nm. Thus, the incorporation of long wave radiation of wavelengths 2800 nm to 100 000 nm, are not included in the calibration of the instruments.

Appendix B: Soil Heat Flux

B1: Soil Thermometer Installation

Good contact was kept between the soil thermometers and the soil. This was done by first digging a hole with a spade and then inserting the soil thermometers into the sidewall of the hole as illustrated in Figure B1. The soil was then replaced and packed to the original density. The remaining length of cable between the logger and thermometers was kept cool underground to avoid heating from the sun. Data were logged every 30 minutes at both depths of 50 and 250 mm.

Figure B1: Installation of soil thermometers/thermocouples

B2: Soil Thermometer Data Downloading

For the period October 2004 to March 2005, HOBO soil thermometers were used to log a potential difference or voltage. These were calibrated prior to installation in the field. The calibration equation can be seen in Section 2.2.1.2. Two sets of MCS soil thermometers were used in the latter stages of the project. The first set of thermometers was installed in mid April 2005, with the second set being installed in mid June 2005. This is illustrated in Figure 1.3 of Part 1. These MCS soil thermometers logged temperature after having been factory calibrated. Downloading of data took place weekly, using a laptop as shown in Figure B2. The loggers were placed in water proof boxes so as to prevent moisture from entering the logger and thus affecting the data.

.

Figure B2: Transferral of data from a MCS soil thermometer logger onto a laptop.

B3: MCS Soil Thermometers Specifications

The MCS soil temperature logger is a low cost 2 channel data logger used for the measurement of soil temperature. It can be programmed to record average, minimum and maximum values at a set recording rate. For the purposes of this project, 30 minute average temperatures were recorded. The micro-power design allows the logger to run unattended for one to two years from a single Lithium Battery, depending on the recording rate. The logger is protected from extreme climatic conditions in a splash proof PVC casing (Figure B3). According to Cotton (2004b), the logger is well suited to record data in agricultural experiments.

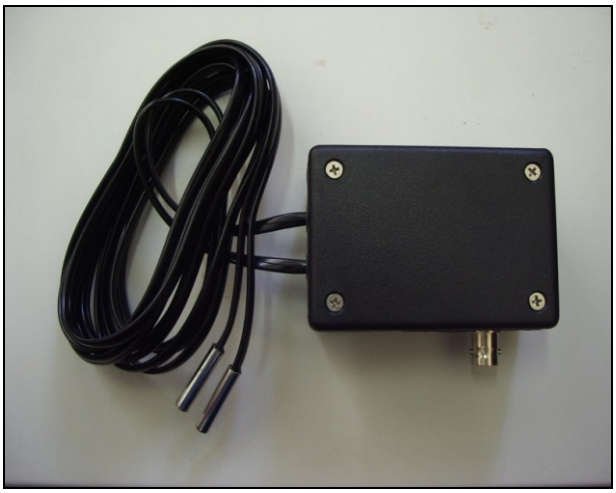

Figure B3: Two-channel soil temperature thermometers and MCS logger.

B4: MCS Soil Thermometer Calibration – Set 1

From Figure B4, the soil thermometers proved to be accurate when compared to the mercury thermometer. This is confirmed by R^2 values of 0.9996 and 0.9995 for channel 1 and 2 respectively. The factory calibration coefficients were thus confirmed.

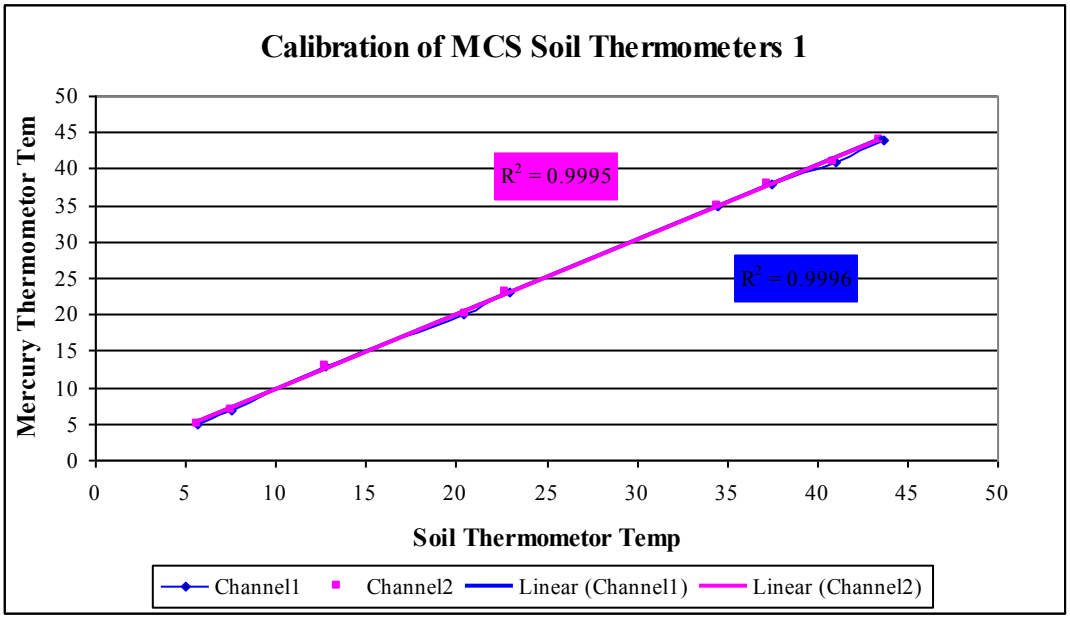

Figure B4: Calibration of MCS soil thermometers 1 against a mercury thermometer for the range 5-45 ^{o}C.

B5: MCS Soil Thermometer Calibration – Set 2

The second set of soil thermometers also proved to log temperatures accurately with R^2 values of 0.9994 and 0.9993 for channel 1 and 2 respectively. The calibration represented in Figure B5 was thus not used in the analysis of data collected but show that the temperatures recorded were accurate and thus also confirm the factory calibration.

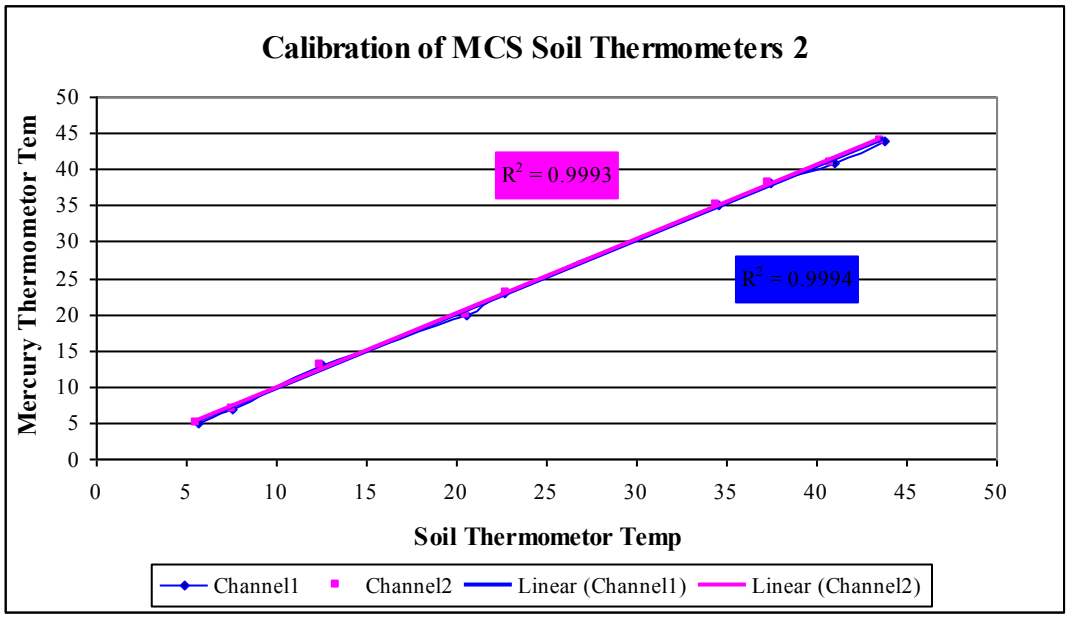

Figure B5: Calibration of MCS soil thermometers 2 against a mercury thermometer for the range 5-45^{o}C.

B6: Hobo Soil Thermometer Specifications

The HOBO soil thermocouples were used over the period November 2004 to March 2005, and logged 30 minute averages of potential difference (voltage). These potential differences were then calibrated against a mercury thermometer for temperatures ranging from approximately 6^{o}C up to approximately 86^{o}C. A calibration curve was thus produced for this range of temperatures. It was however decided to focus on the lower range of temperatures, from 6^{o}C up to 35^{o}C, as this is more realistic in terms of soil temperatures and resulted in a more accurate calibration which has been represented in Figure B6.

B7: Hobo Soil Thermometer Calibration

From Figure B6, it is evident that the calibration coefficients obtained provide a good representation of actual soil temperatures with a good linear fit indicated by having a R^2 value of 0.9941. This once again proved that the temperatures logged were accurate. The calibration represented in Figure B6 was thus used with high confidence in the conversion of the estimated potential difference to soil temperatures.

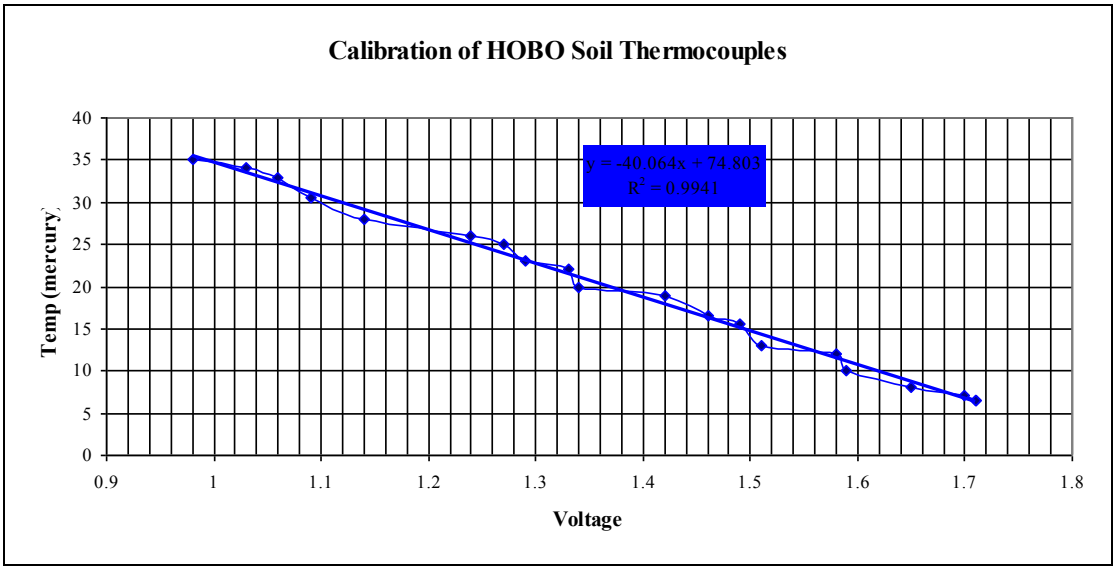

Figure B6: Calibration of HOBO thermocouples against a mercury thermometer for the range 6 to 35^{o}C.

B8: Soil Density

Excess soil was cut off with a hacksaw (Figure B7) leaving only the core sampler filled with undisturbed soil from the profile. The volume of the core sampler was measured as well as the mass of soil within the sampler once oven dried. This allowed for the calculation of soil bulk density in the laboratory.

Figure B7: Method used in the estimation of soil bulk density.

Appendix C: Sensible Heat Flux

C1: Scintillometer Transmitter

The BLS 900 transmitter emits radiation through 924 light emitting diodes (LED). Two round cases each house a disk with 444 infrared and 18 red LED's. The transmitter can be operated at four different frequencies as seen in Table C1. The pulse rate of 125 Hz produces maximum accuracy and allows for the measurement of transverse wind speed. Although running the transmitter at 125 Hz results in large power consumption, the availability of a constant power supply meant that the transmitter was operated at this maximum frequency to provide maximum accuracy for the duration of the project (Scintec, 2004).

Table C1: Options for frequency rates at which the transmitter operates (Scintec, 2004).

Rate	Frequency (Hz)
1	1
2	5
3	25
4	125

Figure C1: BLS 900 transmitter (left) and fire tower on which it was mounted (right)

C2: Scintillometer Receiver

The receiver is able to run for approximately 7 to 10 days on two 96Ah batteries in parallel. Batteries were therefore changed weekly and the instrument re-launched and re-aligned. Data collection took place at the receiver and was logged at one minute intervals. The receiver was bolted onto a strong box, in which the signal processing unit (SPU) is located, as were the batteries (Figure C2). The data were transferred onto a laptop on a weekly basis.

At the receiver, radiation is collimated by a plan convex lens onto 2 photodiodes. The receiver was mounted on a 3 axis positioning device which was used during alignment of the instrument. A telescope is also mounted on the receiver and was used for aligning with the transmitter (Scintec, 2004).

Figure C2: BLS 900 receiver (left) and strong box (right)

C3: Scintillometer Signal Processing Unit

The signal processing unit (SPU) or logger for the BLS 900 has two plugged-in cards. The signal processing card filters, demodulates and digitises the received signals and the microprocessor card evaluates and stores the converted data. The microprocessor also controls the communication to a PC via a serial interface (Scintec, 2004).

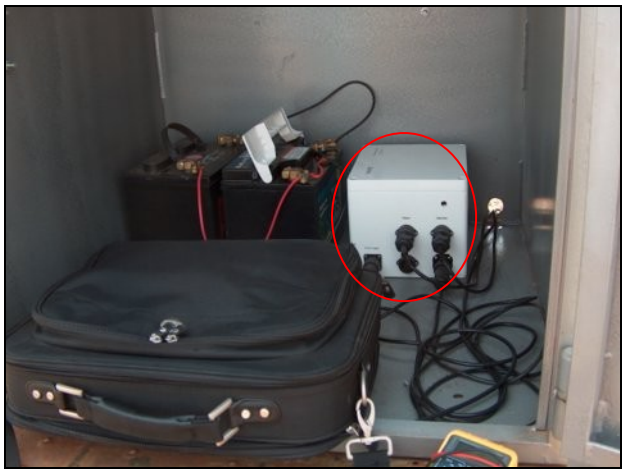

Figure C3: Signal Processing Unit for the BLS 900 scintillometer.

The SPU operates using a 'loop storage' system whereby the RAM capacity allows for storage of up to 4 weeks. Once the storage capacity is exceeded by the amount of data, the first data points are overwritten.

One of the major shortfalls of the BLS 900 is that the data are stored in a 2 Mbyte volatile RAM. This means that if power is cut or battery voltage drops too low, all data are lost. This proved to be a slight problem with valuable data being lost at the inception of the project in October 2004. Consequently, the field procedure was changed to allow for the replacing of batteries every 7 to 10 days to ensure that data would not be lost. After power to the SPU was removed, all data stored were deleted as well as the program which the SPU used to operate. Therefore, upon reconnection of recharged batteries, the SPU program was transferred from the laptop to the SPU. This therefore formed part of the weekly download and re-launching procedure.

The BLS 900 has independent air temperature and atmospheric pressure sensors. The data measured by these sensors are used in the calculation of sensible heat flux. The atmospheric pressure and air temperature were read 20 times per minute with averaged values being used in the heat flux calculation (Scintec, 2004). The sensible heat flux component is calculated using internal computation recalibration routines. Details of sensible heat flux computation are not addressed in this study.

Appendix D: TDR Soil Water Content Sensor

A Time Domain Reflectometry method was used to estimate volumetric moisture content at the experimental site. The TRIME-FM TDR model was used in this study (Figure D1). This is a portable moisture measurement instrument, which has been developed for mobile field use. According to Imko (2001), the measuring of soil water content with Time Domain Reflectometry is now a well established method. A measuring accuracy of ± 2 vol.-% is possible, provided that soil and access tube are in close contact (Imko 2001).

Figure D1: TRIME-FM and access tube used to estimate volumetric soil water content content.